5-2019

Modeling Color Appearance in Augmented Reality

Nargess Hassani
nh2305@rit.edu

Modeling Color Appearance in Augmented Reality

Nargess Hassani

May, 2019

COLLEGE OF SCIENCE
ROCHESTER INSTITUTE OF TECHNOLOGY
ROCHESTER, NEW YORK

CERTIFICATE OF APPROVAL

Ph.D. DEGREE DISSERTATION

The Ph.D. Degree Dissertation of Nargess Hassani
has been examined and approved by the
committee as satisfactory for the
dissertation required for the
Ph.D. degree in Color Science

Reynold Bailey, Chair

Michael J. Murdoch, Advisor

Mark D. Fairchild

James Ferwerda

Date

Declaration

This dissertation is a presentation of my original research work. Wherever contributions of others are involved, every effort is made to indicate this clearly, with due reference to the literature, and acknowledgment of collaborative research and discussions.

I hereby grant permission to Wallace Center Library of R.I.T. to reproduce my thesis in whole or in part. Any reproduction will not be for commercial use or profit.

Rochester, May, 2019

Nargess Hassani

Rochester Institute of Technology

College of Science

Program of Color Science

Munsell Color Science Laboratory

Ph.D. Dissertation

A Dissertation Submitted in

Partial Fulfillment of the Requirements for the

Degree of Doctorate of Philosophy in Color Science

Modeling Color Appearance in Augmented Reality

Nargess Hassani

May, 2019

Signature of Author _____

Accepted by _____

Graduate Program Director Date

Nargess Hassani

Modeling Color Appearance in Augmented Reality

Ph.D. Dissertation, May, 2019

Advisor: Michael J. Murdoch

Committee Chair: Reynold Bailey

Committee Members: Mark D. Fairchild and James Ferwerda

Rochester Institute of Technology

College of Science

1 Lomb Memorial Dr

14623 and Rochester

Abstract

Augmented reality (AR) is a developing technology that is expected to become the next interface between humans and computers. One of the most common designs of AR devices is the optical see-through head-mounted display (HMD). In this design, the virtual content presented on the displays embedded inside the device gets optically superimposed on the real world which results in the virtual content being transparent. Color appearance in see-through designs of AR is a complicated subject, because it depends on many factors including the ambient light, the color appearance of the virtual content and color appearance of the real background. Similar to display technology, it is vital to control the color appearance of content for many applications of AR.

In this research, color appearance in the see-through design of augmented reality environment is studied and modeled. Using a bench-top optical mixing apparatus as an AR simulator, objective measurements of mixed colors in AR were performed to study the light behavior in AR environment. Psychophysical color matching experiments were performed to understand color perception in AR. These experiments were performed first for simple 2D stimuli with single color both as background and foreground and later for more visually complex stimuli to better represent real content that is presented in AR. Color perception in AR environment was compared to color perception on a display which showed they are different from each other.

The applicability of the CAM16 color appearance model, one of the most comprehensive current color appearance models, in AR environment was evaluated. The results showed that the CAM16 is not accurate in predicting the color appearance in AR environment. In order to model color appearance in AR environment, four approaches were developed using modifications in tristimulus and color appearance spaces, and the best performance was found to be for Approach 2 which was based on predicting the tristimulus values of the mixed content from the background and foreground color.

Acknowledgement

First, I would like to thank my advisor Dr. Michael Murdoch, for all his help and guidance that he has given me over the past four years. He is the nicest advisor one can ask for. I thank him for his valuable and constructive suggestions during the planning and development of this research work. I would like to express my sincere gratitude to Dr. Mark Fairchild for his help and support both as my committee member and my professor. I also thank my other advisory committee members, Dr. James Ferwerda and Dr. Reynold Bailey for their thoughtful comments and suggestions.

I would also like to express my gratitude to my professors at color science program, Dr. Roy Berns and Dr. Susan Farnand and Dr. David Wyble for their help and guidance. Special thanks to Valerie Hemink for her help with the administrative tasks and continuous support.

I would like to thank my fellow students/colleagues at RIT who helped me during my Ph.D. study and generously participated in my experiments, Yixuan Wang, Christopher Thorstenson, Dr. Yuta Asano, Dr. Adrià Forés Herranz, Dr. Farhad Moghareh Abed, Dr. Brittany Cox, Dr. David L. Long, Joel Witwer, Fu Jiang, Lili Zhang, Anku, Matthew Ronnenberg, Adi Robinson, Katherine Carpenter, Morteza Maali Amiri, Garav Sheth, Olivia Kuzio, Josh Glaro, Hao Hie, Yongmin Park, Mingming Wang, Jenible Paray, Yue Yuan, Luke Helwig, David Liu, Rik Spieringhs, Xiangzhen Kong, Kensuke Fukumoto, and Mahshad Mahdavi.

Special thanks to Jeff Cox who always helped with problems of studying abroad. I would also like to thank my friends: Dr. Baharak Eshghipour, Dr. Hamid Tofighi, Paarth Mehta, Sahar Hashemgeloogerdi, Dr. Mohammad Kazemi Dehkordi, Dr. Niaz Abdolrahim, Dr. Hesam Askari, Shima Khamooshi, Koosha Abdolrahim, Dr.Majid Rabbani and Dr.Mojgan Rabbani who made great memories for me during my Ph.D. study.

I also wish to thank my family for supporting and understanding me pursuing a PhD in the United States: Soraya, Ali , Samaneh and Mohammad Reza.

Finally, I would like to thank my dearest Yashar Seyed Vahedein for all his love and support through these years and for always being there for me.

Contents

List of Figures

List of Tables

1 Introduction

1.1 Motivations

Augmented reality (AR) is a technology that enhances human perception, enabling observers to perceive the world in a more enriched way. Telecommunication, education, design, navigation and many other areas can benefit from AR technology [Van Krevelen and Poelman, 2007]. AR will be a revolution in human computer interaction. It will completely change the way information is presented and reduce the efforts that the user makes while switching back and forth between the real world and computer screens [Feiner, 2002]. Using AR, a tourist can see navigation and historic information of places, a surgeon can see medical pictures overlaid on patient's body, firefighters can see structure information of a building, and gamers can fight fantasy creatures while traveling. There has been a lot of effort to bring this technology to production. There are different types of AR devices developed so far. One common design is called optical see-through head mounted displays (HMDs). In these devices, the virtual content is optically overlaid on top of the real world. These devices are wearable and usually interactive.

Color perception in AR is a very important subject as the quality of the experience in AR could be greatly impacted by the color quality of the content. In many applications of AR, knowing the color appearance and being able to control it is critical; applications such as design, education, medicine etc. There are cases where the color appearance should stay stable regardless of changes in background or lighting or other cases where we want the virtual content to look as realistic as possible, therefore, with regard to changes in lighting and background, we want the same appearance changes for the virtual content as it would happen for a real object's appearance. Color is a major concern for optical see-through HMDs. This is because the color of the virtual content blends with the background. Therefore, when looking at different backgrounds or under different lightings, the mix appearance perceived will be impacted.

Since AR is relatively a new technology, most of the effort has been focused on bringing this technology to life. Therefore, most of the research has been done on the technology side of AR. There has not been much research done on color quality and perception in AR. For reflective objects, color appearance has been studied for decades and it has been well modeled. Also, perception of transparency has been studied for

over decades. However, there hasn't been any research on trying to model color appearance in this new environment.

If AR is going to become the next interface between human and computer, we should be able to know color perception in such environment and be able to control it. In case of see-through HMDs (which are a very common design in AR), the light behavior should be studied. How the real world, virtual content and the final mixed light is impacted by the optics of the device, and how the light behaves when the light from the background is mixed with the overlay light coming from the displays embedded in the device.

The impact of background should also be studied. How the color appearance of the background impacts the color appearance of the mix and how changing the background from one color to another impacts the mix appearance are vital to know. The background can vary a lot. It can be indoors or outdoors, with different objects in the scene and different distances from the observer.

Another factor that affects the mix color appearance in AR is the virtual content that is presented on the devices displays and reflects into user's eyes using the optics of the device. The display has a limited brightness range and a limited color gamut which limits the final mix appearance. One big problem with brightness limitations is showing the virtual content in bright outdoor environments would be very difficult and sometimes impossible. Also, the color gamut of the AR device would be limited by the displays color gamut and the color features of background objects.

The other factor in color perception in AR is lighting. Lighting will change the adaptation state of the observer and the background brightness is impacted by the brightness of the lights in the environment. The lighting can be simple (one source for indoor or daylight in outdoor environments) or more complex (cases with multiple sources of light).

In order to be able to control the color in AR devices, we need to model color appearance in this environment. This modeling should at least include impacts of background color, foreground color, visual complexity of the content and lighting on perceived color. This model will help create better color quality in AR devices and adjusting the color appearance to the intended appearance.

1.2 Approach

There are two approaches to model color appearance in AR. One is starting from scratch and try to model all the color perception phenomena in AR, and the other approach is to use an already existing color appearance

model and modify it for AR applications. Since color perception in AR environment shares some similarities to color perception in real world, the second method was chosen in this project. For this purpose, CAM16 color appearance model was chosen as the starting color appearance model. CAM16 is a comprehensive yet practical color appearance model [Li et al., 2017a], which is a recent modification of CIECAM02 [Moroney et al., 2002], it covers a wide range of stimulus and adapting intensities, a range of viewing conditions from dark to dim to average surrounds, and it is computationally reversible. Neither CIECAM02 nor CAM16 include dynamic light adaptation nor chromatic surrounds/backgrounds for the stimulus. Also, there has been a lot of research works focused on transparency. Since in optical see-though AR designs the virtual content is transparent, the results of these research works were used in modeling color appearance in AR. As reviewed above, there has been some work on color in augmented reality environment, however, there has not been any work on modeling color perception in augmented reality. In this research, color appearance in AR is studied.

The first step was to study very simple situations in AR using 2D solid color patches both as background and foreground stimuli in a controllable AR simulator. When color appearance in this simple example of AR is understood, more complex situations can be further studied. CAM16 was used to test its suitability for AR applications, then modified to improve the accuracy of its predictions of the AR color matching data. The second step was to compare color perception in AR environment to color perception on a single display. For this purpose, an experiment was performed with a similar color matching task, but on a single (non-AR) display in order to understand the differences between our AR example and corresponding 2D patches. The results showed that color perception is different in these two environments. At the end to further understand color perception in AR, new experiments were conducted with more visually complex stimuli. This was done to study cases that are more similar to real applications of AR. First a scaling experiment was designed to scale visual complexity of stimuli with 2D and 3D designs with different levels of texture. Then a color matching experiment was performed in the AR environment to study color perception for more visually complex stimuli. All the results of these experiments were then used to model color appearance in AR environments.

1.3 Novelty

Since there has not been much research on color perception in AR, this research is the first attempt to study and model color perception in AR. In this research, three main novel contributions are provided including:

- physical and psychophysical datasets for AR environment
- a model framework for AR

- a perceptual scale for visual complexity

In terms of the datasets, a dataset of physical measurements of foreground, background and mixed colors is provided. Two psychophysical datasets of the perceived mixed colors are provided for color appearance of simple solid color virtual patches in AR mixed over simple solid color real color patches as background under two different illuminants. Also, another psychophysical dataset was built for virtual content with different levels of visual complexity overlaid on simple solid color patches as real background. Different approaches are taken to model color appearance in AR using the aforementioned datasets. First an already existing color appearance model was chosen (CAM16) and modified for AR purposes by adding the impact of chromatic simultaneous contrast. Then four other approaches were taken: one based on modifying the CAM16 calculations in JAB space regarding the background and foreground color, another based on modeling the transparency of the foreground stimuli using the background and foreground colors in XYZ space. Tow other approaches were 1) adding the impact of simultaneous contrast to the second approach and 2) combining the first and second approach. A scale of the visual complexity of the stimuli was also build in this research.

First, measurements are made from light coming from the background, display and the mixed light in AR environment. These measurements were done using a Photo Research PR655 spectrophotometer.

This led to building a dataset from these measurements. Two other datasets are built from psychophysical color matching experiments in AR environments for simple 2D solid color stimuli and visually complex stimuli and another one for color matching on a display.

The main contribution of this research is the framework provided for color appearance modeling in AR environments which are based on the results of all the experiments that are explained in this dissertation. These approaches are the first approaches to model color appearance in AR environment.

Another contribution of this research is building a scale for stimuli with different levels of visual complexity. This scale can be used for psychophysical experiments which use stimuli with different levels of visual complexity to include the impact of visual complexity in a more quantitative way.

1.4 Dissertation Structure

Chapter 2 goes over the AR technology and history. In this chapter, AR technology and different designs of AR devices are explained and reviewed.

In Chapter 3, research that has been done in the field of color in AR is reviewed. Although there have not been many research studies on color in AR (especially color perception), there are few researches which focus on color.

Chapter 4 discusses the measurements that were performed in AR simulator. The AR simulator is a prototype built in our lab to simulate AR environment with simple optics. The design of the AR simulator and stimuli that were measured are all explained in this chapter. The results of the measurements are provided and discussed in this chapter.

Chapter 5 goes through the color matching experiment in the AR simulator for simple 2D solid color patches as stimuli. The design of the stimuli and the experiment are explained. The results are presented and discussed. The measurements done in chapter 4 are then used as input to CAM16 to predict the color appearance in this environment.

Chapter 6 explains the color matching experiment on a single display which was designed to evaluate the differences between the color perception in an AR environment vs on a single display. The results are then compared to the results obtained in chapter 5.

Chapter 7 includes discussion of a direct scaling experiment to scale visual complexity. Stimuli with different shapes, dimensions and texture levels are used in this experiment. The design of the stimuli and graphical user interface (GUI) is explained. The results are presented and a scale is built based on the results.

Chapter 8 goes over the final psychophysical color matching experiment which was performed to study color perception in AR for more realistic stimuli with higher levels of visual complexity.

Chapter 9 uses all the obtained results from all the chapters to provides new framework to model color appearance in AR environment. Several related approaches are explained and the performances are discussed.

Chapter 10 goes through conclusions and reviews all the results obtained in previous chapters.

2 Augmented Reality Technology

Augmented reality is part of the mixed reality area in the reality-virtuality continuum [Milgram and Kishino, 1994]. In augmented reality, virtual content is mixed with the real content. AR systems mix the virtual and real content in a 3D fashion and in real time. Therefore, they are often interactive systems.

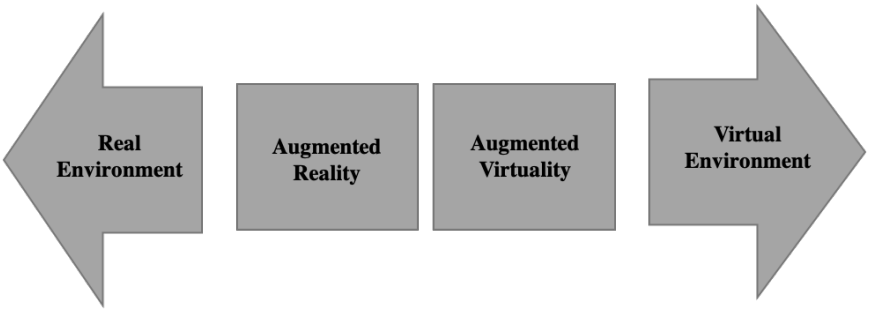

Fig. 2.1 – Diagram of reality-virtuality continuum.

In the diagram above, the left most part of the chart is the real environment. Then there is augmented reality which is the real environment with virtual content added and then we see augmented virtuality which is the virtual world with some contents added from real world. On the furthest right there is virtual environment, which is a completely virtual world. It should be mentioned that AR is not restricted only to sight. Virtual contents can also be in forms of sound, touch, and smell. However, when talking about AR, mostly visual virtual content is mentioned. In this dissertation, we only talk about the visually augmented reality.

The first AR device was built in 1968 by Ivan Sutherland and his students at the University of Utah [Sutherland, 1968]. Their device was a see-through design including a computer, two mini cathode ray tube displays and a variety of equipment to enable the user to move. Figure 2.2 shows the device.

Figure 2.2 shows pictures of the first AR device built by Ivan Sutherland. This device was called a 3-D display. The picture on the right in Figure 2.2 shows the device worn by an observer. The picture on the left, shows all the equipment used to enable the device. Figure 2.3 shows a schematic of the design of this device and the equipment used.

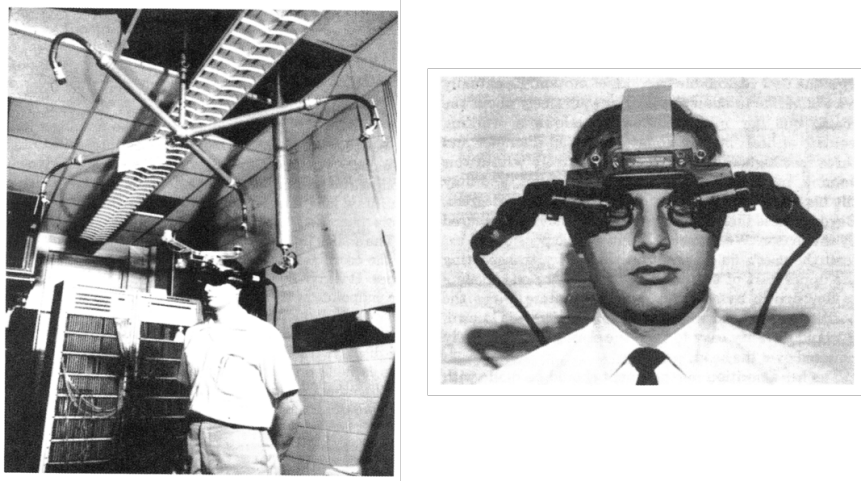

Fig. 2.2 – Ivan Sutherland's augmented reality device. The left picture shows a user using the device. The right picture depicts the optics of the device [Sutherland, 1968].

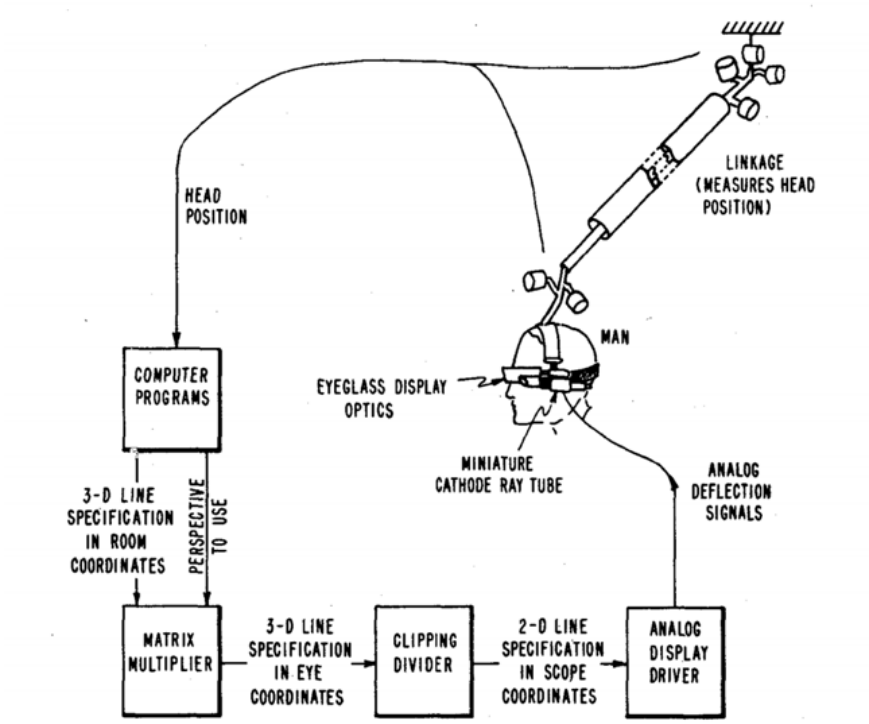

Fig. 2.3 – The equipment used in the 3-D display design.

From Figure 2.3, it is noticeable that there was a variety of equipment used. The device included two miniature cathode ray tubes (also visible in Figure 2.2 on the right). There was a linkage connected to user's head to detect user's movements. These movements were then transferred to the computer which would rebuild the projection matrix and update the clipping window to show proper content with regards to the movements.

Nowadays, AR devices can be categorized into four groups based on the display positioning: retinal, spatial, hand-held and head-worn (or head mounted). Retinal AR displays present the virtual context on a retinal display (like a contact lens). In projective spatial AR devices, the virtual content is projected in real environment. In handheld displays the virtual content is shown in a display that the user is holding it in their hands (also showing the real environment). Most AR devices are usually designed as head mounted displays, which are designed in a way that user wears them on their head (usually like a helmet or glasses). HMD designs are either optical see-through or video see-through.

2.1 Retinal AR displays

Micro fabricated contact lenses, sometimes called smart contact lenses or bionic lenses, with embedded electronics, optoelectronics or sensors can be used for AR purposes which use micro-light- emitting diode (LEDs) for producing images [Pandey et al., 2010]. Also, the tear fluid in eyes contains biomarkers that closely correlate to levels found in blood [Shum et al., 2009]. Therefore, these contact lenses can be used as medical sensing instruments to measure glucose, cholesterol, sodium, and potassium [Ho et al., 2008]. The picture below shows the basic design for these lenses.

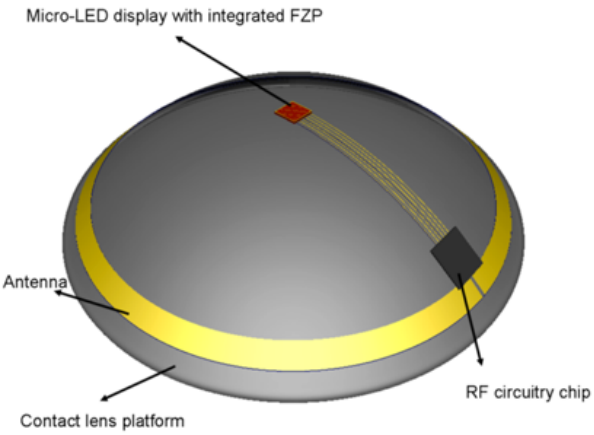

Fig. 2.4 – Conceptual design of a contact lens with embedded electronics [Shum et al., 2009].

As seen in the picture above, this design contains a contact lens platform (which is a biocompatible polymer), an antenna, a radio-frequency circuitry chip for power harvesting and communication, and a micro LED display. There are lots of dilemmas in producing these contact lenses. One difficulty with a contact lens display is producing in-focus images [Mirjalili and Parviz, 2012]. As human eyes can accommodate from 7-40 cm, they cannot focus on images that are placed directly on the cornea. To solve this problem, Mirjalili et al. embedded integrated Fresnel zone plate (FZP) micro lenses in between the micro LED and the eye to bring the image into focus [Shum et al., 2009]. These FZP lenses use diffraction from circular gratings to focus the light into a point.

Other difficulties in producing these instruments include energy provision, power efficiency, biocompatibility, integration and manufacturability, eye movements, and controller chip [Mirjalili and Parviz, 2012].

2.2 Spatial AR displays

This technology is detached from the user and is instead integrated into the environment. Three different approaches exist in this category: video-see through, optical see-through or direct augmentation [Smet et al., 2013].

2.2.1 Spatial video see-through

This approach which is also called screen-based video see through [Smet et al., 2013] or window on the world [Bimber and Raskar, 2005] uses a regular monitor (e.g. a desktop monitor or a phone display) to merge the virtual content with camera-captured real content. In this approach, the AR field of view of the observer is limited to the display size. Also, a big disadvantage of this approach is the decreased resolution of the merged images, in comparison with the perceived real environment by the observer, which is limited to the monitor's resolution. However, this approach can be used where mobile applications are not required and is the most cost efficient approach as only a regular display, PC and camera are required.

2.2.2 Spatial optical see-through

In this approach, the virtual content is aligned with the physical environment using spatial optical combiners. These combiners can be planar, curved, mirror beam combiners, transparent screens, or optical holograms [Smet et al., 2013]. A famous example of this method is "Pepper's ghost" effect, which was an old example of spatial see through augmented reality; invented by professor John Henry Peppers in 1862, Pepper's ghost effect contained appearance of ghostly objects in the scene or transforming objects in the room into different objects. The application was mainly for entertainment purposes usually used in theaters and later in some concerts.

Using spatial optical see-through displays, users cannot benefit from mobile applications since the optics need to be spatially aligned with the environment. Also, as the display is see-through, a mutual occlusion between the real and virtual content does not happen. Most displays of this type prevent a direct interaction with the user as well. However, this approach benefits from easier eye accommodation, larger field of view, higher resolution, and better controllable environment.

Fig. 2.5 – An example of a spatial optical see-through display AR [*Holograms 3D Holographic Projection - Laser Magic Productions*].

2.2.3 Spatial direct augmentation

Using this method, the virtual content is projected on a real model (see Figure 2.6). These displays can cover a wide field of view and can project the virtual content on a wide range of surfaces from simple models such as flat walls to more complex three-dimensional models. The projection can be done using a single or multiple projectors.

This method has been used in bigger scales for entertainment or advertisement purposes in projecting buildings. Figure 2.7 shows an example.

For simple projections on the surfaces, one projector can be sufficient. However, if there is projection of a three-dimensional graphic in front of or behind the surface object, then stereoscopic projection is needed, as the correct depth perception is not provided by the real surface object anymore. Geometrical complexity of the real surface object is one of the main concerns in this approach. This makes the alignment of the virtual content on the real surface a difficult task. Also, the display area is limited by the real surface's appearance features such as size, shape and color.

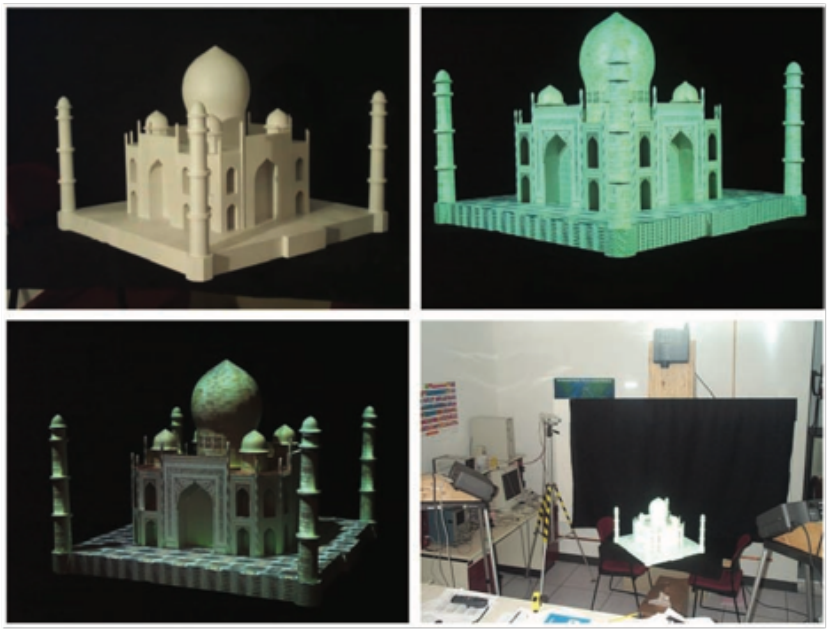

Fig. 2.6 – Projecting the virtual content on a real model [Bimber and Raskar, 2005].

Fig. 2.7 – Castle projection in Disneyland.

2.3 Hand-held AR displays

In this approach, using a hand-held display (usually a cell phone), the virtual content is overlaid on the real environment. The overlaying method can be both video see-through or optical see-through. This method

has been widely used to introduce AR to a mass market as it is very cost efficient and easy to use. A recent example of this method is the AR mobile game “Pokémon Go” [*The Pokémon Company, Niantic*]. This is an AR mobile game that uses cell phone’s display to superimpose virtual game objects into the camera-captured surrounding environment. The game was released in 2016 by Niantic and was very popular at the time.

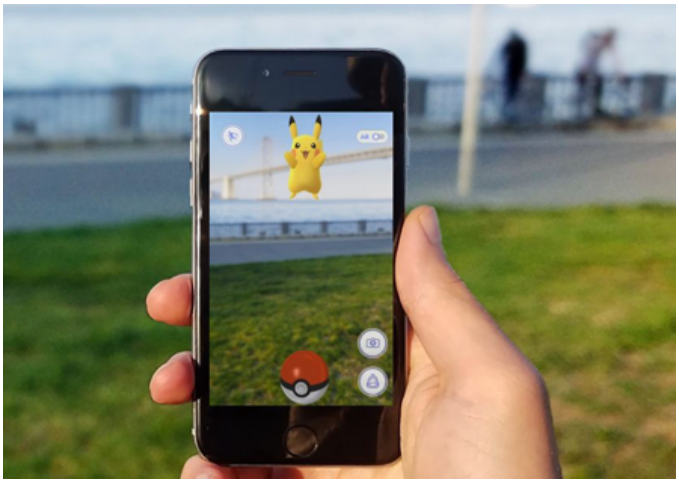

Fig. 2.8 – AR mobile game “Pokémon Go”

2.4 Head-worn AR displays

Currently HMDs are one of the most favored approaches in AR as they are mobile, can be interactive, and give an immersive experience to the user. In this approach, the user wears the display on their head, and through the optics of the display, experiences the AR. There are two methods in designing HMDs. One is called video see-through and the other is optical see-through. Each design is explained in detail below.

2.4.1 Video see-through HMDs

In standard designs of video see-through HMDs, the user does not see the real world directly [Azuma, 1997]. These HMDs can have one or two head-mounted cameras which provide the user’s view of the real world. This view then gets combined with the virtual objects rendered by the graphics of the device. There are different methods in composing the image in video see-through HMDs. These methods include chroma-keying and using the depth information. In the chroma-keying method, the background of the virtual image is set to a color that does not exist in the virtual object intended for the scene, then all the areas of the image that have that color will be replaced with the video from the real world [Beato et al., 2009]. The depth information technique uses the depth information in each pixel for real world images and replaces the virtual object in the intended location [Beato et al., 2009].

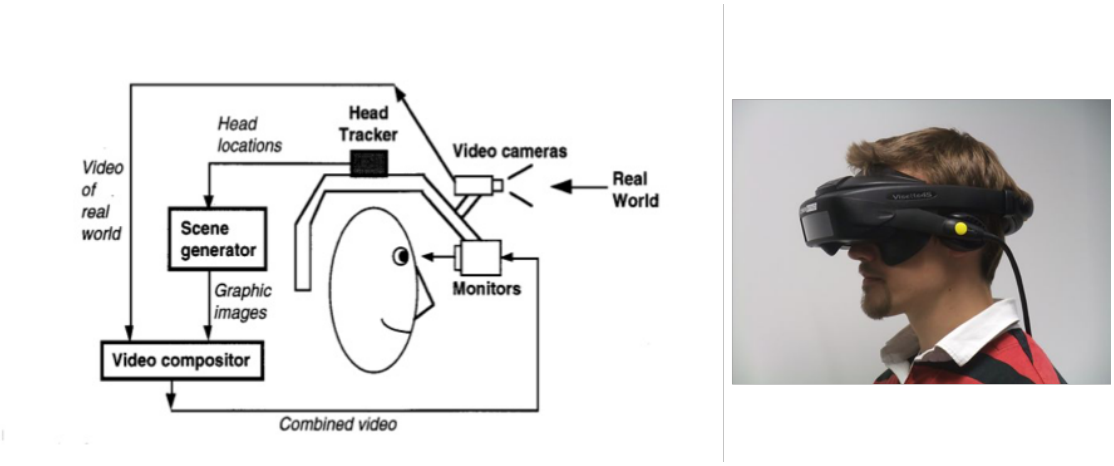

Fig. 2.9 – Left: A schematic of a video see-through AR design. Right: a user wearing a video-see through HMD (Visette 45 SXGA VST) [Beato et al., 2009]

The left picture in Figure 2.9 shows a conceptual design of a video see-through HMD. From this picture we see that the view of the real world is captured with a video camera, then this video is fed into a video composer along with the information from the head tracker which also goes through the scene generator. Then these two videos get combined and are sent to the monitors which show the mixed reality to the viewer. The right picture in Figure 2.9 shows a person using a video see-through HMD.

2.4.2 Optical see-through HMDs

In optical see-through HMDs, optical combiners are used. These combiners are partially transparent; therefore, the user sees the real environment directly through the device. The optical combiners are also partially reflective. The virtual context is then added to the real world using the reflective properties of the combiners which reflect the image of the virtual context from the displays in the HMD into the user's eyes [Bimber and Raskar, 2005]. Figure 2.10 below shows a see-through HMD design.

From the left picture in Figure 2.10, which depict a conceptual design of optical see-through HMDs, we see that the head tracker information is fed to the scene generator, then the generated scene regarding the head position is sent to the monitor; The scene is then overlaid on top of the real world using optical combiners. The user sees the real world directly through the optics of the see-through HMD. The picture on the right in Figure 2.10 shows an observer using an optical see-through HMD (in this case Microsoft HoloLens).

In the common design, the optics of the device usually reduce the amount of light coming from the real world so, when turned off, they act similar to sunglasses. The semi-transparent mirrors used in these devices transmit part (for example 30%) of the light coming through and reflect part (for example about 70%) of the

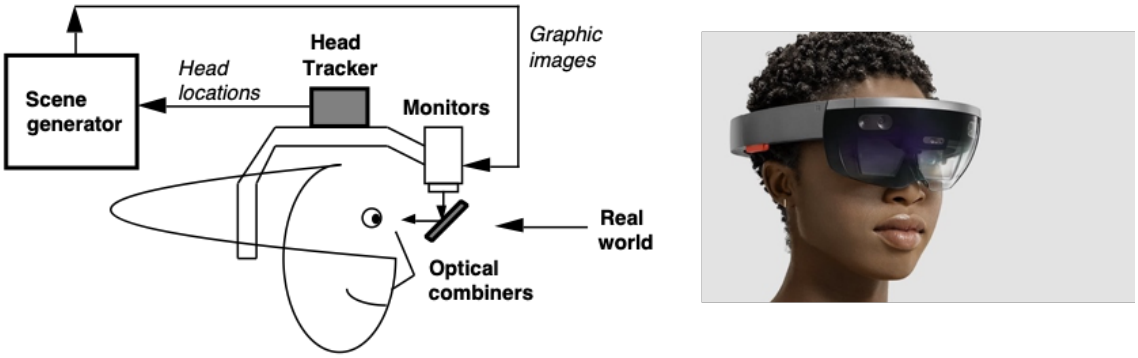

Fig. 2.10 – Left: A schematic of an optical see-through AR design. Right: A user wearing Microsoft HoloLens (a see-through AR device) [Bimber and Raskar, 2005] and [*Microsoft HoloLens*]

light falling upon them. In another design, the optics of the device is designed to reflect only light from certain wavelengths and transmit light from other wavelengths. This design works best with the monochrome displays. Many different methods are used to design the optics in the optical see-through HMDs. Figure 2.11 shows two traditional designs. In the first method, shown on the top of the figure, an intermediate image is formed. This is called a pupil forming design. This design allows integration of optical functionalities such as exit pupil expanders (EPE), which is expanding the image to fill up the viewer's field of view. Also, using this design there is more flexibility on the optics used in the device as the intermediate mage size can vary with custom made display sizes [Raskar et al., 2001].

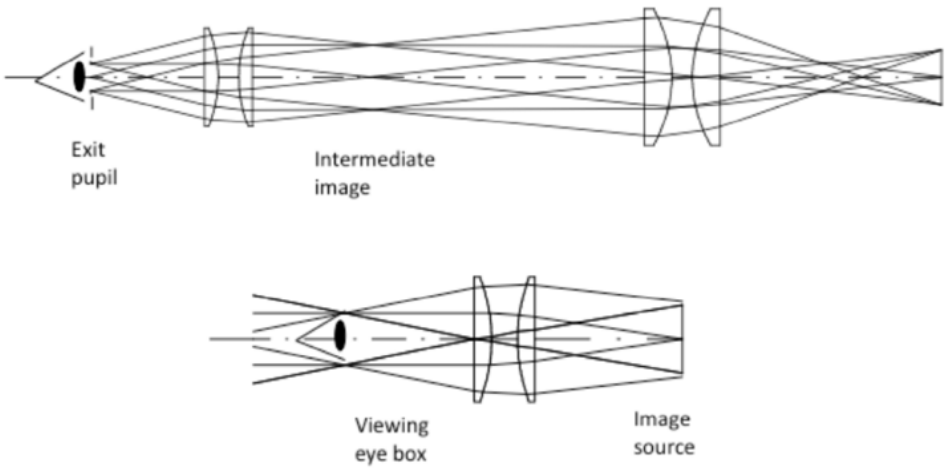

Fig. 2.11 – Two traditional optical designs for optical see-through HMDs [Raskar et al., 2001].

The bottom picture in Figure 2.11 shows a non-pupil forming design. As it is clear from the picture, this design is much more compact and more common in consumer HMDs. There is no intermediate image formed in this design, therefore, it does not allow functionalities such as EPE and there is a need for an additional EPE for HMDs that use this design. Other optical designs include: curved combiners, Total internal reflection (TIR) prism lenses, waveguide Holographic, and cascade extractors.

Today a conventional method to design a see-through HMD, which is currently used by many manufacturers, is using a non-pupil forming optical system (magnifier lens) and a beam splitter or waveguide. In design of the see-through HMDs, cameras are used for interaction and registration purposes. As we see in Figure 2.10 , these cameras are embedded in front of the HMD in Microsoft design of the HoloLens.

2.4.3 Optical see-through vs video see-through

Each design of AR devices has their pros and cons and are appropriate for certain applications. Optical see-through HMDs are simpler in design, they keep the resolution of the real world intact, they are safer (if there is a power failure the user still can see their surroundings), there is no eye offset and they are cheaper overall. Also due to no eye offset, observer would not experience motion sickness in Optical see-through design. However, optical see-through HMDs have limited field of view and reduce the brightness and the contrast due to their optical design. Retinal scanning displays (RSDs) however, can fix the problem of low brightness and limited field of view by using low power lasers and drawing the virtual image directly into the retina [North et al., 2016]. Optical see-through HMDs are also less suited for outdoor use. Another problem that optical see-through HMDs face is occlusion. Due to the design of optical see-through HMDs, virtual content cannot occlude the real objects. There has been some work on this problem and Kiyokawa et al [Kiyokawa et al., 2003]. solved this problem by using an opaque overlay for an LCD panel with pixels that cover the areas desired to get occluded. Video see-through HMDs are more flexible in design, they have a wider field of view, the real and virtual delays can be matched in them, there are additional registration strategies available for them, and it is easier to match the brightness of the real and virtual images in them.

In this research a device with an optical see-through design (similar to optical see-through HMD) was used.

3 Prior Research on Color Appearance

In this chapter research on color appearance models and perceptual transparency is reviewed. The reason for choosing these topics is that optical see-through AR environment includes real objects and virtual contents overlaid on top of them (which look transparent). Therefore, it is necessary to review previous research in these areas. First color appearance models for reflective objects (opaque objects) are mentioned. Later, studies on transparency and simultaneous color contrast are reviewed. At the end, the research works on color in AR environments are discussed.

3.1 Traditional Color Appearance Models

In the Color Appearance Models book by Fairchild [Fairchild, 2013], he describes color appearance models as "any model that includes predictions of at least the relative color appearance attributes of lightness, chroma, and hue." There have been many color appearance models developed over the decades, from simpler models such as CIELAB [CIE, 1986] to more complex ones such as CIECAM02 [Moroney et al., 2002]. All these models include an adaptation transform and predictions of relative color appearance attributes. Some of the more complex color appearance models have predictions of brightness, colorfulness or other color phenomena.

CIELAB was suggested by CIE in 1976. Although it was developed as a color space, it meets the criteria for a color appearance model. This model uses dimensions L*, a*, and b*, which represent lightness, red versus green and blue versus yellow percepts respectively. Using this model one can also predict chroma (C) and hue (h). Although CIELAB predicts attributes such as lightness, chroma, and hue, it is inadequate for color appearance predictions especially in more complex situations (for example it does not include the impact of background). Therefore, there have been many efforts to provide more adequate color appearance models [Nayatani et al., 1990] [Fairchild and Berns, 1993].

Hunt's model is one of the most comprehensive color appearance model [Hunt, 1991]. It covers a wide range of adaptation and it predicts a wide range of visual phenomena. However, this comprehensiveness comes with complexity. Hunt's model is one of the most complex color appearance models and it is not analytically

reversible due to its complexity. Hunt uses a Von-Kris type of adaptation transfer with significant modifications which includes nonlinear behavior of visual responses. Hunt's model predicts color phenomena such as Bezold-Brucke hue shift, Abney effect, Helmholtz-Kohlrausch effect, Hunt effect, Simultaneous Contrast, Helson-Judd effect, Stevens effect, and Bartleson-Breneman observations [Fairchild, 2013].

In 2002, CIE recommended a new color appearance model called CIECAM02 which was based on the previous color appearance model CIECAM97S [CIE, 1998]. Both models have similar structure, however, CIECAM02 solved some problems with CAM97S. One significant improvement was that CIECAM02 is a reversible model while CAM97S is not. CIECAM02 was suggested by CIE to be a comprehensive standard color appearance model. It was aimed to cover a wide range of stimulus intensities (from very dark to very bright), adaptation levels, and viewing conditions [Fairchild, 2013]. CIECAM02 predict appearance features including hue (both hue angle and hue quadrature), chroma, lightness, saturation, brightness, and colorfulness. The inputs to the model include tristimulus values of the stimulus and the white point, the adapting luminance, and the relative luminance of the surround. The viewing condition can be chosen from "Average", "Dim", and "Dark" levels; for each level there are constant values defined in calculations of the model. However, these values are continuous and can be interpolated between the defined levels. CIECAM02 uses a linear Von Kries type chromatic adaptation. It provides an optimized transform matrix (CAT02) for chromatic adaptation calculations which is based on the matrix used in Hunt's color appearance model [Hunt, 1991] and it is normalized to give equal L,M, and S (cone response values) outputs when transforming tristimulus values of the equal energy illuminant's tristimulus values to cone responses. In order to modify the appearance dimensions in CIECAM02 to include the weighting that is usually used in color difference formulas such as CIE DE2000 to make the color difference calculations easier. Later a uniform color space base on CIECAM02 was suggested (CAM02-UCS color space) [Luo et al., 2006].

Although CIECAM02 is a relatively comprehensive color appearance model and is recommended by CIE as a standard model, it has some computational failures. In research work, Li et al. reported that CIECAM02 has some computational failures in certain cases such as cross-media color calculations [Li et al., 2017b]. They claimed that although there have been efforts to address these problems, all the solutions are based on keeping the structure of CIECAM02 intact. However, in this research work, they suggested a new model called CAM16. They claimed that this model solves these problems and outperforms CIECAM02 in predicting visual results. Also , they claimed that the new model is simpler than CIECAM02 to use. The main change in CAM16 over CIECAM02, is combining the chromatic and luminance adaptation to take place in a new cone-like space. They provided CAT16 (a new chromatic adaptation transform) and CAM16-UCS (a new uniform color space) to replace CAT02 and CAM02-UCS respectively. By comparing CAM16 and CIECAM02, CAM16 performed equal to or better than CIECAM02 when using different datasets. CAM16 was significantly better in predicting hue and colorfulness than CIECAM02.

3.2 Perception of Transparent Color

Color transparency has been studied since 1867 when Helmholtz's Treatise on Physiological Optics mentions his study of transparency by superimposing strips of papers of different colors over each other using a simple optical device [Helmholtz and Southall, 2005]. Since then, two schools of thought have emerged: The additive and subtractive models. These two schools of thoughts are explained in the following. First research works that are based on additive concept are reviewed and then the studies which focused on subtractive model are discussed.

3.2.1 Additive Models

One of the important recent studies on transparency was done by Metelli [Metelli, 1970] [Metelli, 1974]. Metelli studied transparency of achromatic stimuli. He stated that physical transparency is different than perceptual transparency and physical transparency is neither a necessary nor a sufficient condition for perceptual transparency [Metelli, 1974]. Also, he mentioned that perceptual transparency is impossible when the underlying field is homogenous. By using an Episcotister (which is depicted in Figure 3.1), he claimed that transparency can be explained using perceptual scission (decomposition of color layers) which assumably follows the law of color fusion (Talbot's law [Talbot, 1834]). When the episcotister is rotated fast, it induces an impression of transparency. Matelli tried to explain transparency mathematically based on Tablot's law.

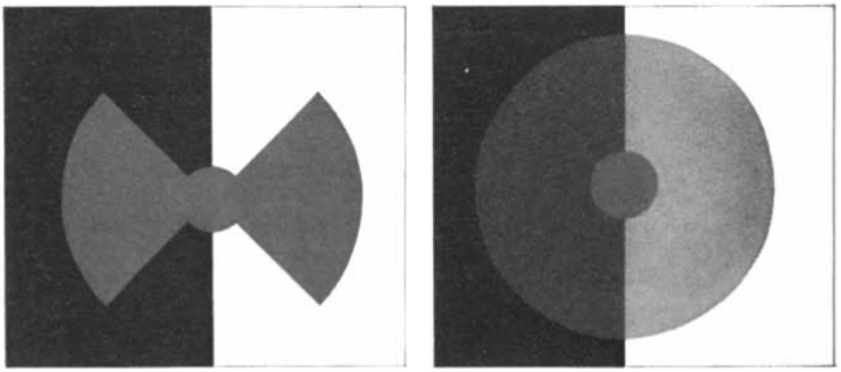

Fig. 3.1 – Episcoster used in study by Metelli [Metelli, 1974]. When the wheel is rotated fast, it gives a transparency impression. left: the wheel when it is static, right: the wheel when rotating fast

Figure 3.2, shows the schematics of perceptual transparency and equations predicting the phenomenon. Surfaces A and B in two different luminance level are the background when P and Q are on top of them. In this Figure, P and Q are perceived as a whole transparent layer (t) superimposed on top of A and B. The reflectance values of these surfaces are shown as a, b, p, and q respectively. Metelli assumed that perception of transparency is a case of color splitting and by assuming that the laws for color fusion work in this case, he

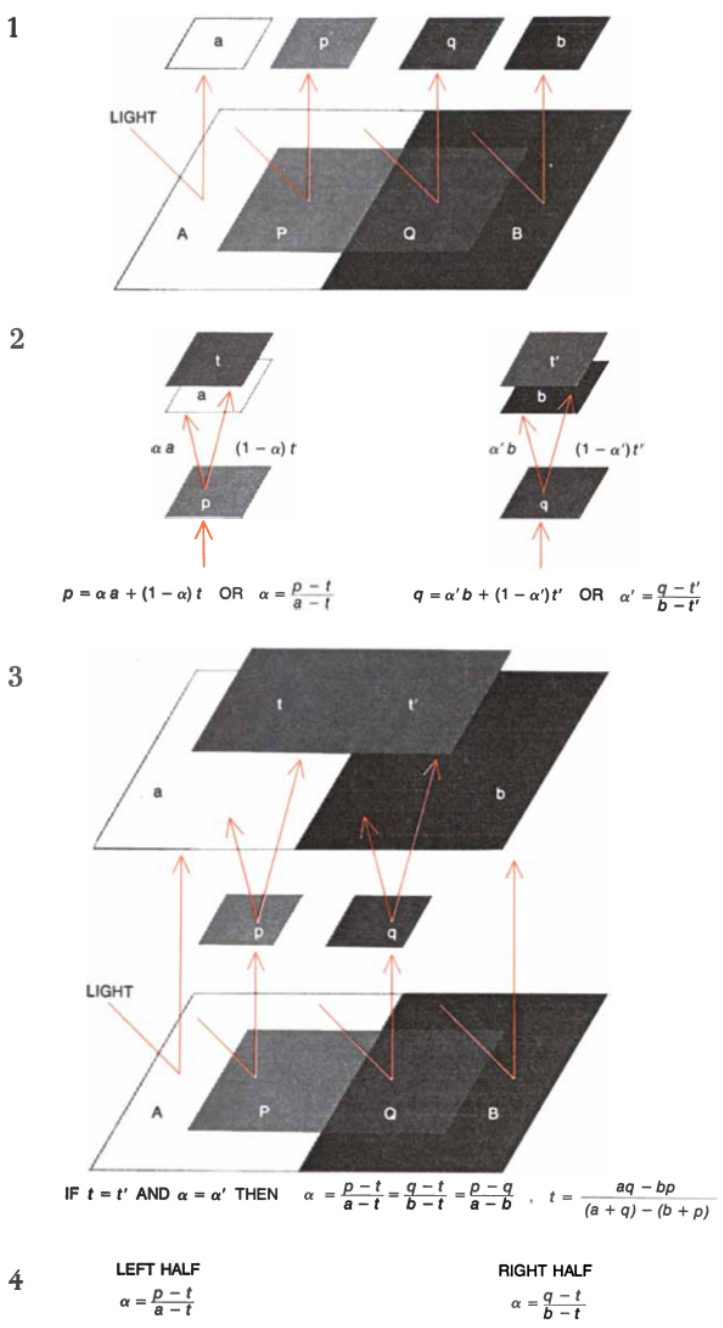

Fig. 3.2 – Explanation of transparency by Metelli [Metelli, 1974].

explained the perceived surfaces relative lightness values using algebraic equations. By these assumptions, p results when t is mixed with a, and q results when t is mixed with b. Therefore:

$$p = \alpha a + (1 - \alpha)t \tag{3.1}$$

$$q = \alpha' b + (1 - \alpha')t' \tag{3.2}$$

and if $t = t'$ then:

$$\alpha = \frac{p - t}{a - t} \tag{3.3}$$

or

$$\alpha = \frac{q - t}{b - t} \tag{3.4}$$

For these equations, α (transparency) varies from zero to one. Variables a, b, p, q, and t are reflectance values of the regarding achromatic stimulus. Metelli mentions that based on this model, relative lightness predictions about the layers can be made. for example a > p > t and b > q > t (the > sign means lighter). The equations became the basis of modeling the physics of transparency in later studies. Metelli also stated that for perception of transparency to occur, three main figural conditions should exist: figural unity of the transparent layer, continuity of the boundary, and adequate stratification. The figural unity of the transparent layer means that the central region of the transparent layer should be uniform. The continuity of the boundary states that there should not be a break in the boundary of the transparent and the opaque background. Otherwise, the perception of transparency is disrupted. The stratifications condition means the background should be perceived as being "under the whole of the transparent layer".

He mentions that in this research work they studied balanced transparency (when the transparent layer is uniform in degree of transparency and color). However, other percepts of transparency exist as well; these include unbalanced transparency (the degree of transparency is non uniform over the transparent layer) and partial transparency (part of the upper layer is perceived as transparent and the other as opaque). These cases of transparency require different formulas.

D'Zmura et al. studied chromatic changes that induce transparency [D'Zmura et al., 1997]. First they used a flat array of color papers and a small square sheet of transparent color plastic. Then they generated simulated images to have images representing a similar display to the array of color papers. They superimposed a square region on the array which the chromaticity of the underlying color squares were changed; these changes represented different chromatic changes including: translation, convergence, rotation and shear in

a equiluminous fashion along the L&M-cone and S-cone axes of MacLeod and Boynton color space. They argued that transparency can be perceived for stimuli with equiluminous translation (a translation with no changes in the luminance level which is mathematically similar to convergence) [MacLeod and Boynton, 1979]. Figure 3.3 shows one of the simulated images representing convergence towards red.

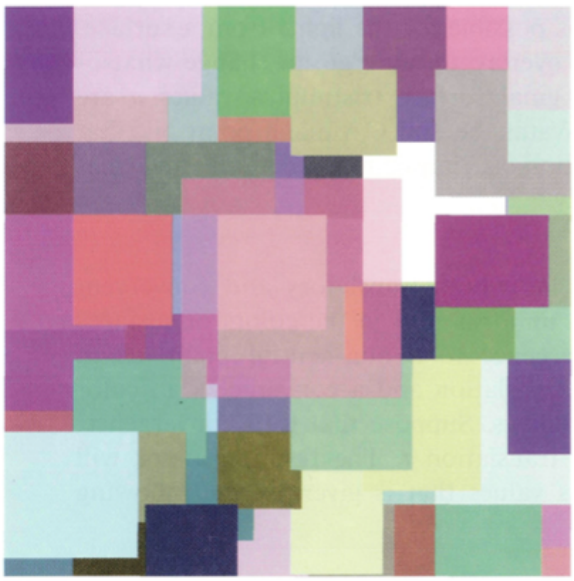

Fig. 3.3 – Simulated image showing an array of colors with a central superimposed color square representing a convergence towards red [D'Zmura et al., 1997].

These images were then used to conduct psychophysical experiments. The experiment included two adjacent simulated images, one with the superimposed square with the color squares being darker (served as a standard achromatic example of transparency) and the other image with the superimposed square representing a chromatic shift. The observers were asked to adjust the physical color contrast of the equiluminous translation to match the transparency of the superimposed color square to the achromatic one. They reported that chromatic translation, convergence and combinations of the two induces the perception of transparency.

$$b = (1 - \alpha)a + \alpha g \tag{3.5}$$

$$0 < \alpha < 1$$

In this equation, a is the background surface color , g is the target color (transparent layer), b is the result of the convergence from a to g (all in tristimulus values), and α determines the extent to which color of b changes from a to b. Also, they conclude that the perception of transparency does not require systematic changes in luminance.

In another study by Chen and D'Zmura, the convergence model of transparency was tested [Chen and D'Zmura, 1998]. They used a stimulus with four color areas. Figure 3.4 shows the stimulus design. The color of the three areas were selected in advance (the two large squares and one of the small middle squares) and the task of the observer was to choose the color of the fourth square so that the small squares appear as a central transparent region. Results showed that the convergence model describes the data. However, they found out that the model has two flaws, one that it does not provide a basis for analyzing the error in prediction and second that in certain color combinations, the model predicts transparency while transparency was not perceived; these cases include colors that caused the two central squares to have opposite hue or lightness.

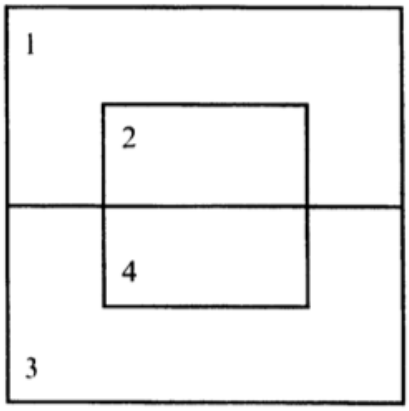

Fig. 3.4 – Stimulus design in a research work by Chen and D'Zmura [**ChenAndD'Zmura**].

D'Zmura et al. further studied color transparency in another study [D'Zmura et al., 2000]. In this research, they evaluated their convergence model in predicting the color of the surfaces behind a color filter. For this purpose, they conducted an asymmetric color matching experiment in which the observers would modify the color of a surface behind a filter to the color of the surface viewed without the filter. Figure 3.5 shows the stimulus design in this experiment. They compared predictions of the convergence model to predictions of other models including a general affine-transformation model and von Kries scaling model and the results showed that the convergence model provides better predictions in comparison to the other models.

3.2.2 Subtractive Models

In 1984, Beck published a paper claiming that for achromatic colors, a model based on subtractive mixture yield similar results to additive mixture (based on Metelli's theory) [Beck, 1978]. In another study, Beck et al tested Metelli's model [Beck et al., 1984]. They designed different experiments to test constraints of the Metelli's model. Since Metelli's model of perception is based on Talbot's law, there are four constraints (first

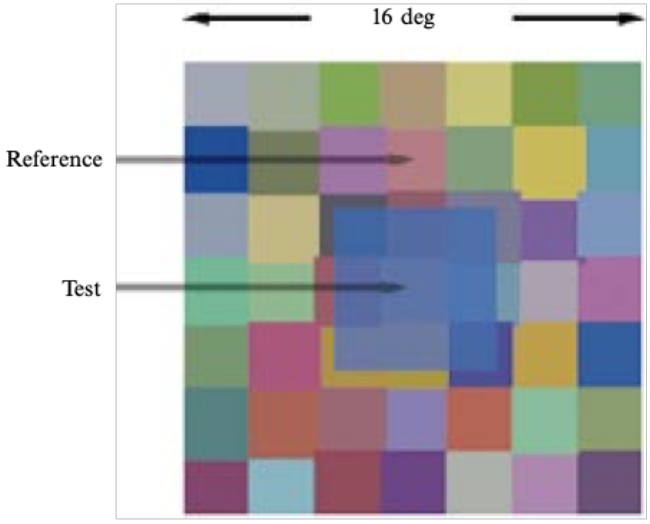

Fig. 3.5 – Stimulus design in study by D'Zmura et al. [D'Zmura et al., 2000]. Observers were asked to modify the color of the test surface to match it to the reference surface.

two mentioned in Metelli's model [Metelli, 1974]. Figure 3.6 shows surfaces in a rotating episcotister which the constraints are explained based on them.

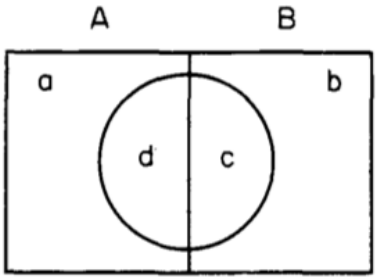

Fig. 3.6 – Schematics of surfaces on a rotating episcotister [Beck et al., 1984].

The first constraint in Talbot's law is that if a > b (see Figure 3.6), then d > c and vice versa. Constraint (ii) is that the absolute difference of a and b (|a-b|) must be greater than absolute differences between c and d (|c-d|). Constraint (iii) is if (a + c) > (b + d) then ac > bd and vice versa. The fourth constraint is that the absolute difference | (a + c) - (b + d)| must be equal or greater than |ac - bd|. Beck et al. mention that in Metelli's statement, transparency happens when the first two constraints are met and it fail to occur when these constraints are violated. However, Metelli does not mention consequences of violating constraints (iii) and (iv).

In Beck et al.'s work, the first two experiments were designed to test constraints (i), (ii) and (iii), (iv) respectively. Results showed that when constraints (i) and (ii) were violated strongly, perception of transparency did not occur. However, when these constraints were violated less severely, with strong figural cues were present,

transparency was perceived by some observers. It was also resulted that constraints iii and iV were not necessary for perception of transparency to occur.

Beck et al. suggest a subtractive model to model the physical transparency. The equations of the model are presented in Equations 3.6, 3.7, 3.8, and 3.9.

$$d = f + (t^2 a)/(1 - fa) \tag{3.6}$$

$$c = f + (t^2 b)/(1 - fb) \tag{3.7}$$

$$t = \sqrt{\frac{(C - bcd + bd^2 - d)(b - a - abc + a^2 c)}{(b - a + abd - abc)^2}} \tag{3.8}$$

$$f = (bd - ac)/b(1 + ad) - a(1 + bc) \tag{3.9}$$

In these equations, a, b, c, d, f, and t are reflectance of surfaces A, B, filter on B, filter on A , Filter reflectance and transmittance values. These surfaces are depicted in Figure 3.7.

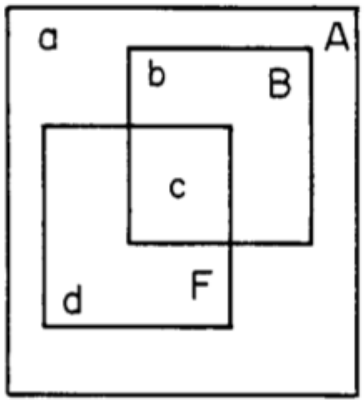

Fig. 3.7 – Surfaces involved in Beck et al.'s subtractive model of transparency [Beck et al., 1984].

Since predictions of this model and Metelli's model of the achromatic stimuli were very similar, Beck et al. concluded that the physical occurrence of transparency involves both additive and subtractive equations. They

designed an experiment (experiment3) to test if perception of transparency varies linearly with lightness or reflectance differences. The results showed that perceptual transparency is based on lightness rather than luminance or reflectance value. Therefore, they concluded that Talbot's law is not an appropriate approach for modeling perceptual transparency. They suggest that using lightness values instead of reflectance values in Talbot's law results in accurate predictions of the quantitative transparency judgments.

Experiment 4 was designed to test how balanced transparency is perceived and to evaluate relationship of degree of transparency with reflectance value. Results showed that suggested the α variable (by Metelli [Metelli, 1974]) fails to predict the perceived degree of transparency. Also, in terms of partial transparency, Talbot's law requires the overlapping surface (perceived as the transparent surface) to have a luminance value between the two non overlapping surfaces (see Figure 3.8. However, the results showed that when this requirement was violated (the luminance of the overlapping surface was not between the luminance values of the two non overlapping surfaces), some observers perceived the overlapping surface as transparent.

Fig. 3.8 – Surfaces involved in partial transparency [Beck et al., 1984].

Beck et al. concluded that color scissioning does not follow a reverse of Talbot's law and its a higher order cognitive encoding. Their results show that when the figural cues are strong, transparency is perceived even if the lightness relationships are incorrect (violating constrains (i) or (ii) or both). Also, the perception of transparency can occur without the occurrence of scissioning. When this happens, the impression of transparency is evoked but the colors in the overlapping regions are wrong.

Later, Metelli et al. published a study to address Beck et al. comments [Metelli et al., 1985]. They argued that in Metelli's theory , limitations relative to α $(0 < \alpha < 1)$ and t $(0 < t < 1)$ apply for balanced transparency. When perception of unbalanced or partial transparency happens, this theory does not claim anything about these constraints. Therefore, cases that Beck et al. study does not test this model. In regards of Beck et al.'s statement about using lightness instead of reflectance value, Metelli et al. explained that Beck uses the same equation that was suggested for prediction of physical transparency and only substituted reflectance values with lightness values and this resulted in good predictions of perceptual transparency. The reason

that this worked is because the equations for predicting the physical transparency are formally identical to equations that would be resulted from lightness estimations of the surfaces involved (Metelli et al. claim that they noticed this when they deduced the equations they provided). They also mention that in their study, they use experienced observers when Beck et al. used naive observers and therefore they obtained different results.

Singh and Anderson studied perception of transparency to understand how humans perceive opacity and lightness of a transparent layer [Singh and Anderson, 2002]. They used sinusoidal gratings as background surface and added disparity to the region of transparency so it would appear in front of the background. This approach was used to "evoke a vivid percept of distinct layers". The study included experiment of observers evaluating the stimuli in terms of lightness and opacity (separately). Results showed systematic deviations from Metelli's model's predictions. Their results showed that observers systematically overestimated transparent layers that decreased the background's luminance and systematically underestimated transparency of layers that increased the background's luminance. Therefore, the relationship between perceived degree of transparency and physical transparency depends on how the transparent layer impacts the luminance of the background. They mention that Metelli's model is not adequate in predicting perceptual transparency. One example for this is comparing a white and a black episcotister (the top layer being white or black). Although, Metelli's model predicts similar degrees of transparency for these with similar cut out sizes, the black episcotister is perceived as more transparent. This is because the black episcotister generates a higher Michaelson contrast. Michaelson contrast is depicted in Equation 3.10.

$$\frac{L_{max} - L_{min}}{L_{max} + L_{min}} \tag{3.10}$$

In Equation 3.10, L represents the luminance value. Singh and Anderson concluded that human vision system uses Michelson contrast instead of α to predict degree of perceived transparency.

3.2.3 Other Transparency Effects

One phenomenon that involves perception of transparency (with no physical transparency) is neon color spreading. Neon color spreading happens when a transparent color texture in between black texture is perceived as a transparent layer. Neon color spreading stimuli have been also studied in transparency researches and sometimes used as the stimulus to study transparency perception.

Nakayama et al. studied transparency with regards to depth, subjective contours, luminance, and neon color spreading a transparency illusion [Nakayama et al., 1990]. Using stereoscopic disparity to change perceived

depth, they studied impacts of disparity on the perception of transparency, color spreading, and subjective contours. results showed that perception of neon color spreading requires transparency perception to happen as well , but not vice versa. They also stated that impacts of configuration and luminance relation changes on perception of transparency were major.

In a study by Ekroll and Faul, the impact of different luminance combinations and color combinations on perception of transparency in neon color spreading displays was studied [Ekroll and Faul, 2002]. They conducted two experiments; the first experiment was focused on impact of luminance level combinations (using achromatic stimuli) while the second experiment studied color combinations (using chromatic stimuli). The results of the first experiment showed that the impressions of balanced transparency resulted when the luminance of the inner elements were between the luminance of the outer elements and the background. The results of the second experiment showed that as long as the luminance level of the inner elements are between the luminance level of the outer elements and the background, all color combinations leads to perception of transparency. However, a subset of these color combinations led to more compelling impressions of transparency. This subset was color combinations that was well described by Metelli's additive model.

Another model of transparency was suggested by Ripamonti et al. in 2004. They studied the constraints that are necessary for perception of transparency [Ripamonti et al., 2004]. For this purpose, they conducted two experiments; the first experiment was designed to compare the strength of transparency percept for transparent stimuli designed by the invariant ratio model suggested previously by Ripamonti et al. [Westland and Ripamonti, 2000] and convergence model suggested by D'Zmura et al. [D'Zmura et al., 1997]. The invariant ratio model equations are presented in Equations 3.11 and 3.12.

$$X_P = \beta x_A \tag{3.11}$$

$$X_Q = \beta x_B \tag{3.12}$$

In Equations 3.11 and 3.12 x_P, x_Q, x_A, and x_B represent cone excitation for areas P, Q, A, and B (depicted in Figure 3.2). β is a diagonal matrix with elements on the main diagonal representing the ratio of cone excitations for each cone types. The stimuli were designed to be Mondrian-like chromatic patterns with a transparent overlay in the center. The experiment was a paired comparison and the observers were asked to choose the stimulus that was perceived as more transparent. The results showed that the stimuli that were designed based on the invariant ratio model were perceived as more transparent for most stimuli. In the second experiment, the impact of the number of background colors (in the Mondrian-like patterns) on percept

of transparency was studied. The results showed that as the number of partially covered surfaces (by the transparent filter) was increased, the filter was perceived as more transparent.

In another study, Faul and Ekroll argued that the additive model is not able to correctly predict chromatic transparency [Faul and Ekroll, 2002]. They mention that since the majority of research on transparency used achromatic stimuli, the additive model suggested by Metelli ([Metelli, 1974]), and the subtractive model suggested by Beck ([Beck et al., 1984]) predict similar results. However, when using chromatic stimuli, systematic deviation from the additive model is observed. They claim that additive and subtractive models have a considerable overlap in predictions and since the additive model is simpler and easier to use than subtractive models suggested previously, additive models have been more popular. Therefore, they suggest a simple subtractive psychological model (called scaling model) based on physical model of transparent filters ([Nakauchi et al., 1999]). The scaling model equations are:

$$P_i = \beta_i(A_i + \kappa I_i) \tag{3.13}$$

$$Q_i = \beta_i(B_i + \kappa I_i) \tag{3.14}$$

In these equations, P, Q, A, and B represent colors (in terms of cone excitation) of the background and target (similar configuration shown in Figure 3.2 and $I_i = (A_i + B_i)/2$, $0 < \beta < 1$ and $\kappa > 0$.

They conduct two psychophysical experiments using simulations of transparent filters to compare their model's prediction with predictions from the additive model. The results showed that the predictions from the additive model show a systematic deviation from observers' perception of transparency. Also, they mention that predictions of perceived transparency by the invariant ratio model suggested by Ripamonti et al. ([Westland and Ripamonti, 2000] was poor. They report many cases where the invariant criteria was violated but the observers perceived transparency.

In another study, Faul and Ekroll proposed a parametrization of their filter model of transparency [Ekroll and Faul, 2002] [Faul and Ekroll, 2011]. The parameters that they suggested were hue H, saturation S, transmittance V, and clarity C. They claimed that these parameters reflect the perceptual dimensions of perceptual transparency. In this research, first they try to estimate model parameters from the input in a robust way. Then they experimentally compare a full filter model with a sub-model suggested by Faul and Ekroll [Faul and Ekroll, 2002]. The relationship between these parameters and the physical parameters of the optical

filters was also investigated. Results showed that saturation and transmittance depend on thickness of the filter while clarity depends on the refractive index of the filter.

Faul and Ekroll also studied constancy for transparent layers regarding changes in background color and illumination [Faul and Ekroll, 2012]. They found out that almost complete constancy was obtained for changes in background colors while the changes in illumination resulted in systematic deviation. However, they explained that these differences can be explained as a compromise between proximal match of the mean color and complete constancy.

Later in 2017, Faul published a work on modifying the HSVC model propose in 2011 [Faul and Ekroll, 2011] [Faul, 2017]. In this work, He tried to address issues with the previous model including parameters of the model not being uniquely related to subjective properties, the parameter changes did not necessarily correlate with phenomenal changes, and the parameters were not independent. The modification was made to include features such as independence, equidistance, compatibility, and invertibility in the new model.

Fleming et al. also studied the perception of transparency [Fleming et al., 2011]. In their research, they studied the perception of transparency for thick transparent materials with irregularities in shape and variation in transparency index (for example an ice cube). They performed three psychophysical experiments first to study the impact of physical refractive index on perceived material properties, and then two other experiments had a focus on the impact of the features in the scene on visual cues derived from the distortion fields (induced by a thick transparent object). Their results showed that the distortion fields determine the human perception when judging refractive indices.

3.2.4 Simultaneous Contrast

Some of the other studies in the area of transparency includes studies of simultaneous contrast. Although simultaneous contrast was assumed to only depend on the surround color in older studies ([Hunt, 1991]), recent studies focused on perception of transparency in predicting simultaneous contrast. In 1991, Hunt suggested to use the following equations for calculation of the adapting white point:

$$\rho'_W = \frac{\rho_W \left[(1-p)p_\rho + (1+p)/p_\rho\right]^{1/2}}{\left[(1+p)p_\rho + (1-p)/p_\rho\right]^{1/2}} \tag{3.15}$$

$$\gamma'_W = \frac{\gamma_W \left[(1-p)p_\gamma + (1+p)/p_\gamma\right]^{1/2}}{\left[(1+p)p_\gamma + (1-p)/p_\gamma\right]^{1/2}} \tag{3.16}$$

$$\beta'_W = \frac{\beta_W \left[(1-p)p_\beta + (1+p)/p_\beta\right]^{1/2}}{\left[(1+p)p_\beta + (1-p)/p_\beta\right]^{1/2}} \tag{3.17}$$

Where:

$$p_\rho = (\rho_p/\rho_b) \tag{3.18}$$

$$p_\gamma = (\gamma_p/\gamma_b) \tag{3.19}$$

$$p_\beta = (\beta_p/\beta_b) \tag{3.20}$$

In these equations, $(\rho_W, \gamma_W, \beta_W)$ are the cone response values for the white point before performing the simultaneous contrast transform and $(\rho'_W, \gamma'_W, \beta'_W)$ are the cone response values of the white point after the simultaneous contrast transform [Hunt, 1991].

Ekroll and Faul studied transparency perception to understand simultaneous color contrast [Ekroll and Faul, 2013]. They conducted an experiment in which observers matched the hue, saturation, brightness, and transparency of a uniformly colored target disk on a uniform gray surround by adjusting the color and transmittance of a simulated comparison disk. The simulated disk could be opaque or transparent and was in front of a variegated background consisting of 8 wedge-shaped achromatic regions of different luminance. Their results showed that simple uniform color target-surround stimuli evokes perception of transparency. They conclude that the magnitude and direction of the simultaneous contrast is similar to predictions from transparency models indicating that the direction of simultaneous contrast is identical to the vector from the surround color to the target color ("direction law"). They also mention that the magnitude of the simultaneous contrast follows the "inverse law" (Kirschmann's fourth law [Kirschmann, 1892]) meaning that the magnitude of simultaneous contrast decreases with the distance between the target and surround color.

Ratnasingam and Anderson studied the impacts of target and surround color on strength of simultaneous color contrast [Ratnasingam and Anderson, 2017]. They state that the majority of studies on simultaneous color contrast focus on the influence of the surround color on achromatic targets in which the direction of the simultaneous contrast is only impacted by the surround color and is independent of the target color. However, based on the study by Ekroll and Faul [Ekroll and Faul, 2013], this should be replaced by "direction law". They conduct two paired comparison experiments to determine the target and surround color that generated the

largest difference (each experiment was designed to have one of the target and surround color to change while the other was kept constant). Results showed that the magnitude of simultaneous contrast depends both on the target and surround color. The effect increases as the surround becomes more saturated. It is mentioned that the results do not provide any insight into the rate of this increase and can only represent the range of the saturations that were used in the experiment and no conclusion can be made for surrounds with saturations outside of this range. They conclude that the results of their experiment are consistent with the "direction law", however the results do not support the "inverse size hypothesis" (Kirschmann's fourth law).

As mentioned, two school of thoughts exist in terms of modeling transparency. One is additive models which are based on a research work by Metelli [Metelli, 1974], and the other one is subtractive models which are based on a research work by Beck et al. [Beck et al., 1984].There are arguments in the literature stating that since both of thee models used achromatic stimuli, both of the model predictions are close. Also, since the additive models (based on Metelli's) are simpler, they were more favored. Since in optical see-through designs of AR, there is both reflective content (real surrounding objects) and transparent content (virtual content), the discussed research works on reflective color appearance and perception of transparent color can help model color appearance in AR. In the section below, research works which focus on color in AR are reviewed.

3.3 Color in Augmented Reality

As mentioned before, there are not many studies focused on color in AR. In this section, some of the research studies in AR with focus on color are reviewed.

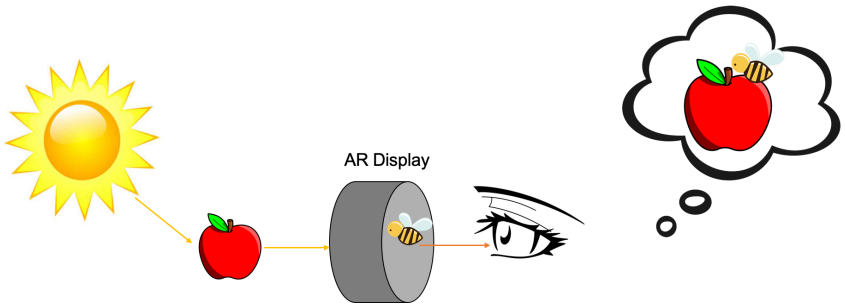

Fig. 3.9 – Light mixture in a see-through head mounted augmented reality device

Color appearance in an AR environment is different than in the real world. Figure 3.9 shows the light mixture in AR. In Figure 3.9, the light coming from the real apple, which is an interaction between the sunlight and the apple's surface, goes through the AR optics (the gray cylinder represents the AR device). The virtual bee is depicted via AR graphics. Therefore, the light coming from the apple gets mixed with the added light by the

device and the observer perceives the mixed appearance. There has been only a small amount of previous research on color in AR.

The light mixture has been studied by Gabbard et al. in which they measured different combinations of foreground and background colors [Gabbard et al., 2010]. They constructed a testbed that emulates the outdoor lighting to measure the mix light of the real background and the virtual color. The testbed contained a colorimeter, light setting and optical equipments (lens, monocle, etc.) for measuring the mixed light. They suggested a model of light mixture with undefined sub functions (see Figure 3.10). They used 6 different test beds as their real backgrounds. Results showed that the mix colors go towards the background color in chromaticity. In another work, Gabbard et al showed that the same result is achieved when using actual real backgrounds instead of posters (for instance using a patch of real grass instead of using a poster of a uniform matching color to it) [Gabbard et al., 2013]. Figure 3.11 shows the results of this study.

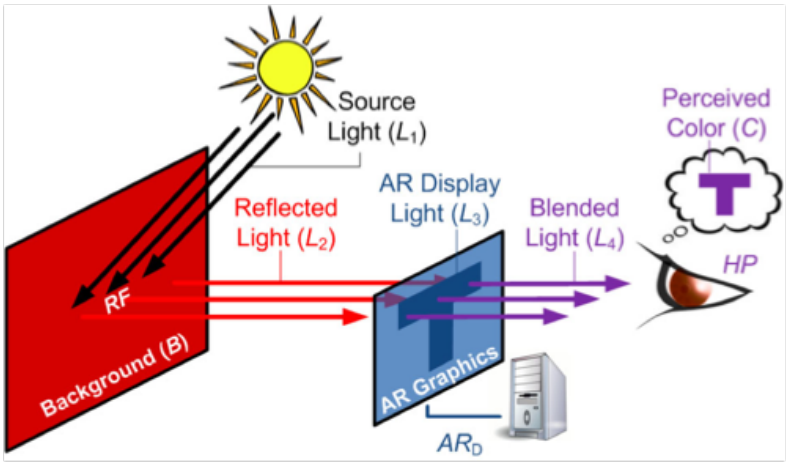

Fig. 3.10 – A model of color blending in AR suggested by [Gabbard et al., 2013].

In Figure 3.10, shows the suggested model of light mixture and color perception in AR by Gabbard et al. In this picture, the light from the source (L_1) interacts with the background (B). This interacted light (L_2) then goes through the optics of the AR device and gets mixed with the AR display light (L_3). The mixed light (L_4) then enters the user's eye and the user perceives a mixed reality appearance.

Figure 3.11 shows parts of the results of the study by Gabbard et. al. in CIE u'v' space [Gabbard et al., 2013]. In this Figure, the outer spots are the measurements from the foreground colors with no background and the center points are the foregrounds on the white background. As it can be seen from the figure, the foreground colors converge towards the background color when overlaid on the background. This research is important in terms of understanding color appearance in AR; Because to do so, first the physics of light mixture in AR should be understood. Later in this dissertation, this study is replicated and later used for modeling color appearance in AR.

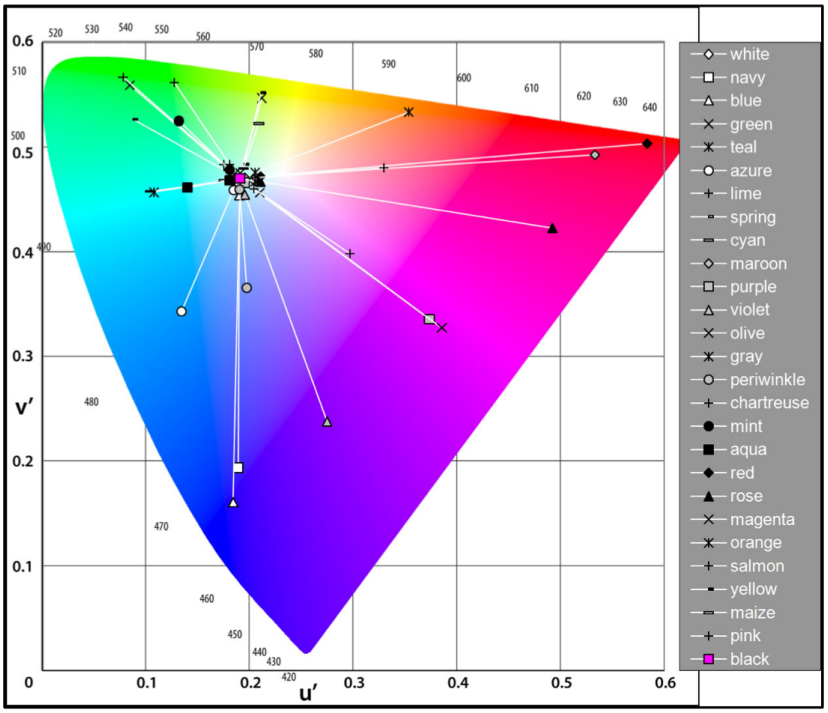

Fig. 3.11 – Results of the study by Gabbard et al. showing "chromatic changes between the no-background condition (outer values) and the white background (inner values). The pink square represents the white background color as seen through the HMD optics" [Gabbard et al., 2013].

Menk and Koch studied the color blending in a projective augmented reality environment [Menk and Koch, 2013]. They worked on altering the color of the virtual context regarding the lighting, the material of the real object (which the virtual context was projected on), the pose and color model of the projector to achieve the desired appearance. They used a physically based computation and by applying a 3D look up table for the color model of the projector, could compute the RGB values for the projector. They provide a method to directly compute RGB values for each projector pixel. In their method, first the projector is calibrated and geometrically registered. Then the ambient light is measured and an HDR image is mapped onto the local geometry and used as the light source in the rendering. After the 3D LUTs are computed, the relationship between the RGB of the projected image and the radiance on the material is described by a matrix. Figure 3.12 shows the setup they used. In this work they do a colorimetric match based on the intended color, the lighting, color of background and the pose. However, no psychophysical experiment is performed to validate these matches.

Livingston et al. studied the visual acuity and color perception in augmented reality [Livingston et al., 2009] . They noticed that observers can achieve the maximum visual acuity with at least the moderate levels of the AR display's contrast. Their color measurements showed distortion for the blended color. They performed a color matching experiment; Figure 3.13 shows the setup.

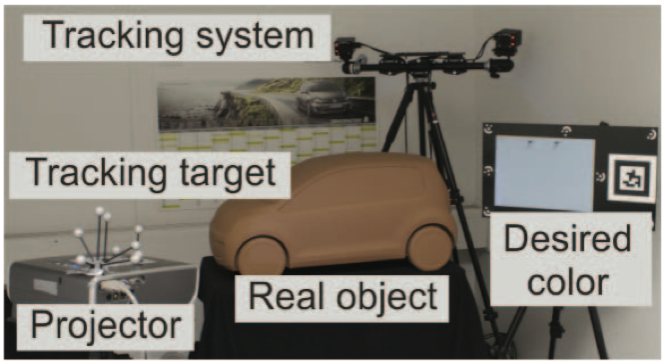

Fig. 3.12 – Experiment setup used in a study on color blending in projective AR [Menk and Koch, 2013].

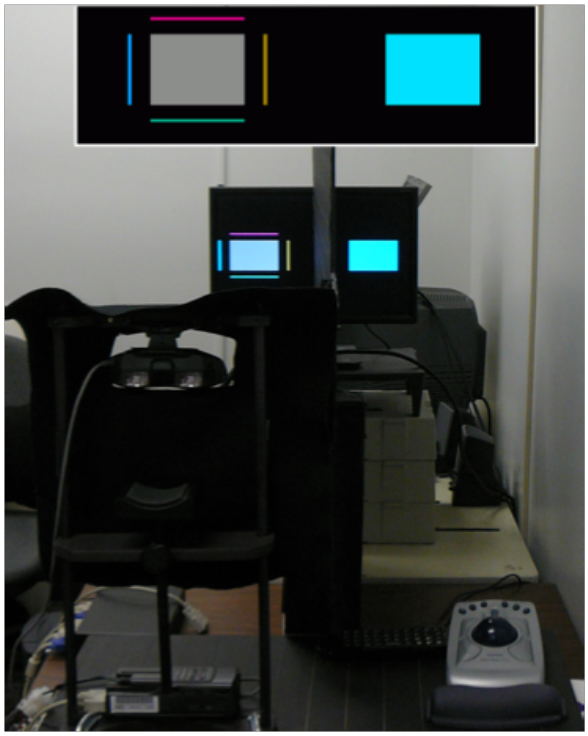

Fig. 3.13 – Setup used in the color matching experiment in a study on visual acuity and color perception in AR [Livingston et al., 2009].

Figure 3.13 shows the setup for the color matching experiment that was performed by Livingstone et.al. in which observers would physically move between the target and reference patch(presented on a display) [Livingston et al., 2009]. They could only see the target patch through an AR device and would modify the appearance of the target patch to match it to the reference patch. Their color measurements showed distortion for the blended color and this distortion was even worse perceptually (resulted from their psychophysical experiment). In this study, the main focus was to evaluate basic visual perception and performances in AR

environment. They studied how the foreground colors get distorted by the color of background and how this distortion is different with different mixes of foreground and background.

In another study, Weiland et al. worked on changing the virtual context using Gaussian or box filters to compensate for adaptation to the lighting that occurs for real context in AR [Weiland et al., 2009]. They suggested a compensation for virtual objects in optical see-through devices. When users see through the HMD, they adopt to the luminance of the real world (by seeing the surrounding through the device). However, this adaptation is not considered for the virtual objects in rendering them. This will result in a clear difference between the real and virtual objects in the AR environment. In their work, Weiland et al. suggested a technique for photometric compensation to avoid this difference. Figure **??** Shows the algorithm suggested by Weiland et al.

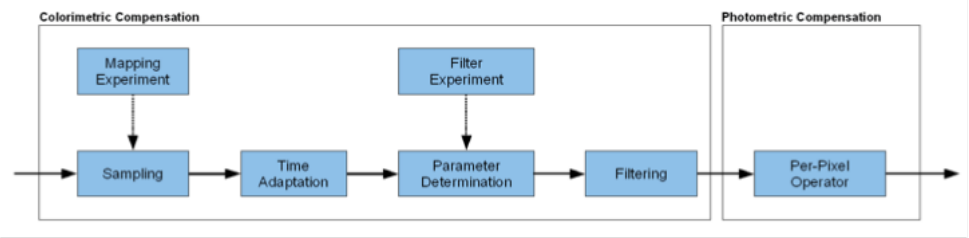

Fig. 3.14 – The algorithm suggested by Weiland et al. for photometric compensation [Weiland et al., 2009].

From Figure 3.14 their technique uses a colorimetric and a photometric compensation. The photometric compensation is performed after the colorimetric compensation and the colorimetrically compensated image and background image are input data for the photometric compensation. In their work, the compensations are not perceptually and the algorithm they provide is based on photometric and colorimetric adjustments. Therefore, it is not clear how these compensations improved the appearance of the virtual content perceptually.

Kirshnamachari and Hincapie-Ramos worked on color correction for optical see-through HMDs [Sridharan et al., 2013]. Their work was on reducing the impact of color blending by finding an alternative color for the virtual context which when mixed with the background, results in the original color. They worked on the distortion resulted from rendering the virtual context. They present a color correction algorithm and middleware called SmartColor for color managements inside the HMD. The middleware manages color corrections and contrast corrections in order to keep a level of contrast needed (for legibility purposes) regardless of the background. In another work Ivanchuk and Hincapie-Ramos applied the color correction at different levels of the OpenGL pipeline for real time color correction and contrast adjustments [Hincapié-Ramos et al., 2014]. Again in this work the focus is on the colorimetrically correcting the color.

In another study, Merenda et al. tried to find most robust colors for optical see-through graphics through different backgrounds for driving purposes [Merenda et al., 2016]. They define robustness as not being

impacted by the background color and support visual search task performance with low visibility. This study was designed with a focus on using AR to present information to drivers while driving. They used three different backgrounds including: brick, grass, and pavement. The observers, who were all drivers, were asked to perform three different tasks; To find a specific letter in a pseudo text, to find a symbol, and to match the presented color with colors from a table. The results showed no significant difference in response time between the background colors, however, for each background, blue, green and yellow colors were more robust than other colors across all the backgrounds. In this research they also use color names to evaluate how robust the foreground color is. This can be practical for applications that the color accuracy is not of interest but the color name is intended to remain constant.

Ryu et al worked on colorimetric estimation of background color, using images of the background and doing a local linear regression [Ryu et al., 2016]. Then, the virtual graphic was compensated regarding the background. For this purpose, they assume the perceived mix image is resulted from the sum of the background and virtual image. To validate their assumptions however, they compare the measured tristimulus value of the mix image with the predictions. However, this comparison cannot tell anything about the actual perception of the mix image and in perceiving the appearance relates not only on the tristimulus values of the object but also on other factors such as: the illuminant, surrounding, etc.

All of the mentioned previous researches add interesting knowledge, but none addresses color appearance generally, and the interactions between foreground, background, and real-world illuminant. In order to be able to control color appearance, it is vital to study these interactions. Therefore, this research work is on studying color appearance in AR regarding the impacts of background color, foreground color, lighting and visual complexity of the content. Then the results of the experiments are used to model color appearance in AR.

4 Measuring Color in Augmented Reality

As discussed in Chapter 3, the appearance in optical see-through augmented reality is a mixture of reflective and transparent objects (objects in the real surrounding are reflective and virtual content is transparent). The first step to study appearance in an AR environment is to study light behavior in such an environment. Therefore, in this chapter, light measurements are reported. The measurements were taken from physical object colors in the AR environment, the virtual content color in AR, and the mix color of virtual overlays on physical backgrounds. Two LED illuminants were used, one similar to tungsten light and the other one a cooler light more similar to D50. The results of the measurements are then discussed.

4.1 Motivations

The first step to understand color perception in augmented reality is to measure color in such an environment. For this purpose, a number of physical background colors, virtual foreground colors and the mixes of those were measured under two different illumination settings. For each set of colors (physical or virtual), the colors were measured both separately and mixed together. These measurements were done to understand the physical light behavior in AR and to validate previous results obtained by [Gabbard et al., 2010]. The chosen colors were similar to colors that Gabbard et al. used and were colors that had more practicality. For example green for greenery backgrounds such as grass, blue for the sky color, etc. Another reason for doing these measurements was to later use them in future experiments and eventually in building a model for color appearance in AR.

An AR simulator was built in order to have a robust and controllable AR environment. The consumer AR devices available lack the color accuracy needed to do research on color in AR [Zhang and Murdoch, 2018], that is why the AR simulator was built to be able to perform color experiments in AR.

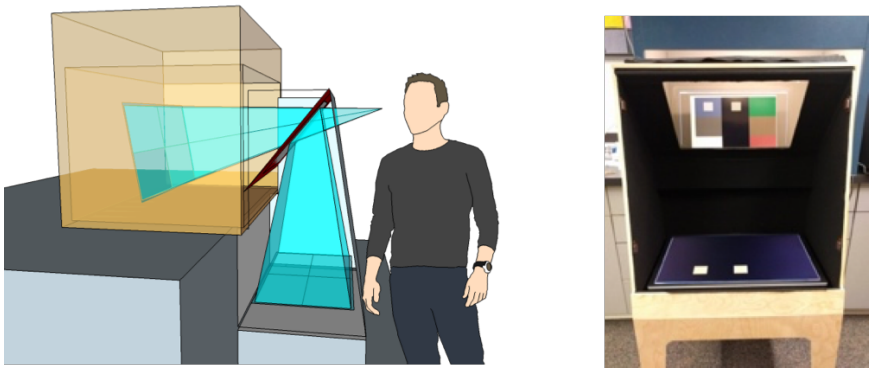

Fig. 4.1 – Design of the AR simulator-Left: The sketch of the AR simulator. The orange box is a light booth. Blue viewing frusta show how the observer sees both light coming from inside the light booth and light from the display at the bottom. The dark red diagonal plane is a half-silvered mirror which mixes the two frusta of light. Right: An actual picture of the AR simulator with the front panel removed, showing the display at the bottom and the optical mix above.

4.2 Building an AR simulator

In order to measure color appearance in AR, an augmented reality simulator was made to overlay the virtual patches on the real backgrounds. The design of the AR simulator is shown in the Figure 4.1: At left is a diagram of its design; at right a photo of the simulator with panel removed to show its interior. In the diagram, the orange box is a viewing booth (85cm wide, 50cm tall, and 59cm deep) containing real backgrounds and adjustable LED lighting and the red diagonal plane is a half-silvered mirror (45cmx33cm, mounted at 50 degree angle with about 30% reflection and 70% transmission). The observer's field of view is shown as blue frusta: one coming directly from the orange box(the viewing booth); the other reflected by the dark red diagonal plane(half-silvered mirror) from an LCD display located near the observer's hip level (at a 56cm distance from the center of the mirror). Therefore, the half-silvered mirror mixes the light coming from the booth and the display. The picture at right shows both the display and the real background. However, a cover panel with a rectangular aperture was used in the experiments so that the observers would not directly see the display and only see the mixed light from the aperture. The observers could freely look into the aperture (no restriction was applied) which was 30cmx15cm. Using this simulator, the virtual patches (light coming from the display) were overlaid on the real, illuminated backgrounds (light coming from the booth).

4.3 Experiment setup

The LCD was a Dell P2715Q 27-inch 4K IPS display being addressed at Full-HD (1920x1080) resolution. The viewing booth light source was a THOUSLITE LED Cube with 11 channels, controlled with LED Navigator-LC V5.6.3 software for spectral tuning.

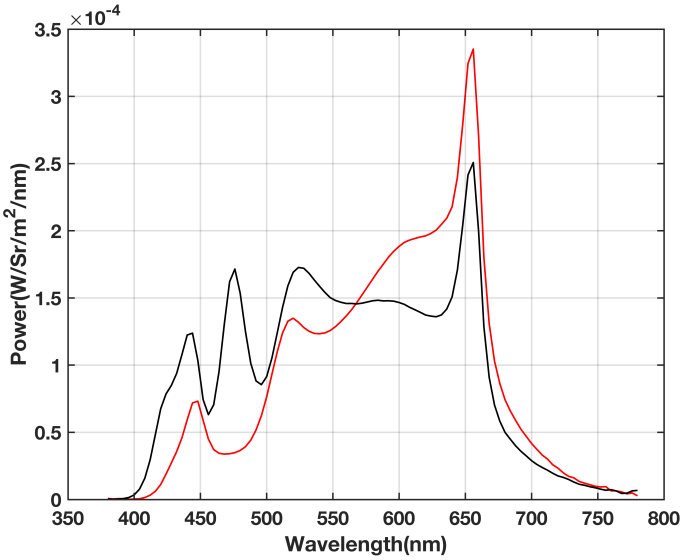

Fig. 4.2 – Spectral power distribution of the illuminants used in the experiments: 2788K (red) and 4334K (black)

All the measurements were done using a Photo Research PR655 spectroradiometer through the half-silvered mirror (from the observers point of view). Figure 4.2 shows the spectral power distributions of the two illuminants that were used in the experiment. Two broad band composite LED spectra were used, one with a correlated color temperature (CCT) of 2788K, referred to as warm light (red line in the plot), and one with a CCT of 4334K, referred to as cool light (black line in the plot). The warm light is similar to incandescent and warm LEDs used in residential applications, while the cool light is similar to light sources used more common in office applications. The illuminance of the light settings was measured from a perfect reflecting diffuser positioned on the bottom of the light booth through the half-silvered mirror. The measured luminance was 22.03 lx and 22.2 lx for the warm light and cool light respectively. The half-silvered mirror was also measured and it was not perfectly uniform over angle and spectrally flat; therefore, all the stimuli and illuminant measurements were done through the mirror to include the impact of the mirror.

The AR stimuli included combinations of virtual color patches and real printed background colors. Figure 4.3 left shows CIE 1976 u'v' chromaticity coordinates of the seven virtual color stimuli that were used in the experiment. The virtual stimuli were small 2D patches (about 4 visual degrees), which were measured on the display from the point of view of the observer (through the reflection of the virtual patches in the half-silvered mirror). Absorbent black felt was used as the background for these measurements. Figure 4.3 right shows a schematic view of the colors chosen for the foreground virtual stimuli. Please note that these colors are not the exact colors that were used in the measurements and are presented here only to better describe the design of the experiment.

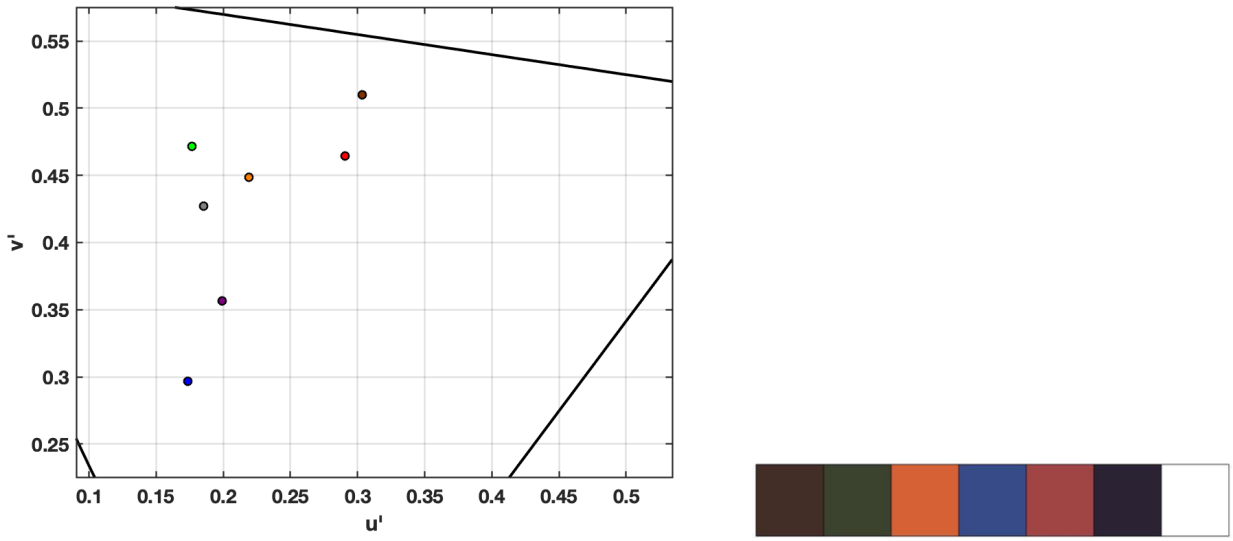

Fig. 4.3 – Left: CIE 1976 UCS plots of virtual color stimuli used in the experiments. Right: The foreground virtual stimuli. Note that the colors are not the exact colors used in the experiments.

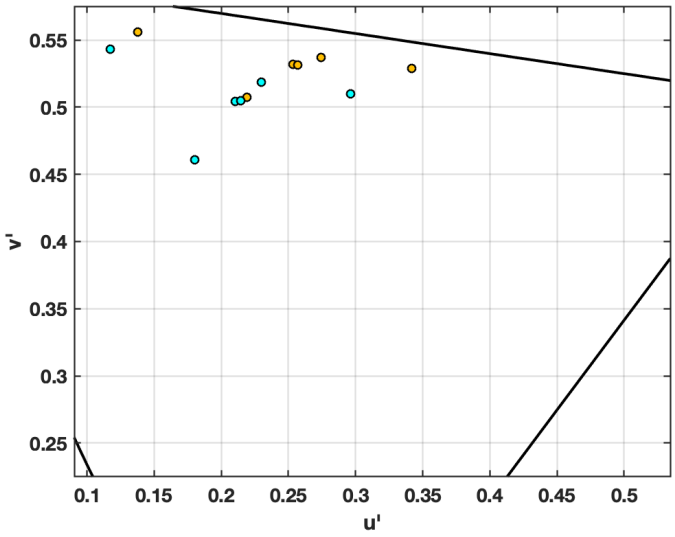

Fig. 4.4 – CIE 1976 UCS plots of illuminated real background colors used in the experiments. yellow circles: measured background colors under the warm light. Blue circles: measured background colors under the cool light. The diagonal lines in the figure are part of the spectrum locus in CIE u'v' color space.

Figure 4.4 shows the chromaticity coordinates of the real physical backgrounds illuminated by the two light sources. The backgrounds were inkjet-printed on paper (43cmx30cm)and then measured under the two light settings from the point of view of the observer (through the transmittance of the half-silvered mirror).

Each background size was about 9 visual degrees. In figure 4.4, yellow circles are the measurements of the background colors under the warm light and blue circles are the analogous measurements for the cool light.

Fig. 4.5 – The real background inside the viewing booth with no virtual foreground (the cool illuminant is on).

Figure 4.5 shows a photograph of the real printed background inside the viewing booth lit by the cool light. The backgrounds were named blue, gray and white (left column from top to bottom) and green, brown and red (right column from top to bottom) to refer to them easier later in the discussion section. The black column in the middle was added based on the requirements for the future psychophysical experiments. The choices for the color of the backgrounds and foregrounds were based on the common colors used in the environment and for virtual content (like blue sky or green grass).

4.4 Measurements results

As described above, the background and foreground stimuli were measured separately using a Photo Research PR655 spectroradiometer from the observer's point of view (through the half-silvered mirror). The virtual patches were then overlaid on the physical backgrounds using the AR simulator and the mixed colors were measured using the spectroradiometer. In the plots in Figure 4.6, the color circles represent the virtual patches (color coded for the virtual stimulus color), the light brown circles are the measured mixed colors and the black diamonds are the background colors. As we see, the mixed light converges towards the physical background color when mixed. This was expected from previous work by Gabbard et al.[Gabbard et al., 2010] (see Figure 3.11). It is clear that the amount of convergence is different for different mixes of virtual foreground colors and real background colors. The degree of convergence depends on the relative brightness of the background color and virtual patch: the maximum convergence happens for the white background (with the maximum lightness among all the backgrounds). Also, the purple virtual patch (the darkest foreground color) had the maximum shift towards the background color for all backgrounds while the white virtual patch (the lightest foreground color) had the minimum shift.

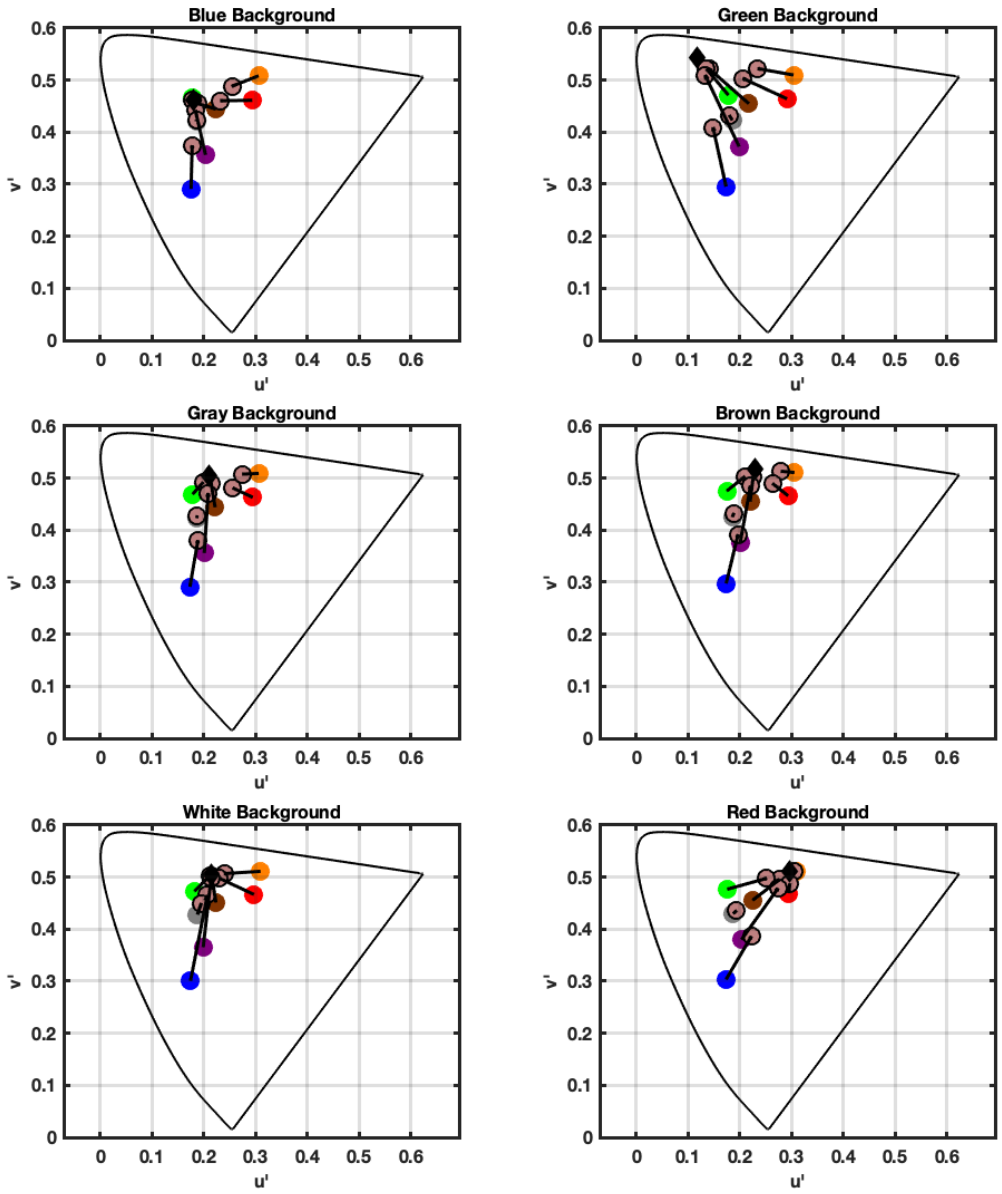

Fig. 4.6 – CIE 1976 UCS plots of physical measurements of the mixed colors under the cool light. Black diamonds depict the background color, light brown circles depict the mixed color and the color points depict the virtual patches and are color coded based on the virtual stimulus color.

Figure 4.7 shows the light measurements under the warm light. The same behavior is observed for measurements under this light as for measurements under the cool light. Again we see that the convergence rate depends on the brightness level of virtual color versus the background color. The brighter the background color, the higher the convergence rate and vice versa. Although the appearances are different under the warm light, convergence rates follow similar behavior for both illuminants for all the mixes.

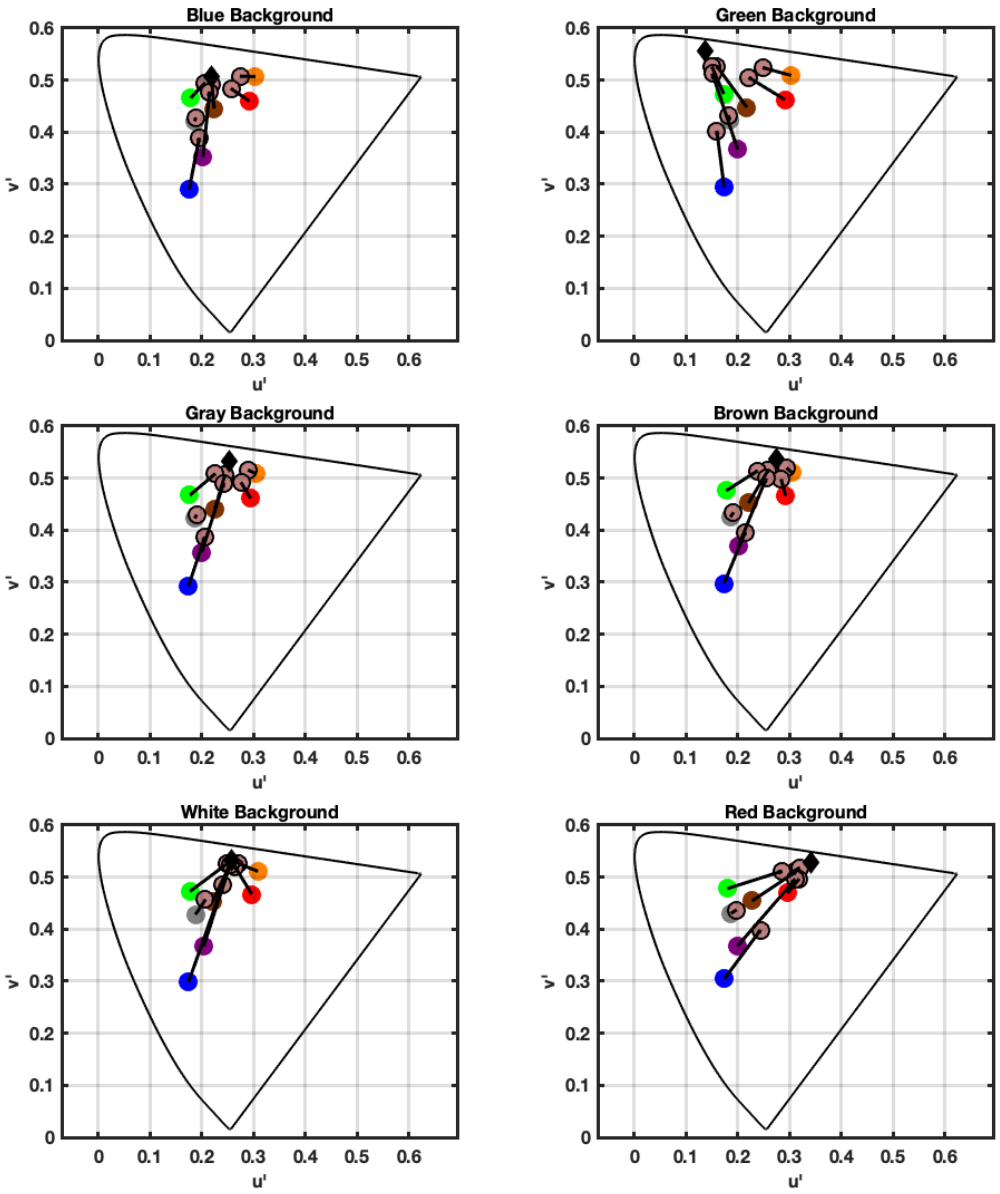

Fig. 4.7 – CIE 1976 UCS plots of physical measurements of the mixed colors under the warm light. Black diamonds depict the background color, light brown circles depict the mixed color and the color points depict the virtual patches and are color coded based on the virtual stimulus color.

4.5 Summary

AR environment is a mix of transparent objects (virtual content) and reflective objects(real surrounding). To understand the light behavior in AR environment and as a requirement for future experiments, analysis and modeling, color measurements were performed in AR. For this purpose, a prototype device was built to simulate AR environment in an accurate and controllable way. This AR simulator was simply designed using a

display, a light booth and a half silvered mirror. The half silvered mirror combines the light coming from the booth and the display and simulates an AR environment.

A set of colors were chosen as physical background colors, which were printed and put inside the light booth. In addition, a series of colors were also chosen for the virtual content colors. These colors were chosen based on similarity to colors previously chosen by [Gabbard et al., 2010] and also by having common applications. The measurements were done using a Photo Research PR655 spectrophotometer. All the measurements were taken through the half silvered mirror (from the observer's point of view). The virtual colors were measure with the lights off and a black felt covering the physical backgrounds while the backgrounds and the mix of virtual and background colors were measured under two lights, a warm and a cool light. These two lights were broad band LEDs.

The results showed that, as expected from [Gabbard et al., 2010] and [D'Zmura et al., 1997], when the virtual and physical colors are mixed, the mix color is a convergence of the virtual color towards the background color. The convergence rate is different depending on the background and virtual color. When the background is brighter, higher convergences rates are obtained while for brighter virtual colors, the convergence rate is smaller.

In this chapter, the physics of light and color in AR was studied. In order to understand and model color perception in AR environment, color perception in AR should also be studied. The next chapter discusses further research on color perception in AR.

5 AR Color Matching with Simple Stimuli

5.1 Motivation

In order to understand color perception in AR, a psychophysical experiment was designed. This experiment was designed to study impacts of color of physical background, virtual foreground and lighting on the mix color perception in AR, building on the physical measurements described in the previous chapter. For this experiment, the stimulus design was tried to be very simple; only 2 dimensional solid color patches were used both as physical background and virtual foreground stimuli. This was done because only the impact of color was being studied and the effect of complexity was not investigated. CAM16 color appearance model [Li et al., 2017a] was used to see if color appearance in AR can be predicted by available color appearance models for the physical objects. For this purpose, the physical measurements of the stimuli and lightings were used as inputs to CAM16. The results of the matches by the observers were then compared to predictions by CAM16 to evaluate the predictions.

5.2 Methodology

A psychophysical color matching experiment was designed to study color perception in AR. In this step, very simple combinations in AR environment were studied when there are 2D virtual color patches overlaid on top of physical 2D color patches (backgrounds). The background and virtual patch colors were the same as the colors that were measured in chapter 4 ; Also, the same light settings were used. The color backgrounds were designed to be printed on a paper while having a black column in the middle so there would be a black background patch next to each color background patch. Figure 5.1 shows this design. A graphical user interface (GUI) was designed in MATLAB to run the color matching experiment in the AR simulator.

For each stimulus presentation, a pair of virtual patches were presented with one patch overlaid on a randomly chosen color background and another patch overlaid on the black background adjacent to the chosen color background (depicted in Figure 5.1). As the display-mirror combination exhibited angular dependence (meaning, the measurements were different for top, middle and bottom of the display), three different display

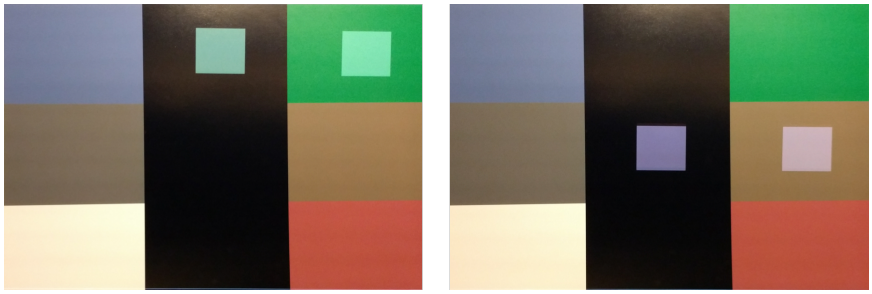

Fig. 5.1 – Two examples of mixed virtual patches overlaid on top of the physical backgrounds in the first color matching experiment. The backgrounds include the six large patches (plotted in Fig 4.4) and black, and the virtual foregrounds are selected from the seven colors plotted in Fig 4.3

characterization models were made for top, middle and bottom parts of the display to make sure the 2D virtual patches were presented with consistent color throughout the display.

The foreground pair of the stimuli were presented at the same depth as the background, therefore, there was no depth difference between the background and foreground patches from the observer's point of view. For each observer, all virtual patches were presented overlaid on all physical backgrounds inside the light booth in random order, which resulted in 42 pairs. The experiment was performed in two sessions, each with the same protocol but differing in the illuminant that was used. Each session included 42 pairs and lasted about 45 minutes and the order of the sessions was randomly chosen for each observer. Observers were about 30 inches away from the half-silvered mirror while the printed physical background (inside the light booth) had a distance of 30 inches from the mirror and the display's distance from the mirror was about 30 inches . The display's specifications were mentioned in Chapter 4. The observers were asked to "adjust the color of the small patch on black to match it to the other small patch". They were given a small keypad (presented in Figure 5.2)with which they could adjust the lightness (left two yellow keys), chroma (middle two yellow keys) and hue (right two yellow keys) of the virtual patch on black background. The steps were 1 unit in terms of hue, saturation or chroma independently (regarding the key pressed). When they were happy with their match, they would press enter (large yellow key in Figure 5.2) and go to the next pair. The starting foreground color was the same for the black and color background and the observers could modify the patch on black.

A total of 21 observers (7 females/14 males, ages range 22-50 years) participated in the first experiment. Participants were screened for deficient color vision using Ishihara color blindness test (24 plates editions) [Ishihara, 1917]. All observers had normal color vision except for one female observer whose data was excluded from the results. The basic hypothesis of the experiment, based on extensive piloting and observations by the authors, was that the visual match between the two patches would be different than a physical match.

Fig. 5.2 – The keyboard that observers used to modify the test color in the color matching experiment

5.3 Results and discussion

Observers' matching results were compared directly with measured mix color appearance obtained using the CAM16 color appearance model. In these calculations, we used tristimulus values of the measured mixed stimuli through the half-silvered mirror as the input to a color appearance model. In CAM16 calculations, the surrounding was set to "dim"(F=0.9, c=0.59, Nc=0.9) with y_w set to 100 and y_b set to 20. Therefore, the adapting luminance (L_a) was set to be 20% of the white point's brightness.

Since the AR simulator has an optical see-through design, the virtual content appears as transparent in front of the real opaque background. Although there has been a lot of work on transparency, there is no color appearance model for transparent stimuli. Therefore, we should choose from the reflective color appearance

models. There were many options for color appearance models for reflective objects to choose from for predicting color appearance in AR. CIELAB is a simple color appearance model and easy to use [CIE, 1986], however, it is not an adequate color appearance model for AR. It does not cover the complexities that are involved in AR environment. Hunt's model [Hunt, 1991] is the most comprehensive color appearance model. However, it is very difficult to use and it is not reversible. Therefore, it would be better to find a color appearance model that is easier to use and is practical (even with modifying it for AR purposes). CIECAM02 is a comprehensive color appearance model and yet not very complex to implement and it is reversible. However, there has been reports of cases that CIECAM02 has some problems in predicting the appearance (especially cross media color calculations) [Li et al., 2017b]. CAM16 is a color appearance model that addresses these problems and has a better performance than CIECAM02. CAM16 allows for incomplete chromatic adaptation and having different adapting surrounds such as dark, dim or average. However, CAM16 has its own deficiencies too; it assumes the background is neutral, which ignores chromatic simultaneous contrast effects.

The viewing condition was considered "dim surround" and the adapting white point was the average of tristimulus values of the white background color under the designated lighting and the white color of the display (both measured through the half-silvered mirror). This white point was chosen because some of the mixed colors appear to be brighter than the white background, and the display is much bluer than the illuminated white background, which results in the white background patch appearing yellowish to the observer even when fully adapted (especially for the session with the warm light on).

Figure 5.3 shows the color matches by the observers for each virtual patch color and background color mixes under the cool light in CAM16 UCS Jab color space (similar in structure to CIELAB). Each plot represents a different background, which is shown as a black diamond in the plots. The small colored diamonds are individual matches, and the large colored diamonds are the average match for all the observers. The colored circles are the color appearance predicted by the CAM16 color appearance model based on the mixed stimuli measured through the half-silvered mirror. The diamonds and circles are color coded for the virtual patch color they represent. From the plots, we see that the CAM16 predictions are not at the average observer match and in some cases they are even outside of the cloud of the matches.The mismatch of CAM16 calculated color appearances with the average match by the observers means the matches by the observers were not colorimetric matches. Also, all the predictions by the model are closer to the background color (black diamond) than the matches by the observers. Not visible in the plots, all the predictions were lighter (higher in lightness J) than the average match by the observers. This difference was similar in magnitude to the a-b difference between the average matches and the predictions. For the white and green backgrounds, the predictions appear worst, and also, we see that observer agreement is poor, with large clouds of observer matches around the average match. The variance in observer matches was even larger in J (lightness) direction for all backgrounds. From the plots, it is visible that there is a shift in appearance for the matches by the observers

(from the colorimetric match). This is assumed to be due to a chromatic simultaneous contrast regarding the color backgrounds used in the experiment.

Figure 5.4 shows the comparison between the observers matches and predictions by CAM16 under the warm light. The same color coding and symbols are used here as they were used in Figure 5.3. Figure 5.4 shows similar trends as Figure 5.3. Similar behavior was also obtained in lightness for the results under the warm light. This was expected from the similar behavior in the measurements that were discussed in Chapter 4. Again, all the predictions were higher in lightness than the average matches by the observers and the observer match variance was larger for lightness. From figures 5.3 and 5.4 it is clear that the observer matches are further away from the background than predicted by CAM16. One possibility is that the observers ignored the background colors to some degree and interpreted the virtual patch color more independently and as an overlay. Another possibility is that, due to chromatic simultaneous contrast effects, the matches have not converged towards the background color as much as CAM16 predicts. Based on this second possibility, CAM16 was modified to account for chromatic simultaneous contrast, as described below.

CAM16 improvement

Simultaneous contrast is the effect of surround color on the appearance of a center color. The color of the background shifts the appearance of the foreground towards the complement of the background color. In our experiment, we use chromatic backgrounds while in CAM16 color appearance model the background is assumed to be neutral. Because the results above show prediction errors in the direction of the background color, the effect of chromatic simultaneous contrast was added in calculating the predictions of the appearance of mixed colors. For this purpose, first a simple classic method of calculating simultaneous contrast was used. This approach was used as it is very simpler to implement than other methods suggested in the literature. In this approach, only the color of the background is considered to impact the simultaneous contrast. The first approach was to use the equations suggested by Hunt for calculating simultaneous contrast [Hunt, 1991]. However, this resulted in minor to no improvement in results. Therefore, another simple approach was developed with similar concepts. For each mix, the adaptation white point was modified based on the color of the background. To achieve this, the chromaticity of the white point was adjusted by adding the chromaticity of the background; This was a weighted average as shown below:

$$NewWP = CW * BackgroundColor + (1 - CW) * OldWP \tag{5.1}$$

In Equation 5.1, NewWP is the modified white point for predictions over each color background, CW is a free parameter, the weighting constant of the color background chromaticity, BackgroundColor is the chromaticity of the color background and OldWP is the unmodified white point. The luminance of the white point was kept unchanged and only the chromaticity of the white point was adjusted. As there was some flare on the black background (due to the impact of the illuminant), the same calculation was done for mixes on black backgrounds as well. The optimum CW (resulting in the smallest Euclidean difference between the predictions and the average match) was found to be 0.2 for all color backgrounds and 0.1 for black backgrounds for both illuminants. The same approach was taken for adding the impact of black background for the matches by the observers as mentioned before (this was done as the black background was not perfectly neutral). The weighting constant was set to 0.1 for black background for both illuminants.

Figure 5.5 shows the observers' perception and perceptual predictions of the mixed colors under the cool light after including the effect of chromatic simultaneous contrast, which can be compared with Figure 5.3. We see that although adding the effect of simultaneous contrast has brought the predictions closer to the average matches, it does not have a very noticeable impact in each case and in some cases, there seem to be no differences. In terms of lightness, again similar improvements were obtained but the impact was not very large for each case.

The same trend can be seen for plots for the warm illuminant. From Figure 5.6, which can be compared with Figure 5.4, we see that adding the simultaneous contrast calculations does not have a big impact. However, now the predictions (for both illuminants) are within the cloud of observer matches yet not exactly at the average.

Figure 5.7 shows the Euclidean color differences between the predictions and the average observer matches of mixed colors in CAM16 UCS color space before and after including the effect of chromatic simultaneous contrast. The boxes show the median and 25%-75% of the distances for colors under the warm light while the black boxes depict the same for the mixes under the cool light. The blue boxes represent the same difference when the effect of the simultaneous contrast is added. We see that by adding the effect of simultaneous contrast, the error of prediction consistently decreases, however some error persists. We conclude that including the effect of simultaneous contrast in this way makes the predictions a little more similar to what observers perceived, but there is room for improvement. To evaluate the intra-observer agreements on the matches, the mean color difference from the mean (MCDM) values were calculated for all the foreground-background combinations.

$$MCDM = \frac{\sum_{i=1}^{N} \Delta E^*_{jabi}}{n} \tag{5.2}$$

$$\Delta E^*_{jabi} = \sqrt{(j_i - j_{mean})^2 + (a_i - a_{mean})^2 + (b_i - b_{mean})^2} \tag{5.3}$$

Equations 5.2 and 5.3 show the calculation of MCDM. In Equation 5.2 and 5.3, MCDM is calculated for each background foreground combination and the terms j_{mean} ,a_{mean} , and b_{mean} represent the average J, a and b for each background-foreground combination. In table 5.1, the MCDM values for the results of the experiments with the cool and warm light are presented.

Tab. 5.1 – Mean Color Difference from the Mean (MCDM) values for the color matches by the observers.

Background	Foreground	$MCDM_{Cool}$	$MCDM_{Warm}$	Background	Foreground	$MCDM_{Cool}$	$MCDM_{Warm}$
Green	Brown	7.67	9.22	Gray	Brown	5.67	5.85
	Green	6.56	6.63		Green	4.33	5.65
	Orange	7.77	7.16		Orange	2.97	3.46
	Blue	7.65	6.51		Blue	5.29	4.82
	Red	7.19	7.42		Red	4.57	4.55
	Purple	11.46	9.11		Purple	9.16	6.65
	White	5.11	3.51		White	6.07	3.94
Blue	Brown	6.31	8.92	Red	Brown	8.11	7.75
	Green	5.70	5.17		Green	10.42	6.56
	Orange	5.49	5.56		Orange	3.47	3.51
	Blue	7.44	6.03		Blue	8.37	6.30
	Red	5.44	4.42		Red	3.89	3.62
	Purple	6.28	6.79		Purple	8.13	7.92
	White	7.55	2.45		White	6.17	6.14
Brown	Brown	7.22	6.40	White	Brown	21.75	23.64
	Green	5.76	6.08		Green	21.08	20.28
	Orange	4.35	4.77		Orange	9.78	9.19
	Blue	6.43	6.22		Blue	13.42	14.97
	Red	5.17	4.59		Red	12.87	9.93
	Purple	9.79	8.86		Purple	25.93	23.39
	White	4.16	4.89		White	8.69	8.51

From Table 5.2, it is clear that the maximum MCDM values are for the mix colors on the white background (with highest MCDM values for both lights) and the brown and purple foreground colors (the darkest foreground colors). This can be because the mix color got washed out by the background color (either with a very light background or very dark foreground) and judging the mix color appearance was difficult for the observers. Note that the MCDM ranges are similar to Euclidian distance ranges between the prediction and the average match by the observers (see Figure 5.7).

Analysis of Variance (ANOVA) was conducted on the dataset (including both light sessions and using predictions with and without the simultaneous contrast). The variable was set to be the Euclidean difference between the prediction and average matched colors. The groups were background color, foreground color, lights and the model (with or without the simultaneous contrast added). Table 5.2 shows the results of the ANOVA.

Tab. 5.2 – Analysis of Variance (ANOVA) table for the color matching data.

Source	Sum Sq.	d.f.	Mean Sq.	F	Prob>F (p)
Model	93.62	1	93.615	21.51	$7.47481e^{-06}$
Lights	203.01	1	203.008	46.64	$1.85579e^{-10}$
Backgrounds	2549.5	5	509.9	117.15	$1.22204e^{-50}$
Foregrounds	1884.73	6	314.122	72.17	$3.03377e^{-42}$
Error	670.31	154	4.353		
Total	5401.17	167			

As seen from Table 5.2 the results of the ANOVA showed p values smaller than 0.001 for all groups meaning that all groups have different distribution regarding the match-prediction difference. This means that the Euclidean difference between the average matched and predicted color is statistically significantly impact by these groups; therefore, from this and the results presented in Figure 5.7, we can conclude that adding the simultaneous contrast improves the overall predictions significantly. This means that although the improvements for each pair looks small, the overall improvements for the predictions was statistically significant.

5.4 Summary

In this chapter a psychophysical color matching experiment was designed and performed. This experiment was designed to study the impacts of background color, foreground color and lighting on mix color perception in AR. All the background and foreground stimuli were designed to be simple 2D solid color patches, this was done to exclude any other factors and only study the impact of background color, foreground color and lighting. Twenty one observers with normal color vision participated in the experiment. The results of the experiment were then compared with predictions from CAM16. The measurements of the stimuli and the lighting (as done in Chapter 4) were used as input to CAM16 to achieve color perception predictions. The comparisons showed that the CAM16 predictions are not accurate and that CAM16 over-predicts the convergences. The mismatch of CAM16 calculated color appearances with the average match by the observers means the matches by the observers were not colorimetric matches. To improve the predictions by CAM16, the impact of chromatic simultaneous contrast was added to the model. The results showed that although the modification made the overall predictions improved (statistically significant improvement), the improvements for each mix was very small.

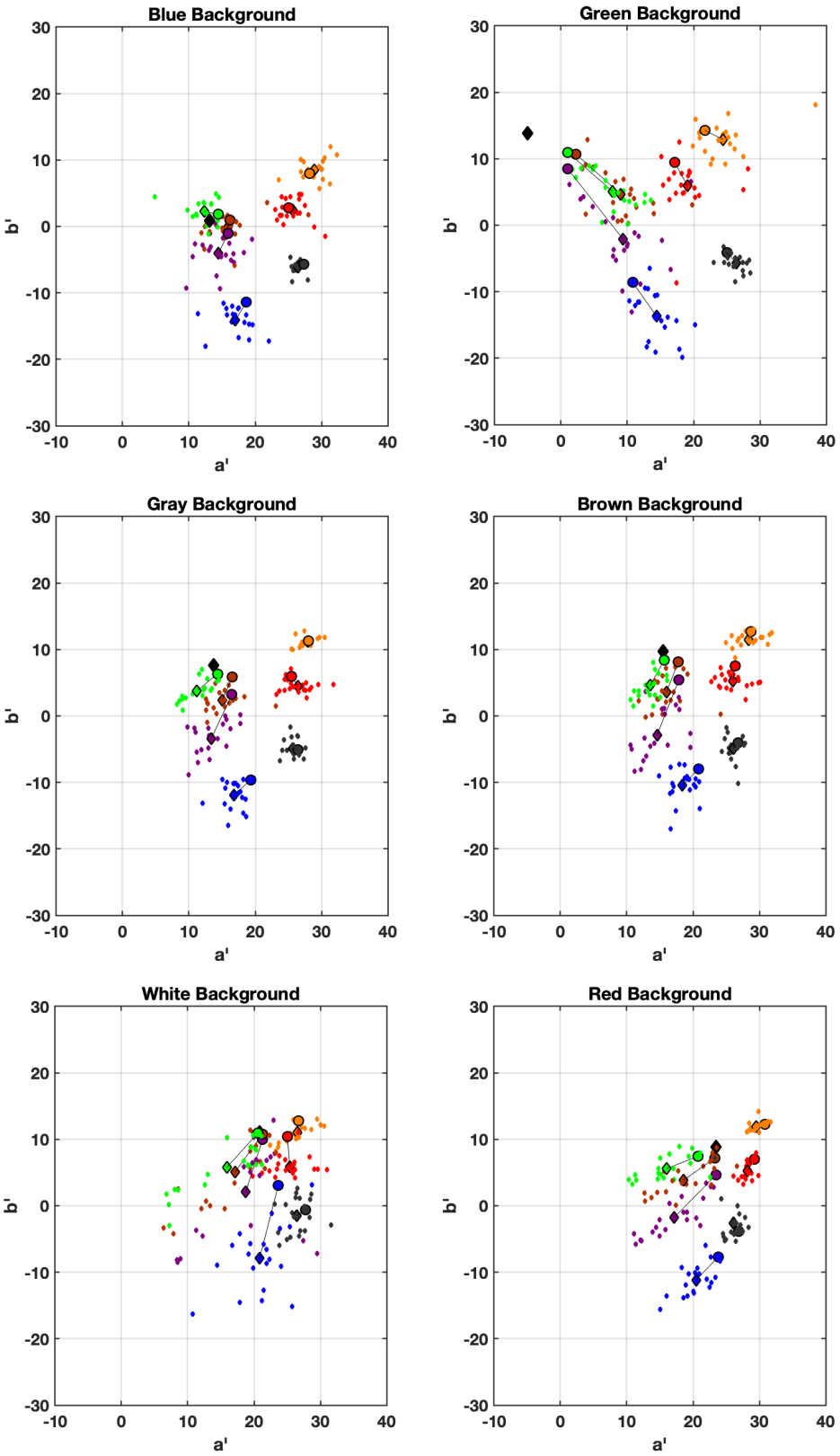

Fig. 5.3 – CAM16 UCS plots of observers' perception and perceptual predictions of the mixed colors by CAM16 under the cool light. The points are color coded for the virtual stimulus color. Small diamonds represent color matches by the observers while the big diamonds are the average of the matches. The black diamond is the color of the background and the circles depict predictions by CAM16.

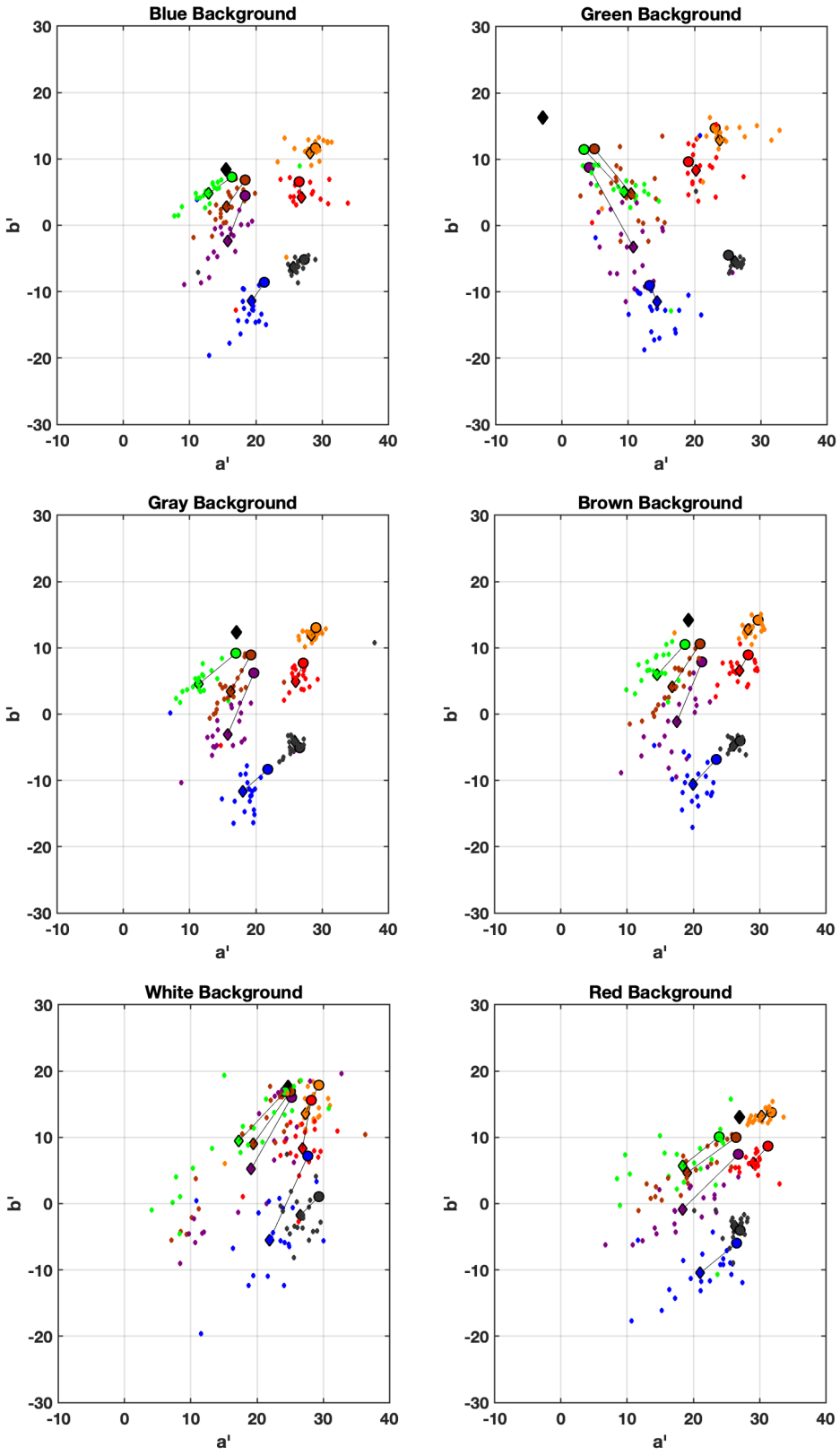

Fig. 5.4 – CAM16 UCS plots of observers' perception and perceptual predictions of the mixed colors by CAM16 under the warm light. The points are color coded for the virtual stimulus color. Small diamonds represent the color matches by the observers while the big diamonds are the average of the matches. The black diamond is the color of the background and the circles depict predictions by CAM16.

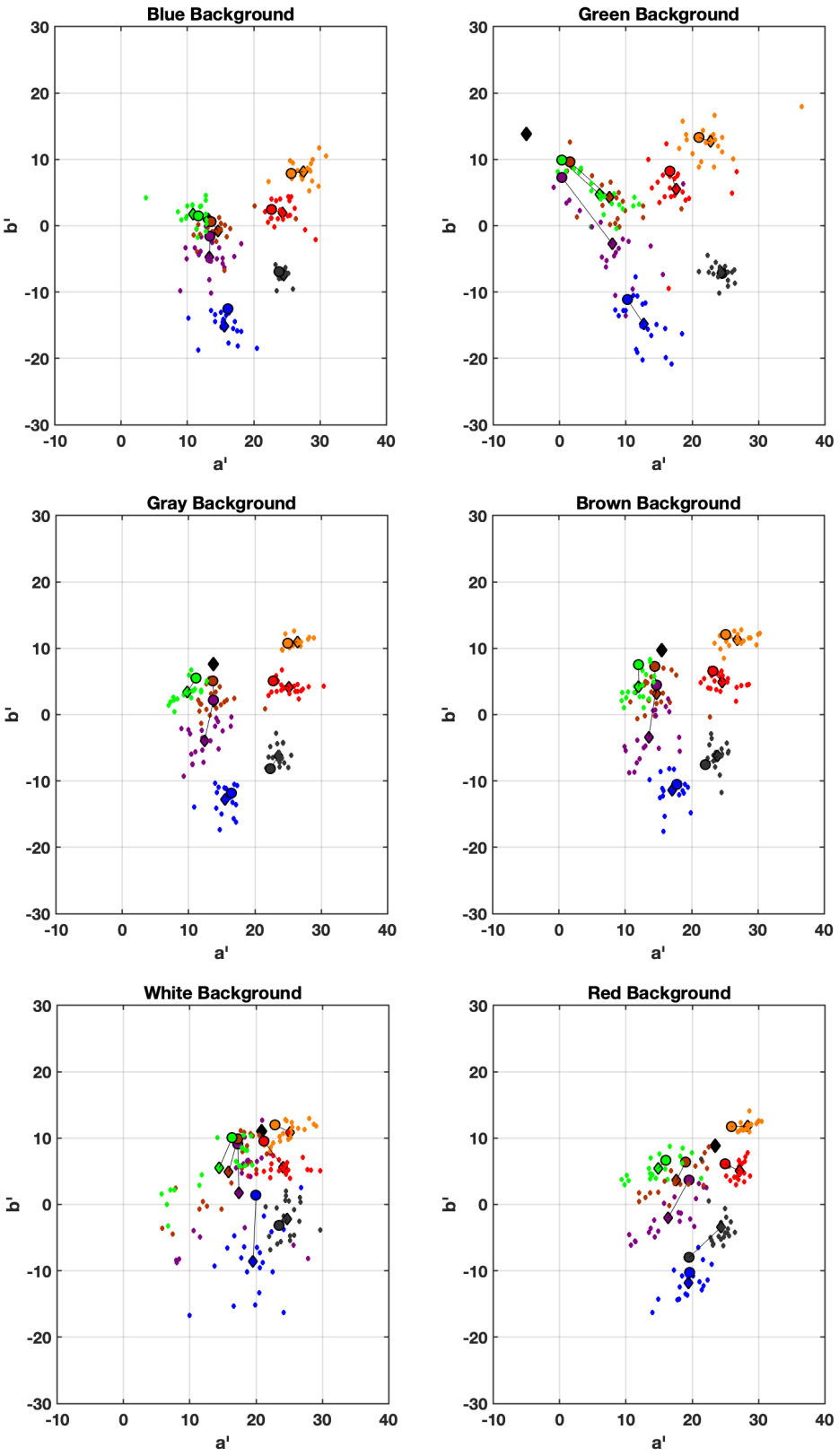

Fig. 5.5 – CAM16 UCS plots showing predictions by CAM16 (circles), including the effect of chromatic simultaneous contrast to perceptual predictions of the mixed colors under the cool light. Small diamonds represent the color matches by the observers while the big diamonds are the average of the matches. The black diamond is the color of the background. The points are color coded for the virtual stimulus color. Similar improvements were also obtained in the lightness direction.

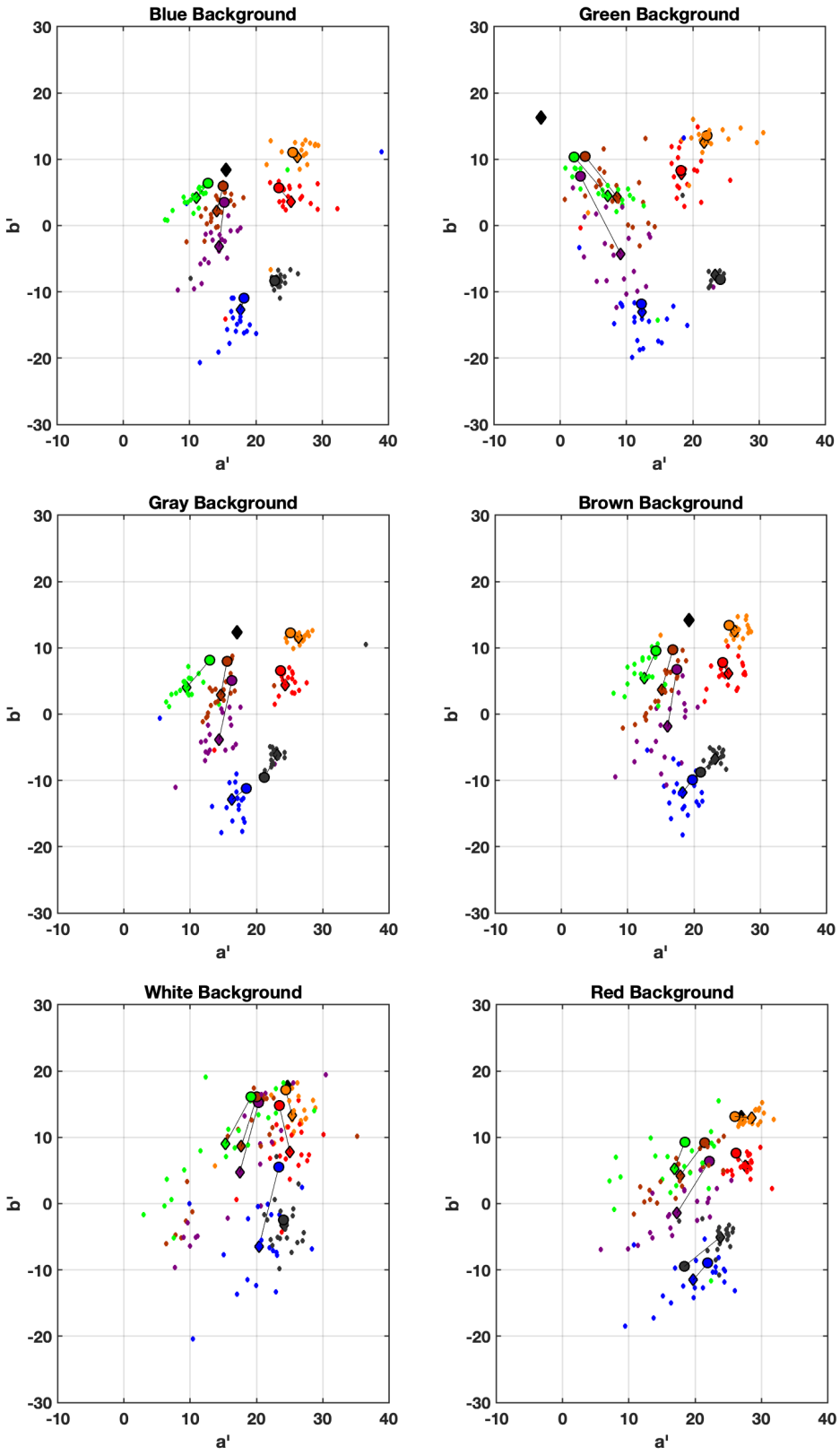

Fig. 5.6 – CAM16 UCS plots showing predictions by CAM16 (circles), including the effect of chromatic simultaneous contrast to perceptual predictions of the mixed colors under the warm light. Small diamonds represent the color matches by the observers while the big diamonds are the average of the matches. The black diamond is the color of the background. The points are color coded for the virtual stimulus color. Similar improvements were also obtained in the lightness direction.

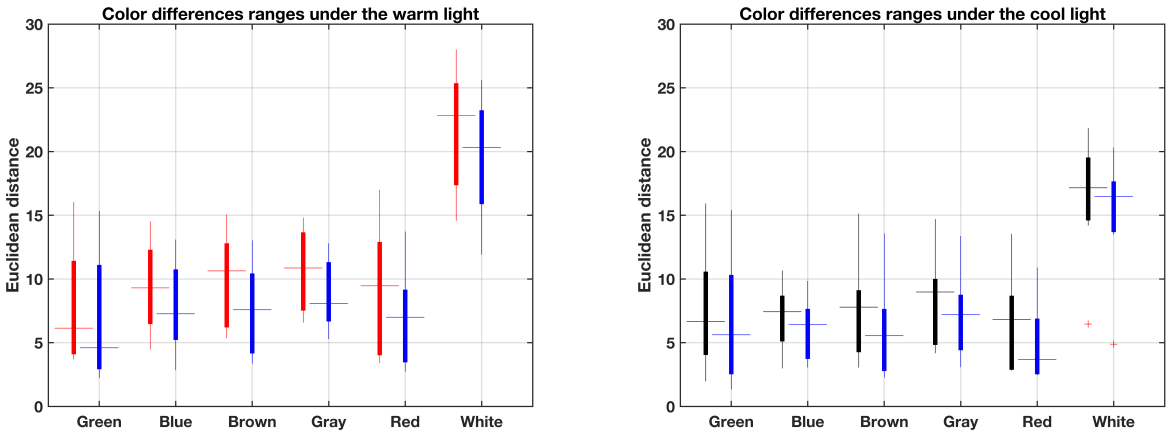

Fig. 5.7 – Color differences in CAM16 UCS color space between the prediction and observer matches of color mixes before and after including the chromatic simultaneous contrast effect. For each background color (labeled axis), solid boxes indicate the 25th to 75th percentiles, with median shown as a horizontal line across the box and vertical whiskers extending to the min and max values over all virtual overlays. The red boxes depict the data for the warm light, the black boxes represent the data for cool light, and the blue boxes show the corresponding data but with the effect of simultaneous contrast added.

6 Color Matching on a Display

6.1 Motivation

In this chapter a color matching psychophysical experiment similar to the previous experiment is discussed. The only difference was that the experiment was performed on a single display instead of the AR simulator and therefore, there was no optical overlaying. This experiment was designed and performed to compare color perception in AR to color perception from a regular display. The results of this experiment were compared to the ones from previous experiment to evaluate the similarity or dissimilarities.

6.2 Methods

A LCD-Dell UP2414QT 24-inch display being addressed at full (3840 x 2160) resolution was used to run the experiment. The same design and color of backgrounds and foregrounds that were used in the previous color matching experiment (Chapter 5) were also used in this experiment. To achieve this, measurements from the background and foreground colors were made from the point of view of the observer (through the half-silvered mirror) and the display was characterized. Using the display color model, the colors were reproduced on the display. To have similar appearances for both experiments, the color of the mixes of foreground and background in the AR color matching experiment (measured from the point of view of the observer) was used as foreground colors for the stimuli on the color backgrounds in this experiment (see Figure 6.1). Similarly, the size of the foreground and background stimuli were about 4 and ten visual degrees. As the impact of illuminant was minimal in previous experiment for the two illuminants used, in this experiment only one session (using the appearances under the cool light) was performed. The white point of the display was set to be similar to the white point used in the previous experiment for the cool light, only scaled up in luminance by a factor of 7 to use the native luminance range of the display.

MATLAB was used to design the graphical user interface for the experiment. Figure 6.1 shows the graphical user interface for the display color matching experiment. The experiment was performed in a dark room and observers sat at about 30 inch distance from the display during the experiment. They used a small keypad to

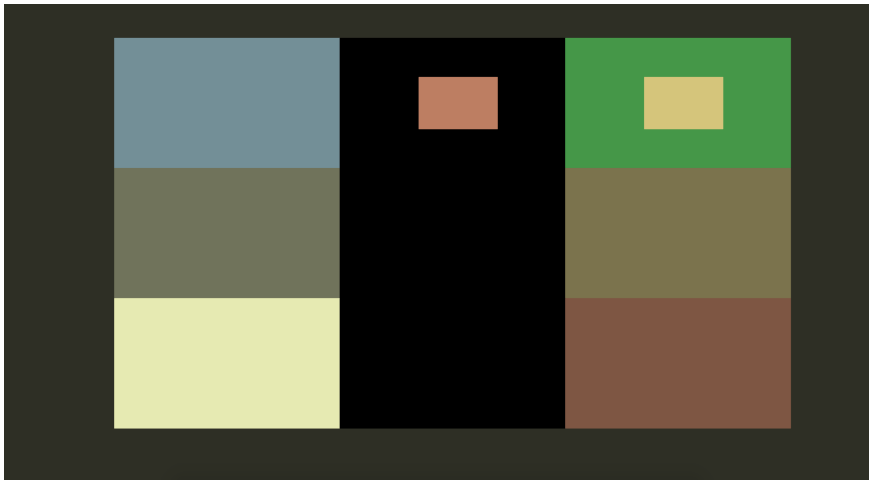

Fig. 6.1 – The graphical user interface (GUI) of the color matching experiment on a display.

adjust the test patch on black in terms of hue, chroma and lightness to match it to the color of the small patch on the color background. Twenty-six observers (14 female 12 male ages range from 20-61) participated in the display color matching experiment. All the participants were screened for color deficiencies using Ishihara color blindness test (24 plates edition) [Ishihara, 1917] and all participants had normal color vision.

6.3 Results and discussion

Figure 6.2 shows the scatter plots of the display color matching experiment results of the observers' matches. In Figure 6.2, the small color squares depict each observer's match, big diamonds depict the average match for all the observers, circles are predictions by the CAM16 color appearance model and black diamonds are the color of the background. The colored circles and diamonds are color coded based on the color of the foreground. From figure 6.2 we see that the results look different from the AR color matching experiment results in terms of variance and average. We also see that the color appearance predictions by CAM16 are even less accurate for the display color matching experiment, especially in case of the white and gray backgrounds. The differences between the predictions and the average match by the observers however, were smaller in the lightness direction. Again these inaccuracies by CAM16 is expected because CAM16 does not predict the impact of chromatic simultaneous contrast.

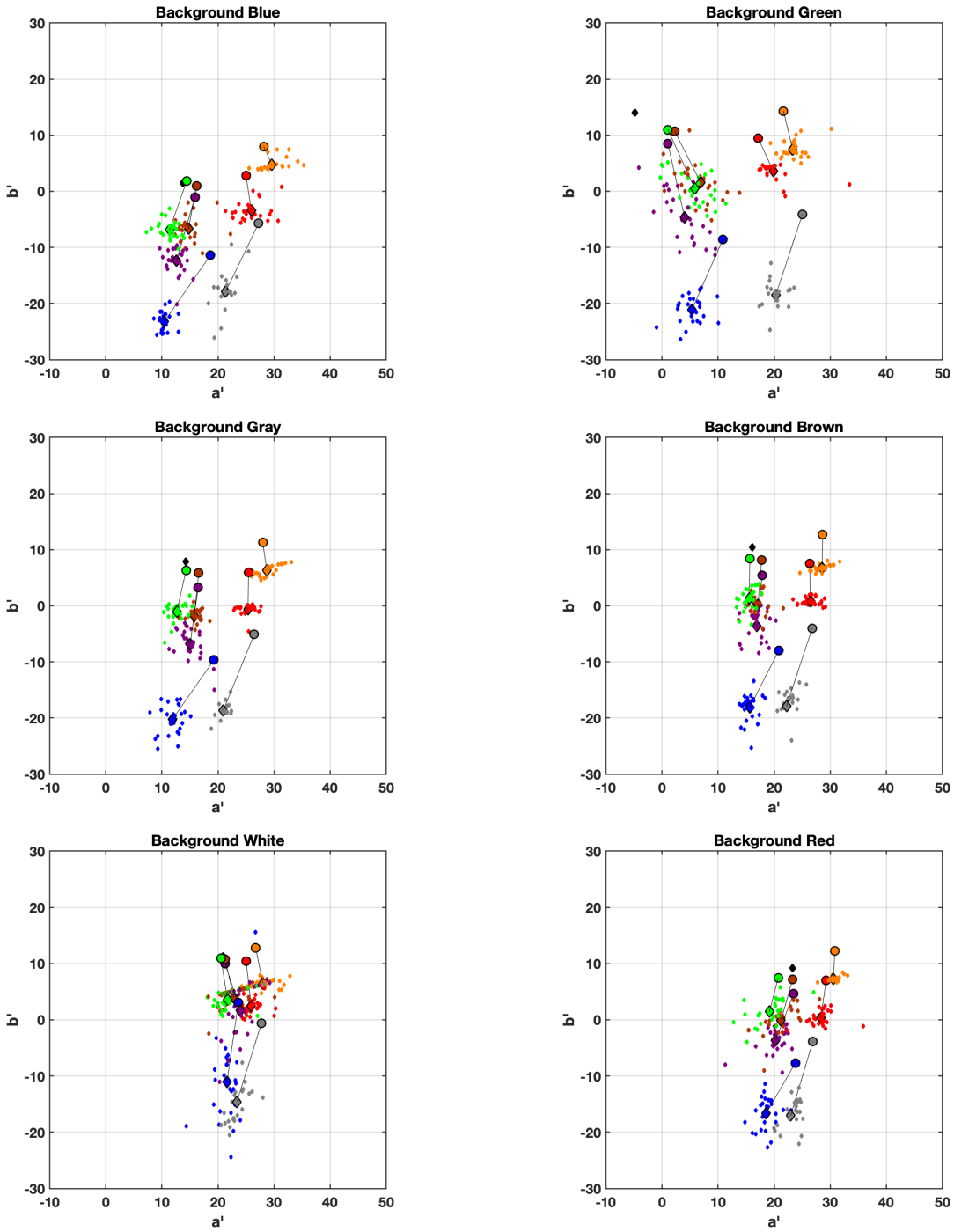

Fig. 6.2 – Scatter plots of the results of the matched color for the display color matching experiment. Small diamonds represent the color matches by the observers while the big diamonds are the average of the matches (color coded for the virtual stimulus foreground color. The black diamonds are the color of the background.

6.4 Cross-Experiment Comparison

Figure 6.3 shows the average match for the results of the two experiments. The points are color coded based on the color of the virtual stimulus. In figure 6.3, triangles represent the average matches from the

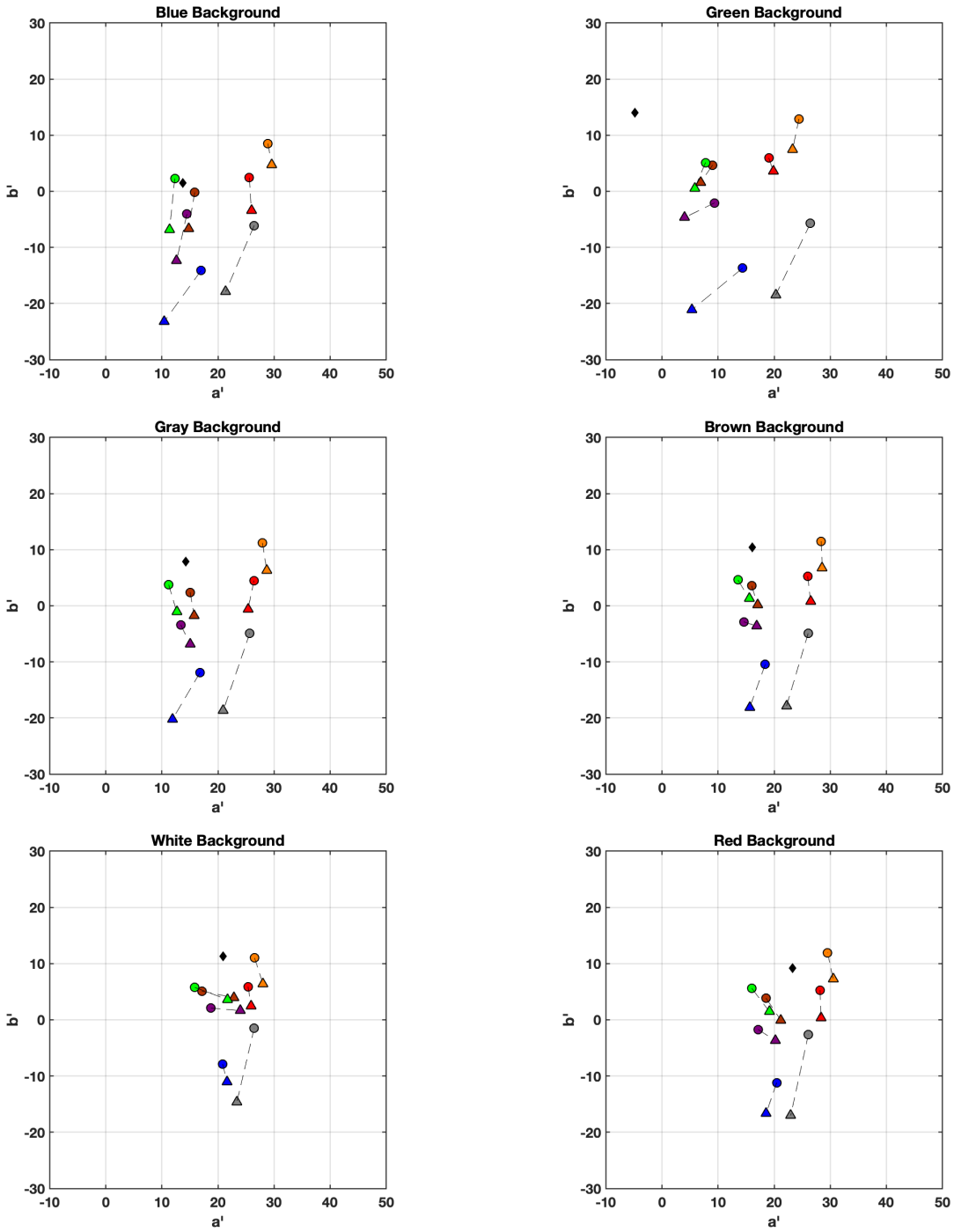

Fig. 6.3 – Scatter plots of the results of the average matched color for the AR (color circles) and display (color triangles) color matching experiment in CAM16 UCS space. All the spots are color coded based on the color of the foreground. The black diamond is the color of the background.

display color matching experiment while circles represent the average matches from the AR color matching experiment (discussed in Chapter5). From figure 6.3 we see that the results from the two experiments are

different. However, to confirm if the difference between the two populations is statistically significant, we need to do some population comparison statistical tests. First, Box's M statistic [Bajorski, 2011] was used to determine the variance-covariance similarities for the two populations (the results from the AR and display color matching experiments for each background-foreground combination). The populations were defined as color matches by the observers for each background-foreground combination for the AR and the display color matching experiment. Therefore, 42 populations for each experiment was defined and each were compared for the two experiments. For example, the matches for the blue foreground on the green background for the AR color matching experiment (by 20 observers) were compared to the matches for the blue foreground on the green background for the second experiment (by 26 observers). The M statistic was then compared against the threshold point (C with = 0.05) to decide upon the null hypothesis (the variance-covariance matrices for the two experiments being equal). Table 6.1 shows the results of the Box's M test.

Tab. 6.1 – The results of the Box's M test for each background-foreground combination.

Background	Foreground	Box's M Test	Background	Foreground	Box's M Test
Green	Brown	*	Blue	Brown	*
	Green			Green	
	Orange	*		Orange	
	Blue	*		Blue	*
	Red	*		Red	
	Purple			Purple	*
	White			White	*
Brown	Brown	*	Gray	Brown	*
	Green	*		Green	
	Orange	*		Orange	
	Blue	*		Blue	
	Red			Red	*
	Purple	*		Purple	*
	White	*		White	*
Red	Brown		White	Brown	*
	Green	*		Green	*
	Orange	*		Orange	*
	Blue	*		Blue	
	Red	*		Red	*
	Purple			Purple	
	White	*		White	*

In table 6.1, asterix sign represents rejected status of the null hypothesis (variance-covariance of the populations being similar). From table 6.1 we see that the null hypothesis is rejected for most of the combinations meaning in most background-foreground combinations, the results from the two experiments were statistically different. Based on the results of the Box's M test, a method of T2 test was used to compare the averages for the two populations [Bajorski, 2011].

The null hypothesis for the averages of the two experiments (being equal), was rejected when the result of the T2 test was greater than the threshold value (taken from the chi-square distribution with α= 0.05). The null hypothesis was rejected for all cases. This means that all the differences between the average matches for the two experiment were statistically significant for all background-foreground combinations. From looking at the data, all matches for the color matching experiment on the display resulted on bluer (lower b values) and in most cases lighter (higher J value) colors than the results from color matching in AR simulator. Therefore, the difference between the two perceptions is most probably a difference in adaptation state.

The mean color difference from the mean (MCDM) was also calculated for the results from the display color matching experiment. The calculations were done in Jab space (see Equations 5.2 and 5.3). Table 6.2 shows these results for all the background-foreground combinations.

Tab. 6.2 – Mean Color Difference from the Mean (MCDM) results for color matching experiment on a display

Background	Foreground	MCDM	Background	Foreground	MCDM
Green	Brown	6.73	Gray	Brown	3.73
	Green	4.18		Green	6.73
	Orange	4.67		Orange	5.03
	Blue	5.00		Blue	5.78
	Red	3.56		Red	5.55
	Purple	6.22		Purple	7.53
	White	2.49		White	5.17
Blue	Brown	5.76	Red	Brown	5.12
	Green	5.22		Green	5.67
	Orange	5.39		Orange	2.94
	Blue	3.40		Blue	4.68
	Red	5.93		Red	3.70
	Purple	5.78		Purple	4.32
	White	4.80		White	4.44
Brown	Brown	4.03	White	Brown	10.26
	Green	3.70		Green	7.64
	Orange	3.65		Orange	7.47
	Blue	3.94		Blue	9.69
	Red	5.71		Red	3.81
	Purple	11.49		Purple	4.79
	White	6.53		White	5.52

From table 6.2 we see that the MCDM values were highest for the white background. However, we see smaller MCDM values for white background in the display color matching experiment compared with the AR color matching experiment (see table 6.1). In both experiments, the maximum MCDM value is for the brown and purple foregrounds on the white background. For other background-foreground combinations we see the same range of MCDM values as for the AR color matching experiment.

6.5 Summary

A psychophysical experiment was designed to understand if the color perception in AR is different than perception from a display. A similar color matching experiment was designed, using a single display instead of the AR simulator, on which the stimuli reproduced the AR color matching experiment's stimuli. As the impact of illuminants were minimal in the previous experiment, only the color stimuli under the cool light were replicated for the display color matching experiment. A comparison between experiments showed statistically significant differences for variance-covariance and for averages: the null hypothesis was rejected for most of the combinations for the variance- covariance and for all combination for the averages between the two experiments. The resulted matched colors of the display color matching experiment were bluer (lower b values) and in most cases lighter (higher J value) than the results from color matching in AR simulator. There are two hypotheses for this: one that it is probably because of differences in adaptation states for the two experiments and two: that the difference is due to the phenomenology difference between the experiment. This is because although the appearance was replicated on the display, in the AR simulator, the observers saw the background as a real physical object while on the display it was an image. Therefore, color appearance perceptions in AR is different than on a single display even for very simple stimuli (two-dimensional single color patches as foreground and background content). Additionally, in the display color matching experiment, CAM16 predictions were again inaccurate meaning the matches by the observers were not colorimetric matches. Inter-observer agreement, however, was similar for the two experiments. Again the white background had the highest MCDM values with the maximum for the brown and purple foreground on the white background, but MCDM values for the white background were smaller for the display color matching experiment than the AR color matching experiment. Therefore, in cases where the mixed color appearance is hard to describe, the observer agreement decreases as the matching task becomes more difficult. Since the perception of color appearance in AR is different than from a single display, available image perception models cannot be used to predict color appearance in AR. Since CAM16 is also inaccurate in predicting color appearance in AR, more data is needed to model color appearance in AR. Therefore, new experiments were designed to gather this dataset.

7 Stimulus Visual Complexity

7.1 Motivation

All the efforts in the previous chapters have been focused on studying simple 2D solid color patch combinations in AR. However, in real applications of AR, we often see more visually complex objects as the virtual content. Therefore, extra steps should be taken to understand perception of combinations of stimuli that are visually more complex. However, first we need to have a scale of visual complexity. For example if a 3D stimulus is visually more complex than a 2D stimulus, what is the scale difference? Since no previous effort has been done to build a scale for visual complexity, to answer this question, a psychophysical direct scaling experiment was designed. This experiment's design and results are discussed in this chapter.

7.2 Methods

A LCD-Dell UP2414QT 24-inch display being addressed at Full (3840 x 2160) resolution was used to run the experiment. In this experiment, only impacts of shape and texture were studied. For this purpose, stimuli with different shapes and different levels of texture were designed. The main shapes of square and circle were chosen and then extended to 3D versions of cube and sphere. The main shapes were then further extended into a spiky and a blob stimulus to have more complexity in terms of shape. Textures were added in two levels.

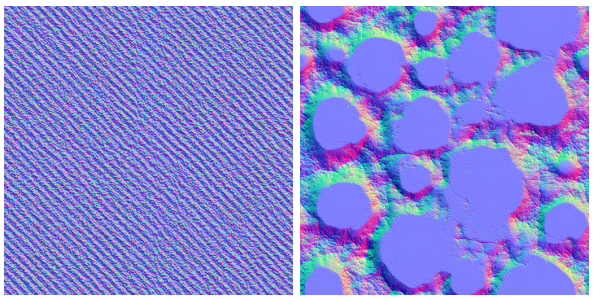

Fig. 7.1 – Images used as normal maps to add texture (level 2 on the left and level 3 on the right) to the stimuli in Blender (level 1 was no texture added)

Level one meant stimuli with no texture; level two was a high frequency and low depth texture while level three was a lower frequency but higher depth texture. The stimuli were designed in Blender using matte surface and a point light. The textures were applied as normal maps to the models in Blender. Figure 7.1 shows the images used for level 2 and level 3 textures (level 1 was no texture added). All stimuli were designed to have diffuse light reflection. These textures were combined with all stimuli resulting in 18 stimuli total. These stimuli are depicted in table 7.1.

Tab. 7.1 – Stimuli used in the visual complexity psychophysical experiment

Texture	Shape: Square	Cube	Spiky	Circle	Sphere	Blob
Level1	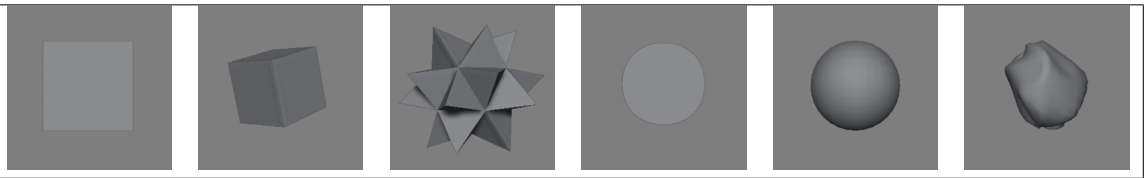					
Level2	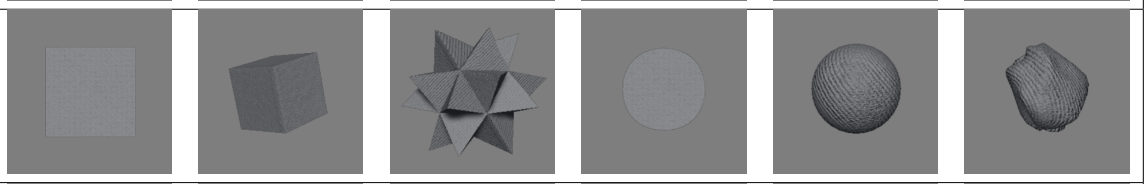					
Level3	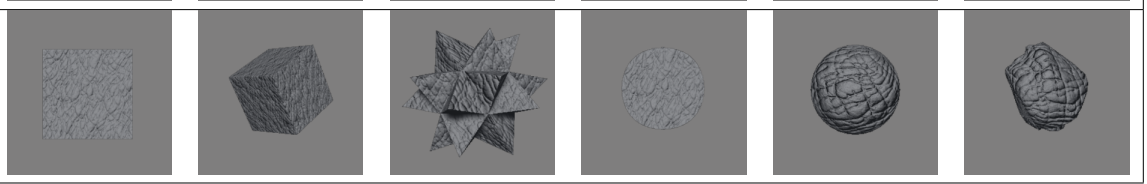					

The experiment was performed in a fully dark room. The only light in the room was the display light and the observers were seated in about 30 inches far from the display while doing the experiment. A graphical user interface (GUI) was designed using unity. Direct scaling method was used for this experiment. Figure 7.2 shows the graphical user interface (GUI) of the experiment made in Unity, As shown in Figure 7.2, there were two anchor stimuli present in all trials. The scale of these two anchor stimuli were assumed to be 15 and 85 (out of 100) and were graphically depicted on the slider present in the GUI. The slider was used to determine the scale of the visual complexity of the test stimulus. The test stimulus was presented in the middle (between the two anchor stimuli) in each trial. The presentation of the test stimulus was designed to follow a random fashion. Observers were then asked to scale the visual complexity of the test stimulus by moving the slider's knob and regarding the two anchor stimuli. As it is visible from Figure 7.2, the stimuli and the background were designed to be neutral as color was not intended to have any impact on the scaling task; only impacts of shape and texture were of interest.

As mentioned above, the experiment included 18 test stimuli; therefore, 18 trials were presented. The observers were brought into the experiment room and while the experiment was explained to them, they got adapted to

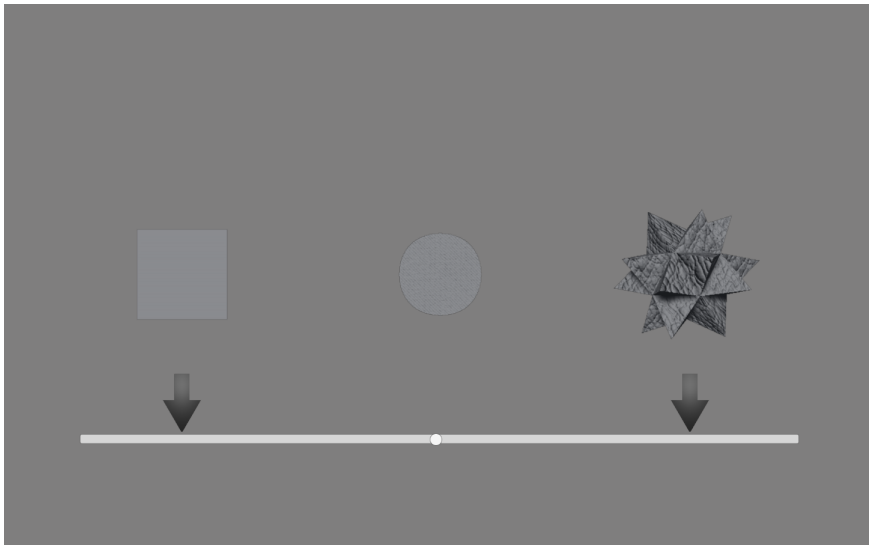

Fig. 7.2 – The graphical user interface (GUI) used in the direct scaling experiment

the darkness. Then started the experiment. The GUI was built into an application, therefore for each observer, the application was played. Test stimuli were randomly presented in the middle and observers moved the slider to the location that represented the visual complexity scale of the test stimulus. The slider started at the middle for each trial. The same task was performed for all the test stimuli. The experiment session took about 15 minutes. At the end of experiment, the observers were asked to repeat the experiment one more time. This repetition was done in order to get more accurate results. A total of 20 observers participated in the experiment. From them, 10 were male and 10 female with ages ranging from 20 to 60 years old.

7.3 Results and discussion

The results of the direct scaling experiment were then averaged and plotted. Figure 7.3 shows the results of the average scaling by the observers.

Figure7.3 shows the results of the direct scaling experiment. In Figure 7.3, the horizontal line shows the stimuli. These stimuli are ordered in terms of basic shape, dimension and texture level. The stimuli with basic shape of square are presented at the top with blue edges. These include square, cube and spiky shaped stimuli with texture levels increasing from left to right. The stimuli with the basic shape of circle are shown in the bottom with magenta edges. These are circle, sphere and blob with texture levels increasing from left to right. The blue and magenta lines represent the standard error (color coded similar to stimuli).

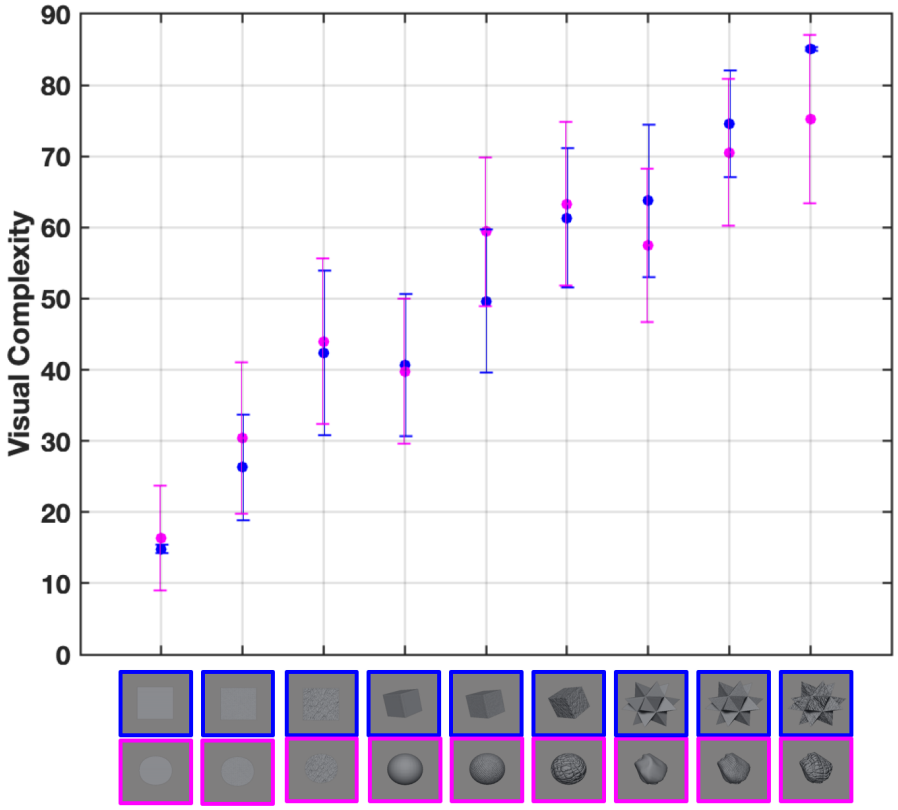

Fig. 7.3 – Average visual complexity scale of the stimuli scaled by the observers. The vertical axis depicts the visual complexity scale while the horizontal axis shows the stimuli (increasing in texture and dimension from left to right). The lines represent standard errors.

From Figure 7.3, it is notable that as more texture is added (stimuli with level1 versus 2 and 3 texture levels), the stimuli is perceived as more visually complex. Also, by adding dimensions to the basic shape , going from 2D to 3D and to more geometrical complex shapes, the stimulus also gains more visual complexity. It is interesting that differences of visual complexity between circle and square is small and the same is true as more dimension and texture added to the same group; Similar behavior and scales are observed from both groups.

Analysis of Variance (ANOVA) was performed on the data. The visual complexity scale was used as the variable and the groups were set to basic shape, shape dimension, and texture level. Table 7.2 shows the ANOVA table. The results of analysis showed p-values of 0.7769 for basic shapes (square versus circle) and zero for shape dimension and texture level. This means that using different basic shapes (square versus circle) does not impact the visual complexity significantly. However, the impacts of dimension and texture level are statistically significant.

Tab. 7.2 – Analysis of Variance (ANOVA) table for the visual complexity scaling data.

Source	Sum Sq.	d.f.	Mean Sq.	F	Prob>F (p)
Basic Shape	8.4	1	8.4	0.08	0.7769
Shape Dimension	186685.5	2	93342.8	898.56	0
Texture Level	56225.8	2	28112.9	270.63	0
Error	64821.1	624	103.9		
Total	307740.8	629			

7.4 Summary

In real applications of AR, virtual objects with different shapes and textures are overlaid on top of the real world. In previous efforts to understand color perception in AR (discussed in previous chapters), the only focus was on impacts of color; Therefore, only simple 2D patches with solid colors were studied. However, it is important to know the impacts of visual complexity on appearance perception. In order to study this, first we need to know the visual complexity scales of stimuli with different shapes, dimensions and textures. In this chapter, perception of visual complexity was studied. A psychophysical direct scaling experiment was designed and performed. In this experiment, stimuli with different shapes, dimensions and texture levels were used. All the stimuli were neutral in color as only impacts of shape and texture were of interest. The results showed that as the dimensions are increased, the stimuli is perceived to have a higher visual complexity. Also, textures with lower frequencies and higher depth, impact the visual complexity more than textures with higher frequency but lower depth. The basic shape did not impact the visual complexity; Therefore, similar results were obtained for the square shaped stimulus and the circle shaped stimulus and extensions of them. Although this experiment was designed to obtain a visual complexity scale of the common stimuli (content) used in AR, the results can also be used in other psychophysical experiments that deal with stimuli with different levels of visual complexity. Results of this chapter were later used in the modeling chapter (Chapter 9).

8 AR Color Matching with Complex Stimuli

8.1 Motivation

As mentioned previously, in AR, usually virtual objects with different shapes and textures are overlaid on top of the real world; therefore, in order to understand the color perception in AR in a practical manner, color perception of complex visual stimuli should be studied. In the previous chapter, visual complexity was studied to understand how different stimuli with different shapes and textured are perceived in terms of visual complexity which resulted in a scale that is used in this chapter (in designing the stimuli) and in the modeling chapter (Chapter 9). In this chapter, a new psychophysical color matching experiment is designed to study color perception in AR for mixture of more complex virtual overlays (compared to simple 2D solid color overlays) and backgrounds. The stimuli used in the experiment are chosen from previously studied stimuli in the the visual complexity experiment discussed in Chapter 7.

8.2 Methods

The psychophysical color matching experiment was designed to be similar to the previous color matching experiments. Simple 2D solid color patches with the same design, as described in Chapter 5, were used as physical background. Figure 8.1 shows the colors used as physical background in the light booth (with the light) on in CIE u'v' space.

Four colors were used for physical background. Although, the design of the printed physical background were similar to the one used in Chapter 5, the virtual foreground stimuli were only presented on 4 of the color backgrounds. This approach was taken to reduce the number of trials. The chosen background colors were blue, brown, gray and red.

Table 8.1 depicts the stimuli that were used in the experiment. The virtual stimuli shapes were chosen from stimuli studied in Chapter 7; They consisted of a simple 2D patch with level1 texture(no texture), a 3D cube with level two texture(high frequency and low depth) and a spiky stimulus with level three texture(low frequency

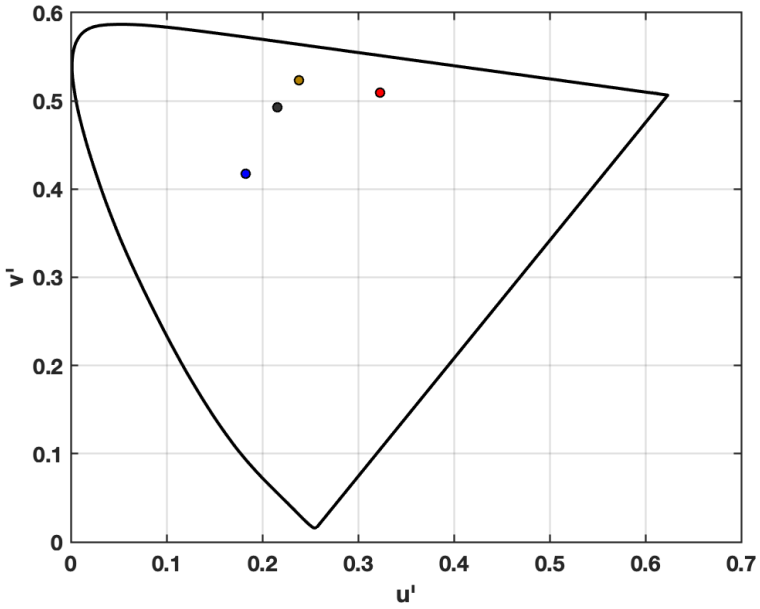

Fig. 8.1 – Color used for physical background in u' v' color space

Tab. 8.1 – Stimuli used in the color matching psychophysical experiment

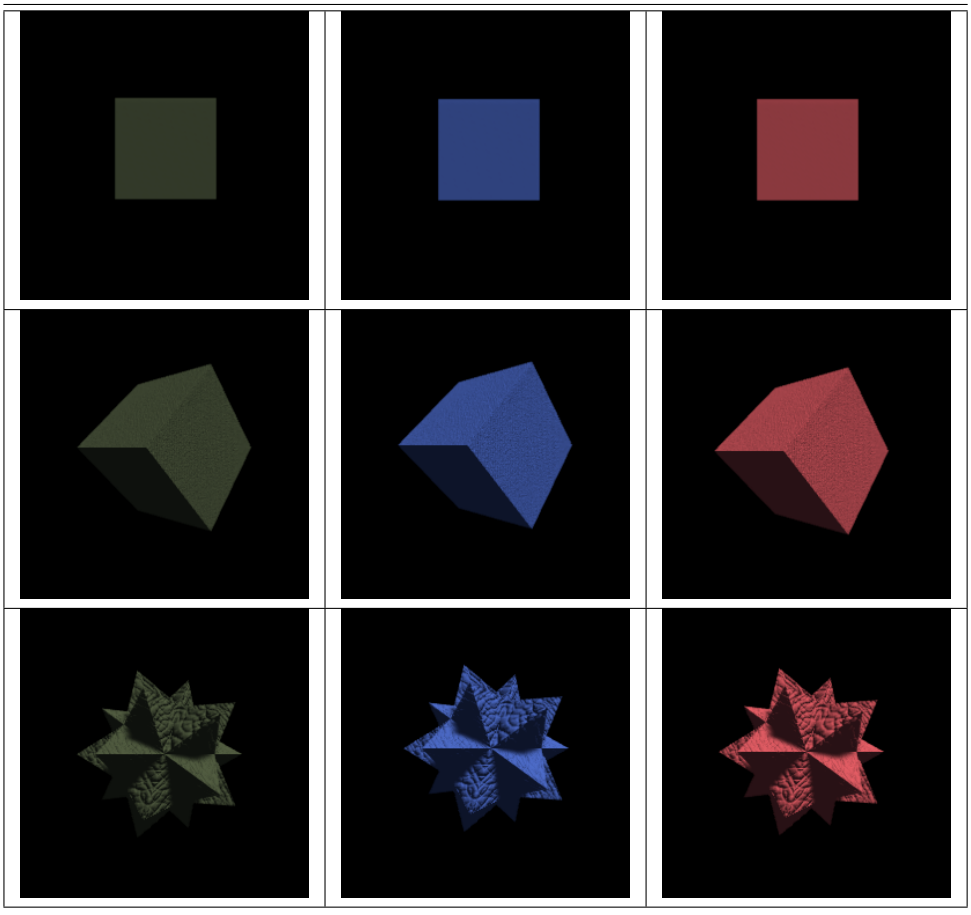

and high depth). The visual complexity scale obtained for these stimuli was about 15, 50, and 85 respectively. As it is visible from Table 8.1 three colors of Green, Blue and Red were used as virtual foreground stimuli color. These colors were combined with the models in Blender (as the albedo color) and then the final results (depicted in Table 8.1) were presented to the observer. The models were made using Blender's default material (matte surface) and they were lit using a point source light with white color and a size of 0.1. The virtual foreground stimuli colors were measured using a Photo Research PR655 spectroradiometer. The measurements were performed through the half silvered mirror, with the virtual foreground stimuli on the middle black physical background with the booth light (in the AR simulator) on. The measurements were taken from the middle part of the stimuli and included the texture. Figure 8.2 shows the colors of foreground stimuli in CIEu'v' space.

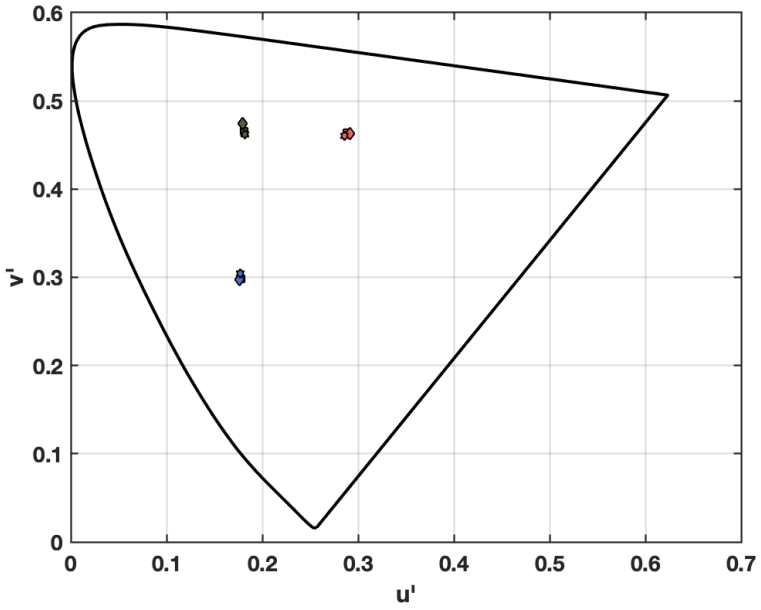

Fig. 8.2 – Color used for virtual foreground in u' v' color space

The LCD was a Dell P2715Q 27-inch 4K IPS display being addressed at Full-HD (1920x1080) resolution (also used in the previous color matching experiment in AR simulator described in Chapter 5). Only one illuminant setting was used which included a pair of Philips Hue "white and color" A19 bulbs with tristimulus values of [14.24, 4.14, 10.43] (reflection of the lamps measured from a perfect reflecting diffuser at the bottom of the booth). A graphical user interface was designed in Unity and developed as an application.This GUI would present the virtual foreground stimuli on the display so that they would get overlaid in the assigned locations through the optics of the AR simulator (explained in chapter 4). Figure 8.3 shows the GUI (overlaid on the real background).

The experiment was consisted of 36 trials. In each trial, a pair of virtual foreground stimuli were presented to the observer; one stimulus on a color background and another on the black background next to it. The

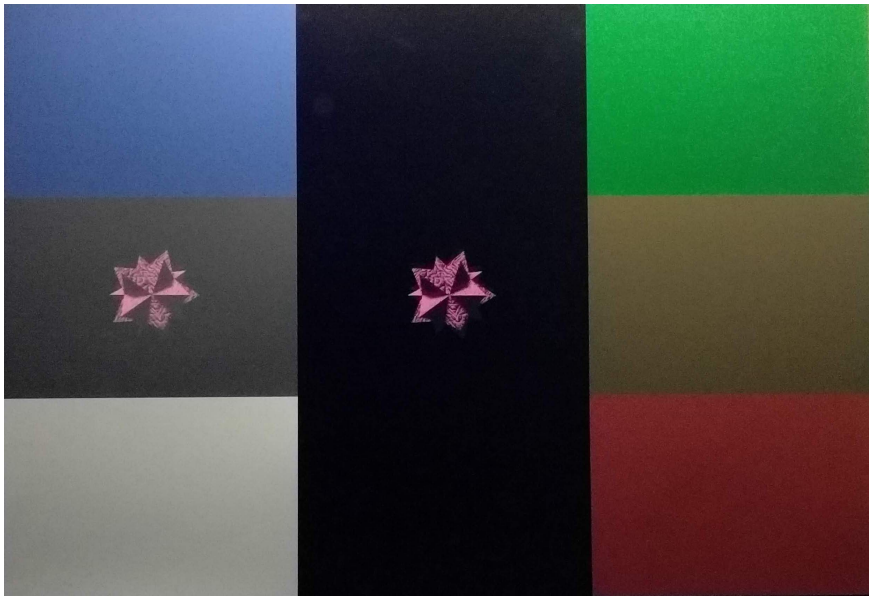

Fig. 8.3 – The graphical user interface (GUI) used in the color matching experiment. The virtual foreground stimuli (small stars in this picture) appeared to be transparent and on top of the real backgrounds.

presentation of stimuli was done in a random order, therefore all backgrounds and foreground stimuli were selected and presented randomly. For each trial, the observers' task was to modify the stimulus on the black background to match it to the stimulus on the color background. Observers were given a small keyboard (the same keyboard shown in Figure 5.2 in Chapter 5 with the same key functions) and a knob by which they could change hue, saturation and value. HSV of the material albedo color was used for the modifications as it was easier than LCH to implement in Unity with c# programming. The knob was used to change hue; based on the feedbacks from the previous color matching experiments, having a knob for changing the hue would be much more convenient for the observer and would reduce the number of clicks needed to reach the desired hue. The hue was also adjustable with the keyboard. Twenty observers participated in the experiment of which 14 were male and 6 female with ages ranging from 23 to 54 with an average age of 31. All the observers had normal color vision (tested with Ishihara color blindness test).

8.3 Results and discussion

The results of the color matching experiment are depicted in Figure 8.4 and 8.5.

In Figures 8.4 and 8.5, the black diamonds are color of the background. other spots are color coded for the color of the foreground (green, blue or red). The spots that are further from the background (black diamond) are the average of the matched colors by the observers. The spots closer to the background (black diamond)

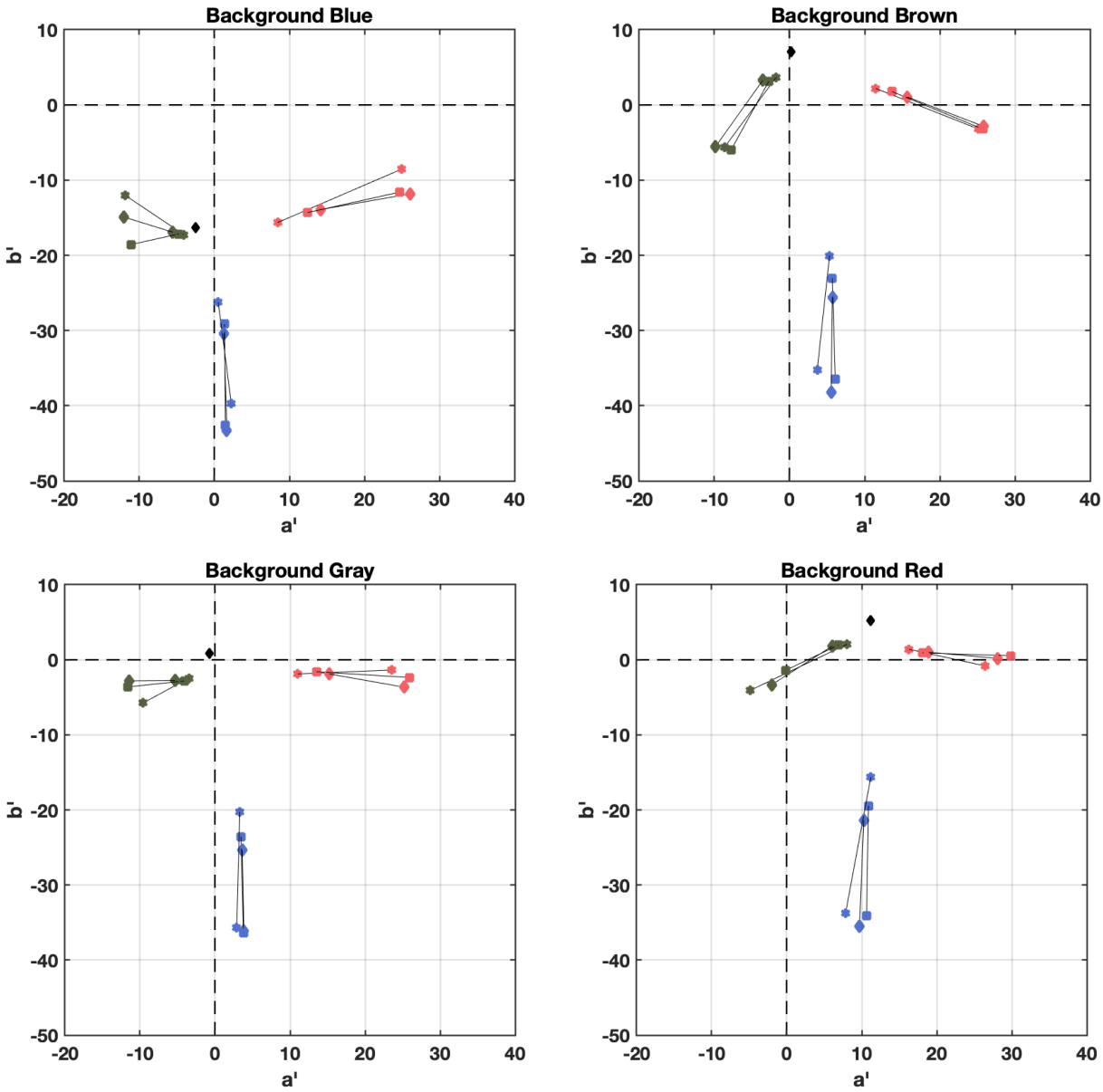

Fig. 8.4 – Average results of the color matching experiments for mixes on each background in a-b plane. The spots are color and shape coded for the color of the foreground and stimulus model. The spots closer to the background (black diamond) show the average matched color by the observers and spots further from the background (black diamond) depict predictions by CAM16. Background color is depicted as a black diamond.

are predictions from CAM16 with measurements of the mix color as input. The color spots are also shape coded for the shape of the stimuli; square spots show the square stimulus, diamonds represent the cube and the star represents the spiky stimulus. As we see from the figures, foreground stimuli with different visual complexity (color spots with no edges) had slightly different overlay color. This is because the texture would slightly impact the color of the stimulus. From the Figure 8.4 in all cases the predictions are far away from the average match by the observers.

From Figure 8.5, we see that the observers' average matched colors are also lighter than what CAM16 predicts. In order to understand the impact of visual complexity, the Euclidean distance between the prediction and average match was calculated for every stimulus. These distances are presented in Table 8.2.

Table 8.2 shows the Euclidean distances of a-b (Δab) and J (ΔJ) in CAM16 UCS color space for each background, foreground and stimulus shape combination; From the table, It is visible that in most cases the Euclidean distance between the prediction and average match is largest for the spiky stimulus in a-b differences.

Figure 8.6 shows the matched colors by the observers for each background-foreground mix and the averages. From Figure 8.6, we see that there are clouds of matches around the average matches. Larger clouds show less consistency on the matched color. We see that for all backgrounds, the cloud of matches are larger for mixes with the green virtual overlay. To investigate this more, the mean color from the mean (MCDM- explained in Chapter 5) was calculated for all combinations of foreground and background color; Table 8.3 shows the MCDMs.

From Table 8.3, we see that the MCDM is not impacted by the stimulus complexity level. In some cases, it increases as the visual complexity increases while in some other cases it decreases with higher visual complexity levels.

In order to further discuss the impact of visual complexity, analysis of variance (ANOVA) was performed on the results from the color matching experiment with 3D stimuli to see if the color matching task was performed significantly different for stimuli with different visual complexity levels. Tables below show the results of the analysis.

Since the dataset (Jab results) was a multivariable dataset, separate one-way ANOVA was performed for each J, a, and b variables with visual complexity as the group. From Tables 8.4, 8.5, and 8.6 it is notable that P values obtained for J, a, and b were $3.94499e^{-40}$, 0.2811 and 0.0621 respectively. Figure 8.7 shows the box plots of the data for J, a, and b for different visual complexity levels. We see that there is a statistically

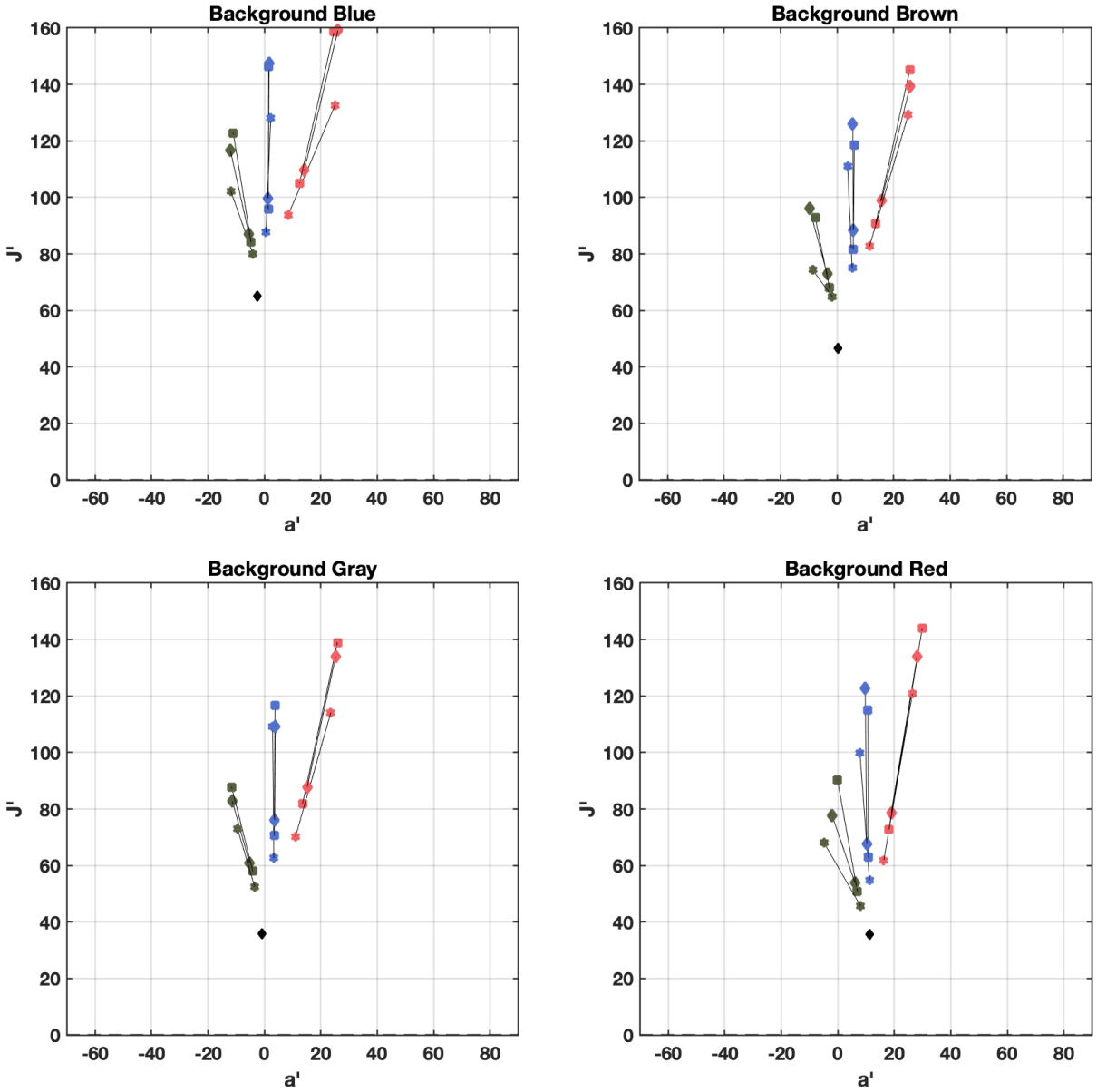

Fig. 8.5 – Average results of the color matching experiments for mixes on each background in J plane. The spots closer to the background (black diamond) show the average matched color by the observers and spots further from the background (black diamond) depict predictions by CAM16. Background color is depicted as a black diamond.

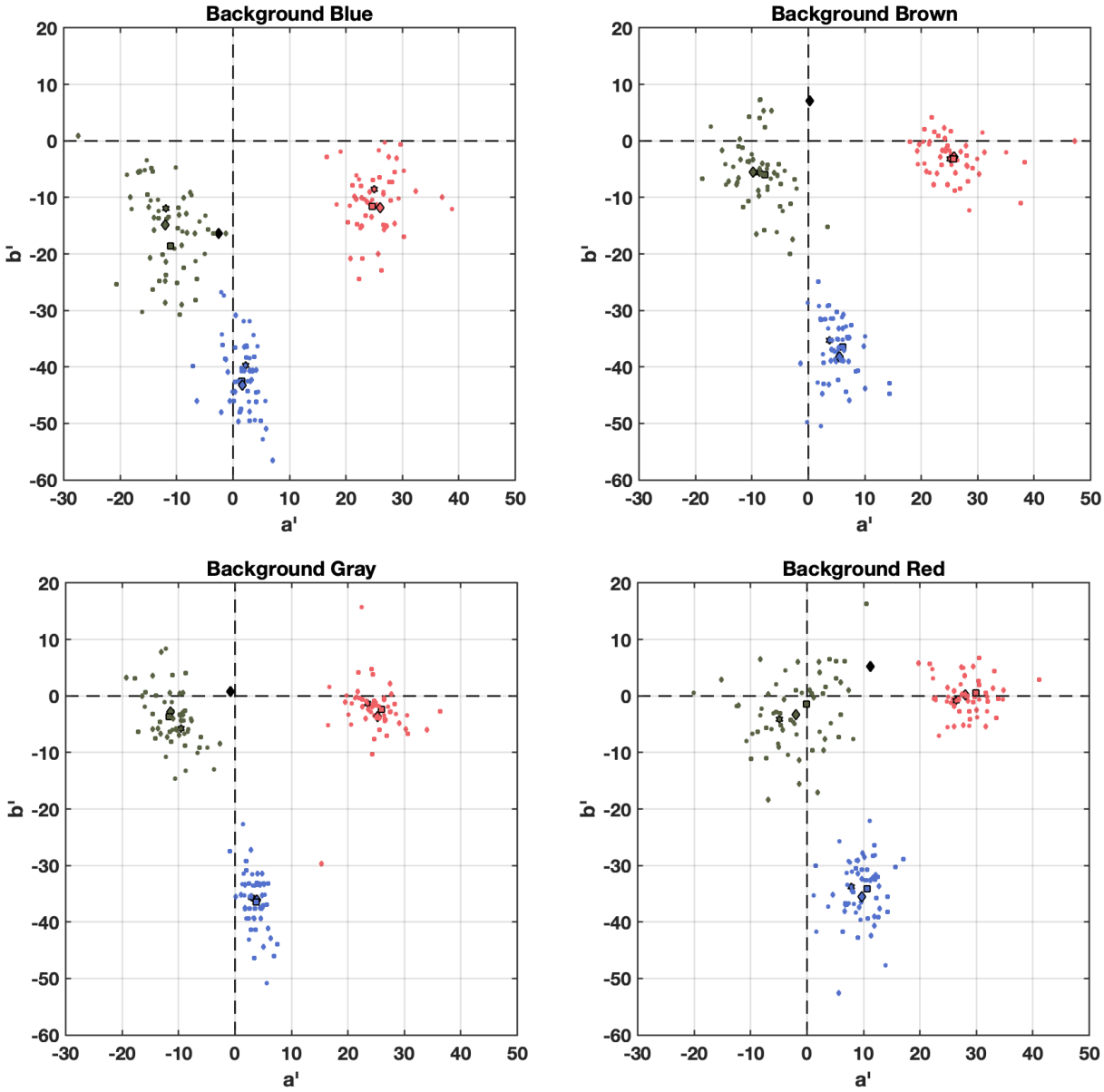

Fig. 8.6 – Results of color matching experiment in CAM16 UCS a'-b' plane for mixes on each background. The spots are color and shape coded for the color of the foreground stimuli (shapes of square, diamond and star for the square, cube and spiky stimuli respectively). The average matches have black edges. Background color is depicted as a black diamond.

Tab. 8.2 – Euclidean distances of average matched color and predicted color by CAM16UCS a-b and J in Jab color space

Background Color	Foreground Color	Shape	Δa'b'	ΔJ
Blue	Green	Square	6.50	38.69
		Cube	6.84	29.55
		Spiky	9.42	22.28
	Blue	Square	13.42	50.43
		Cube	12.87	47.72
		Spiky	13.57	40.41
	Red	Square	12.56	53.80
		Cube	12.06	49.48
		Spiky	17.97	38.65
Brown	Green	Square	10.39	24.66
		Cube	10.84	23.21
		Spiky	11.58	9.49
	Blue	Square	13.44	36.94
		Cube	12.63	37.67
		Spiky	15.31	35.92
	Red	Square	13.03	54.34
		Cube	10.87	40.55
		Spiky	14.70	46.56
Gray	Green	Square	7.56	29.81
		Cube	6.09	21.78
		Spiky	6.94	20.60
	Blue	Square	12.83	46.17
		Cube	10.77	33.19
		Spiky	15.37	46.45
	Red	Square	12.39	57.09
		Cube	10.17	46.05
		Spiky	12.52	43.93
Red	Green	Square	7.78	39.38
		Cube	9.54	23.73
		Spiky	14.24	22.28
	Blue	Square	14.63	52.18
		Cube	14.15	55.03
		Spiky	18.44	44.96
	Red	Square	11.76	71.25
		Cube	9.20	55.27
		Spiky	10.34	58.90

significant effect on J but not a or b. And, from Figure 8.7, the most complex model (spiky stimulus) is significantly lower in J than the others.

Figure 8.7 shows the box plots for results of the color matching experiment with complex stimuli to compare the results of the average matched J, a, and b for stimuli with different visual complexity levels. The top and bottom edges of the blue boxes in the plots show the 75th and 25th percentiles of the data. The red line inside

Tab. 8.3 – Mean color differences (MCDMs) of he matched colors by the observers

Background Color	Foreground Color	Shape	MCDM
Blue	Green	Square	26.11
		Cube	25.23
		Spiky	22.98
	Blue	Square	16.93
		Cube	20.96
		Spiky	25.81
	Red	Square	15.41
		Cube	14.09
		Spiky	21.95
Brown	Green	Square	22.75
		Cube	22.64
		Spiky	20.01
	Blue	Square	22.95
		Cube	15.31
		Spiky	23.35
	Red	Square	15.51
		Cube	18.29
		Spiky	16.30
Gray	Green	Square	20.33
		Cube	18.50
		Spiky	15.64
	Blue	Square	20.41
		Cube	15.92
		Spiky	18.09
	Red	Square	14.70
		Cube	16.87
		Spiky	21.00
Red	Green	Square	21.06
		Cube	22.68
		Spiky	17.48
	Blue	Square	16.33
		Cube	14.42
		Spiky	21.29
	Red	Square	12.57
		Cube	12.96
		Spiky	18.69

Tab. 8.4 – Analysis of Variance (ANOVA) table for the color matching experiment with complex stimuli in terms of 'J'

Source	Sum Sq.	d.f.	Mean Sq.	F	Prob>F (p)
'J'	208750	2	104375	103.25	< 0.01
Error	724844.9	717	1010.9		
Total	933595	719			

the boxes show the median and the black outer line shows the range between the minimum and maximum points. The plus signs show the outliers.

Tab. 8.5 – Analysis of Variance (ANOVA) table for the color matching experiment with complex stimuli in terms of 'a'

Source	Sum Sq.	d.f.	Mean Sq.	F	Prob>F (p)
'a'	565	2	282.517	1.27	0.2811
Error	159345.1	717	222.239		
Total	159910.1	719			

Tab. 8.6 – Analysis of Variance (ANOVA) table for the color matching experiment with complex stimuli in terms of 'b'

Source	Sum Sq.	d.f.	Mean Sq.	F	Prob>F (p)
'b'	1570.1	2	753.549	2.79	0.0621
Error	193656.2	717	270.092		
Total	195163.2	719			

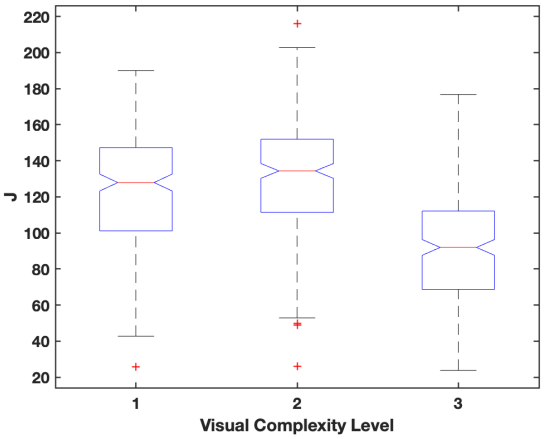

(a) Differences in matched J for stimuli with different visual complexity levels

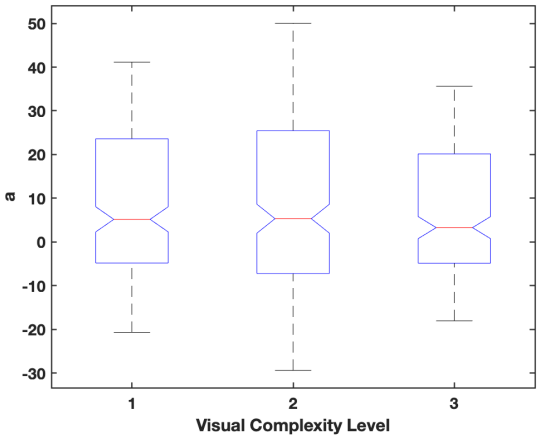

(b) Differences in matched a for stimuli with different visual complexity levels

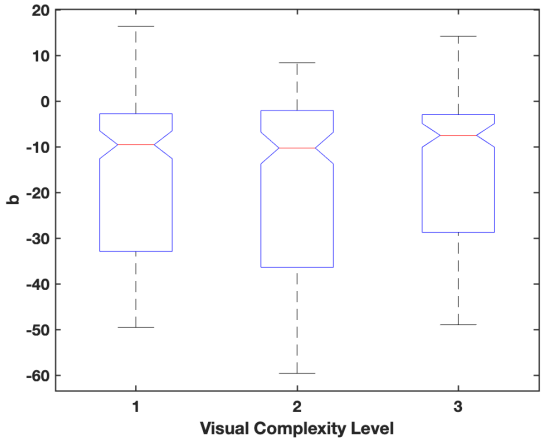

(c) Differences in matched b for stimuli with different visual complexity levels

Fig. 8.7 – Comparing matched Jab results for stimuli with different visual complexity levels

From figure 8.7, we see that in all cases the results of the matches are very similar for stimuli with different visual complexity levels. The only case that a noticeable difference is seen is the J matches for the stimuli with highest visual complexity (spiky shaped stimuli). These stimuli were the hardest to match in terms of brightness (claimed by the observers) and were noticeably darker compared to the other two shapes because of the texture.

8.4 Summary

In this chapter, a color matching experiment with stimuli having different levels of visual complexity was discussed. This experiment was a psychophysical color matching experiment performed inside the AR simulator. It included stimuli at three different visual complexity levels. The stimuli models were chosen from the stimuli used in the visual complexity scaling in chapter 7. The experiment was designed to study more practical AR environments with stimuli having higher visual complexities. The measurements were also used as input to CAM16 to predict the mix appearance in AR. The results showed that the average match by observers is far from predictions by CAM16, which means the observer matches were not colorimetric. As the stimulus became more visually complex, this difference was increased. Also, color matching was more difficult for stimuli with higher visual complexity resulting in larges mean color difference from the mean values. The results of ANOVA showed that the impact of visual complexity is statistically significant for J and non-significant for a and b.

The results of this chapter and the previous chapters were used to provide a color appearance model (discussed in Chapter 9) for AR environment.

9 Color Appearance Model for Augmented Reality

9.1 Motivation

As mentioned before, in several applications of AR, it is necessary to control the color appearance of the optically-mixed AR content. All the effort discussed in previous chapters has been towards modeling mixed content appearance in AR environment. Different experiments were designed and performed to answer different questions regarding color appearance in AR. The results of these experiments helped model color appearance of mixed content in AR. As discussed in Chapter 5, CAM16 was used as a beginning step for calculating the color appearance. In this chapter, model components are tested with the goal of building a single model to describe all the experiments. CAM16 color appearance model was further modified regarding the results of the experiments. Another approach was taken to model color appearance in AR. In this approach, based on the previous researches on transparency, tristimulus values of the stimuli were modified and then used as input to CAM16. These approaches are discussed in this chapter.

9.2 Approach

As reviewed in Chapter 3, color appearance for reflective objects has been studied for over decades. Also, there has been research done on transparency perception. In see-through AR environments, both reflective objects and transparent stimuli are presented to the observer and evoke a mixed appearance perception. Controlling color perception in AR is necessary for many applications. Therefore, in this research work, color appearance in AR is studied to be modeled.

From previous experiments, color appearance in AR has been better understood. From Chapter 4, it was seen that the measured color of mix converges towards the color of background from the overlay color. The amount of this convergence seems to depend on the relative brightness of foreground color versus background color. It was noted that the illuminant's impact is minimal if a broadband and not very chromatic light source is used.

In Chapter 5, a color matching experiment was done in the AR simulator (built in the lab for experiments in AR environment). This experiment was done to study the impact of background color, foreground color and lighting on the mixed color perception. CAM16 was also used to predict color appearance of the mix. CAM16 color appearance model was used as it is one of the comprehensive color appearance models; it allows choices for adapting surround condition and has enough complexity to be appropriate for AR environment. The measurements of the mix colors in AR were used as input to CAM16 with the CAM16 prediction surrounding conditions set to "dim". The results showed that the calculations of appearance by CAM16 (using the measured mixed color as input) are far from the average matched color by the observers. This means that the matches by the observers are not colorimetric matches. To improve the predictions by CAM16, the effect of chromatic simultaneous contrast was added to the calculations; This brought the predictions closer to the average matches and within the cloud of matches by all observers, however, the improvement was small.

To further study color perception in AR, a question to answer was if the color perception in AR is different from perception from just a single display. In typical HMD see-through AR designs, the overlay is simply a display image optically overlaid on top of the real world. In order to answer this question, another color matching experiment was designed and performed (discussed in Chapter 6). The experiment was designed to be very similar to the previous color matching experiment in AR simulator. The results of this experiment showed that the color perception on a single display is different from color perception in AR environment. The resulted matched colors of the display color matching experiment were bluer (lower b values) and in most cases lighter (higher J value) than the results from color matching in AR simulator. This is might be due to differences in adaptation states for the two experiments or due to a difference in phenomenology (since in the experiment performed in the AR simulator the background was a real physical object while in the display experiment it was an image).

Before trying to model the data, it was necessary to understand the impact of visual complexity on color perception in AR. The previous experiment were all designed to have simple 2D patches with solid colors as stimuli. However, in real applications of AR, usually more visually complex content is presented as the overlay. Therefore, modeling color perception in AR just based on this dataset would not represent real AR environment. Also, based on the observations of AR environment, one assumption was that the visual complexity of the stimulus impacts the amount that observers discount the background and treat the virtual content with higher visual complexity level more as a separate layer than mixed with the background.

First an experiment was designed to study visual complexity (discussed in Chapter 7). This was a direct scaling experiment with a GUI designed in Unity. The stimuli included different levels of shape complexity and texture. The results of this experiment was later used in the model. Then, a new color matching experiment was designed to be performed in the AR simulator (discussed in Chapter 8). This experiment was similar to the previous color matching experiments, however, stimuli with different levels of complexity were used in

this experiments. The stimuli were chosen from the stimuli used in the direct scaling experiment. The results showed that the stimuli with more visual complexity were more difficult to match. CAM16 was used again to predict the color appearance in AR. The results showed that predictions by CAM16 were again far from the average matched color by the observers.

An approach was discussed in Chapter 5 to improve predictions by CAM16 by adding the impact of simultaneous contrast to the model. The results showed that although this made the predictions closer to average matches by the observers overall, the impact was very small for each case. Therefore, in this chapter we take new approaches to predict color appearance in AR environment.

9.3 Modeling color appearance in AR

Previous results showed that the predictions using measured mix colors as input to CAM16 are not very accurate (see Figures 5.4, 5.3, 8.4, and 8.5). The average observer matches were further away from the background than the predictions by CAM16. Interestingly, the color matching experiment with simple stimuli has smaller errors, but the results show less systematic behavior. The color matching experiment with complex stimuli shows the systematic bias away from the background. Similar trends can be seen in terms of lightness predictions. One probable reason for these differences between the experiment results can be the difference in appearance of the stimuli in the experiments.

9.3.1 Approach1: Modifications for Augmented Reality in Jab Space (CAM Approach)

In order to model the results of the experiments, the output of CAM16 was modified. The input was kept the same, being XYZ of the mixed color stimuli and using as white point the XYZ of the background white (both measured using a X-Rite PR655 spectrophotometer), and the surround was set to dim for CAM16. All the modifications were done in Jab space. In Chapter 5, the chosen white point was an average of the background and foreground white points (Display white was used as foreground white point and background white was used as background white point). Choosing this white point resulted in colors looking yellow-reddish in CAM16 UCS Jab space (see Figures 5.3 and 5.4) However, using just the white background would result in very bluish appearance for blue foregrounds and from the observation, yellow-reddish appearance was representative of the appearance of the stimuli inside the AR simulator, especially with the warm light on. However, results of the color matching experiment with complex stimuli showed that this white point (average of display white and real background white) results in yellow-reddish appearance predictions which did not

resemble the observed appearance. Therefore, for the modeling, the background white was chosen as white point for both experiments to be more consistent.

To modify the CAM16 Jab predictions based on the systematic biases measured above, the predicted Jab (by CAM16) was pushed away from background color. This was done by defining a normalized vector named V with a direction from the background color towards the predicted mix color (CAM16 output color). Equation 9.1 shows how V was defined.

$$V = Norm(BgJab - MixJab) \tag{9.1}$$

In Equation 9.1, BgJab and MixJab represent the Jab of the background color and the predicted color by CAM16 respectively; Norm is a function which normalized the input vector, in this case BgJab-MixJab.

Next, the predicted colors are moved away from the background color using vector V and a scalar. This transformation is defined as below:

$$NewMixJab_i = MixJab_i - X \times R_i \times V_i \tag{9.2}$$

$$R_i = \frac{BgJ_i}{FgJ_i} \tag{9.3}$$

$$X = Optimize(R, V, MixJab, MatchJab) \tag{9.4}$$

$$Optimize = Min(\sum_i (MatchJab_i - X \times R_i \times V_i)^2) \tag{9.5}$$

In equation 9.2, Mix Jab is the predicted color in Jab space, X is a scaling factor, R is a factor of relative lightness of the foreground and background color defined in Equation 9.3 and V is the normalized vector defined in Equation 9.1. R is defined in Equation 9.3 in which BgJ and FgJ represent the lightness of the background and foreground color respectively. X is a scale factor which is optimized for minimum distance between the prediction and average match for all the datasets resulted from color matching experiments with

simple and complex stimuli. This optimization is defined in Equations 9.4 and 9.5. In these equations, we see that the optimization function uses R, V, MixJab (predicted color in Jab)and MatchJab (average matched color in Jab) of the color matching experiments in AR (both with simple and complex stimuli). This function finds an optimized X that minimizes the distances between the predicted color and average matched color (both in Jab).

As mentioned above, this model was developed based on the datasets from the color matching experiments for simple and complex stimuli. In order to add the impact of visual complexity, another step was designed to push the new modified prediction towards the foreground color. However, when doing this step, the impact was very small and would not satisfy the cost of the model becoming more complicated. Trying to create a general enough model to fit all the data, the impact of visual complexity was excluded from the model. This was done because adding it would not noticeably change the results while it would make the model more complex and that the small difference in J regarding the visual complexity of the stimulus (discussed in Chapter 8) was smaller than the residual error between the two experiments.

Model Performance

The new model was used to predict the appearance for both 2D and 3D color matching experiments. Figures below show the results of the new prediction compared to the CAM16 prediction and the average matched color.

Figures 9.1 , 9.2, and 9.3 shows the predictions by the new model for both 2D and 3D color matching experiments (green points) and comparison to the average matched colors(blue points) and predictions by CAM16 (magenta points) The points are shape coded; square for the square stimuli, diamond for the cube stimuli and star for the spiky shaped stimuli. We see that the new predictions (green points) are closer to the average matched color (blue points) than the old predictions (magenta points). This is especially better for the 3D color matching experiment results as the average matched colors being away from the background on the background-mix vector was true for all color mixes in the 3D color matching experiment, however this was not true for some cases in the 2D color matching experiment. The new predictions (green points) were closer to observers average matched colors than the old prediction in terms of J too.

The average Euclidean differences between the prediction and average matched color in Jab space was calculated for both the old and new model predictions. Average Euclidean differences were 42.13, 17.92, and 14.96 for Jab differences between the average match color and the predicted color by CAM16 for color matching experiment with 3D stimuli and 2D stimuli under the warm and cool light respectively. These values were reduced to 26.24, 12.57, and 10.67 respectively.

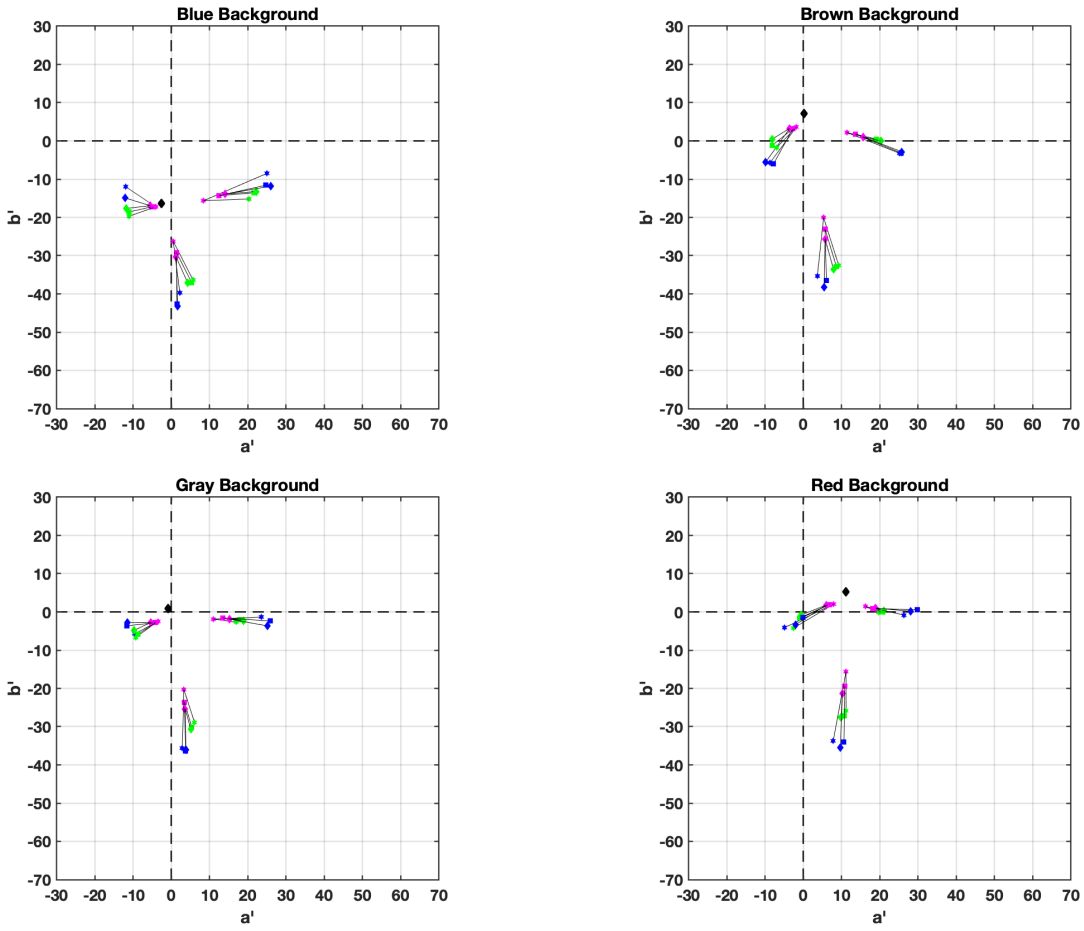

Fig. 9.1 – Comparing the average results of the color matching experiment(blue points) with complex stimuli, the prediction by CAM16 (magenta points) and the prediction by CAM Approach (green points) in CAM16 UCS a-b plane

9.3.2 Approach 2: Modifications for Augmented Reality in XYZ Space (XYZ Approach)

Based on the previous research works on transparency reviewed in Chapter 3, a new approach was taken to modify the tristimulus values of the stimuli in order to predict the perceived appearance in AR. This model is based on the model by D'Zmura et al. [D'Zmura et al., 1997]. The reason to choose this method over other transparency models was that the stimulus design in their work ([D'Zmura et al., 1997]) is somewhat similar to the stimuli that was used in previously discussed color matching experiments (see Chapters 5 and 8).

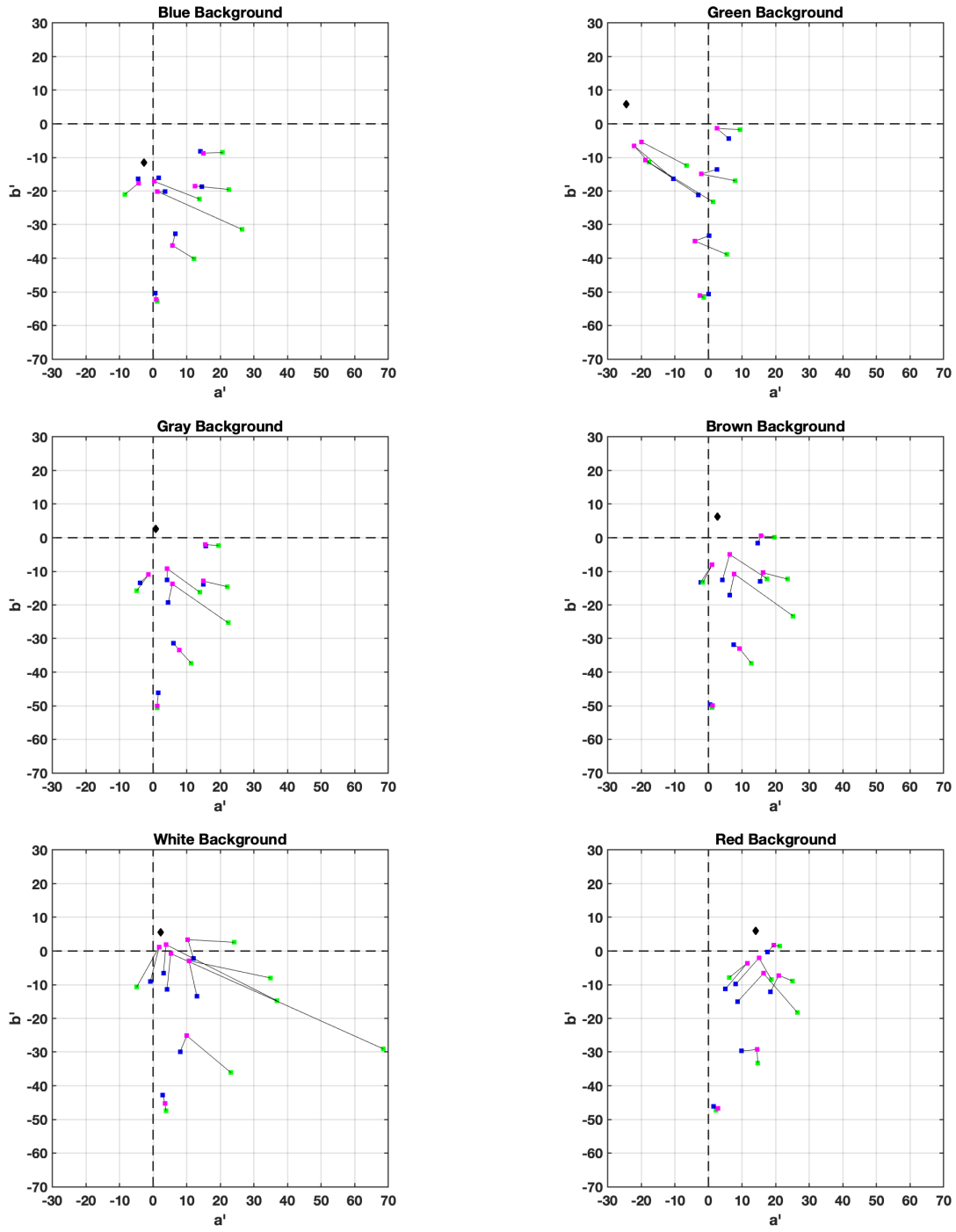

Fig. 9.2 – Comparing the average results of the color matching experiment with simple stimuli under the warm light (blue points), the prediction by CAM16 (magenta points) and the prediction by CAM Approach (green points) in CAM16 UCS a-b plane

Also, the convergence behavior that was observed in results of these experiments (see Chapter 5 and 8) was similar to D'Zmura et al. 's work. The equation that D'Zmura et al suggest for convergence is as follows:

$$b = (1 - \alpha)a + \alpha g \tag{9.6}$$

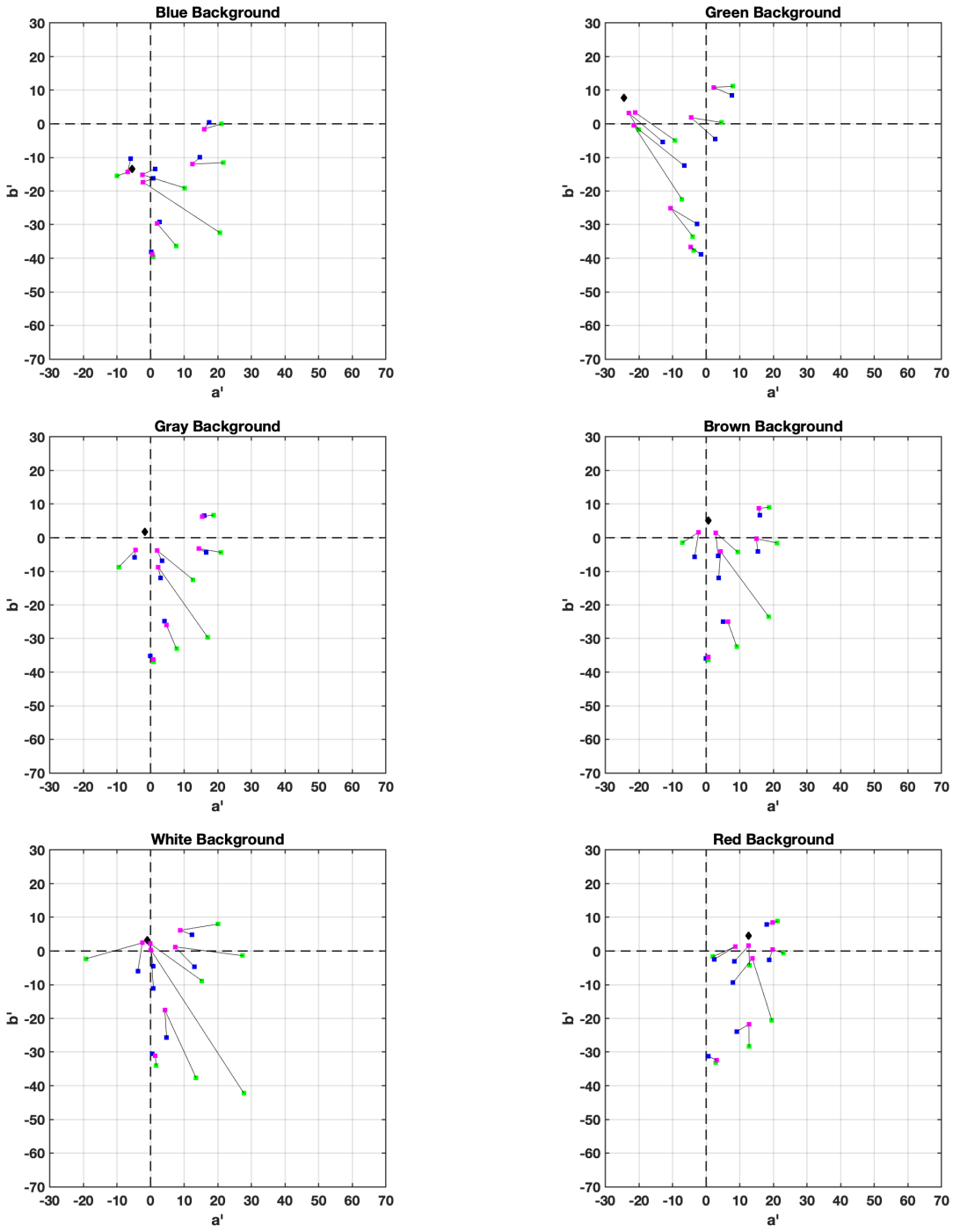

Fig. 9.3 – Comparing the average results of the color matching experiment with simple stimuli under the cool light (blue points), the prediction by CAM16 (magenta points) and the prediction by CAM Approach (green points) in CAM16 UCS a-b plane

In Equation 9.6, b, a, and g represent tristimulus values of the mix, background and overlay stimulus respectively; in this equation, α (opacity) should be between zero and one. The suggested equations in Approach

2 are presented in below: Equation 9.7 was developed for AR environment and was used in Approach 2; in this equation, instead of alpha being a scalar (representing opacity), it is a vector of two scalars: one for background color ($\alpha(1)$) and one for foreground color ($\alpha(2)$).

$$b = \alpha(1)a + \alpha(2)g \tag{9.7}$$

The constrain of α being between zero and one for Equation 9.6 is resulted from the physics of having opaque backgrounds covered by transparent overlays (filter). In usual situations, α cannot physically be outside of this range. However, in the AR environment, light is added to the physical background. Therefore, this constraint does not hold for AR. Although α values should be larger than zero, we can expect getting values larger than one.

Model Performance

Figure 9.4 and 9.5 show the results of using this approach in CIE u' v' space for color matching experiment with simple stimuli for the warm and cool light sessions and color matching experiment with complex stimuli respectively.

Figures 9.4. 9.5, and 9.6 show predictions by the XYZ approach in CIE 1976 UCS space. Black diamonds show the color of the background, magenta diamonds show the foreground color, blue diamonds depict the average matched color by the observers and the cyan diamonds are predictions by the new approach. We see that using this approach, tristimulus values of the matched colors and the convergences are very well predicted by the second approach.

In these predictions, α values were obtained for each experiment separately by fitting the datasets with the model. The optimization found α values that minimized the total Euclidean difference between the prediction and average matched color in XYZ space. The α values were as following:

Tab. 9.1 – Values of the constant α in the second approach (see Equation 9.6)

Experiment	$\alpha(1)$	$\alpha(2)$	$\frac{\alpha(2)}{\alpha(1)}$
Color Matching with simple stimuli (Warm light)	0.51	1.02	1.99
Color Matching with simple stimuli (Cool light)	0.58	1.14	1.96
Color Matching with complex stimuli	1.08	3.12	2.86

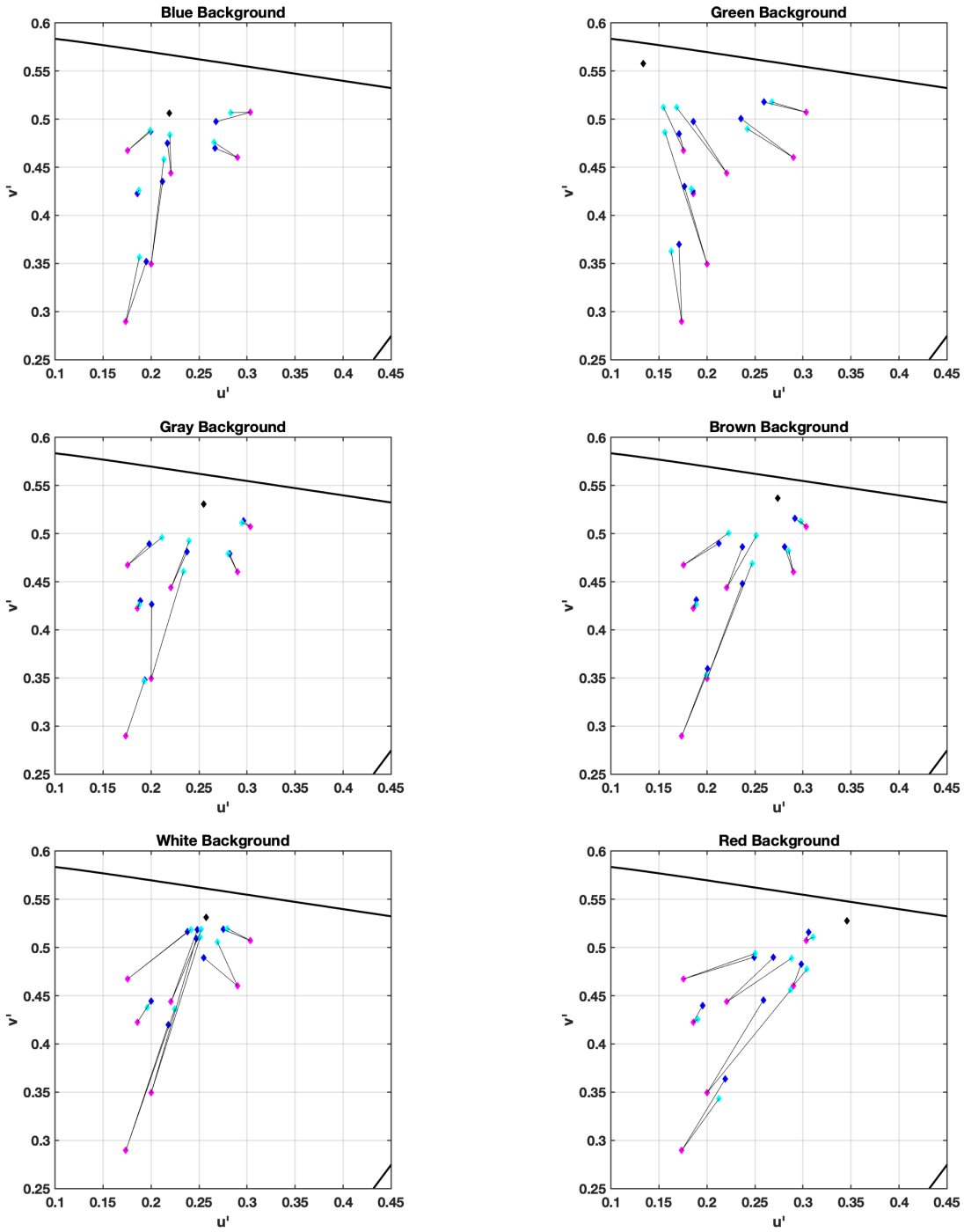

Fig. 9.4 – Results of using XYZ approach to predict perception of the mix content in AR in CIE 1976 UCS space for color matching experiment with simple stimuli (warm light session). The black, magenta, blue and cyan diamonds represent background color, foreground color, average color match by observers and predicted color by tristimulus modification approach respectively.

From Table 9.1, we see that the α values for color matching experiment with simple stimuli are very similar for both sessions (with different lighting). However, α values for the color matching experiment with complex

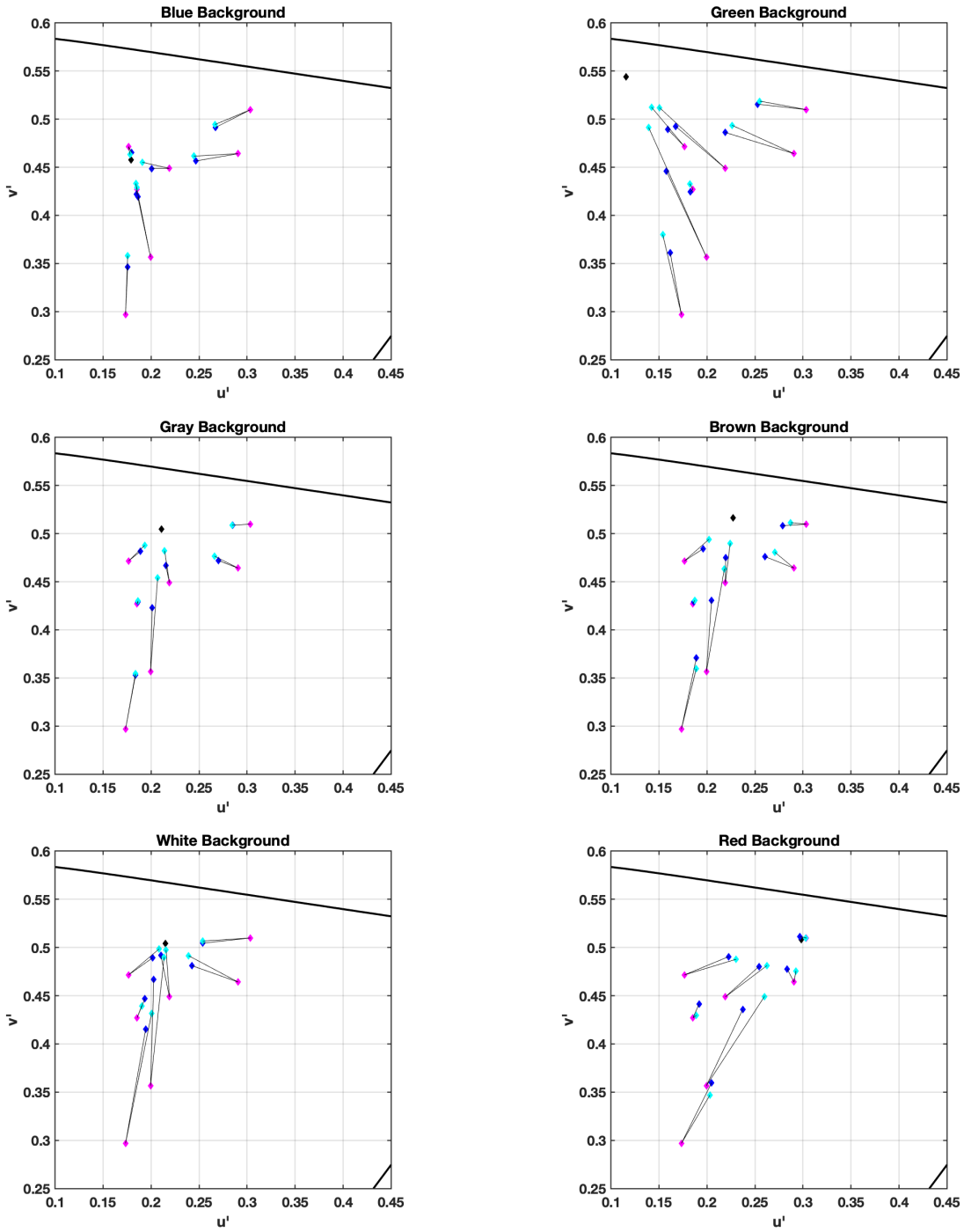

Fig. 9.5 – Results of using XYZ approach to predict perception of the mix content in AR in CIE 1976 UCS space for color matching experiment with simple stimuli (cool light session). The black, magenta, blue and cyan diamonds represent background color, foreground color, average color match by observers and predicted color by tristimulus modification approach respectively.

stimuli are different. We see that the ratio of $\frac{\alpha(2)}{\alpha(1)}$ is larger in comparison to the same values for the other two

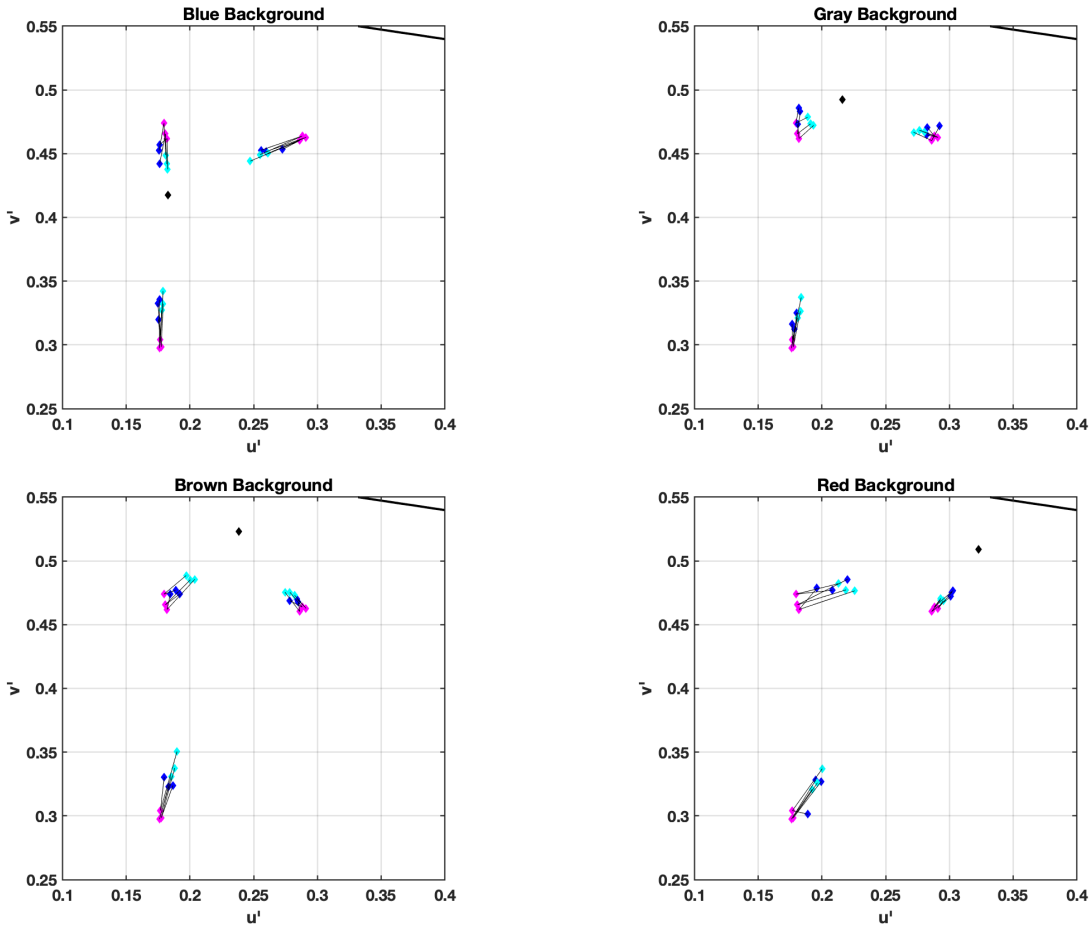

Fig. 9.6 – Results of using XYZ approach to predict perception of the mix content in AR in CIE 1976 UCS space for color matching experiment with complex stimuli. The black, magenta, blue and cyan diamonds represent background color, foreground color, average color match by observers and predicted color by tristimulus modification approach respectively.

experiments. This can be because since in the color matching experiment with complex stimuli, there were more cues available to the observers revealing the transparency (dimension and texture), observers see the stimuli more as a separate layers than mixed. To further study this, α was fitted separately for each subset of the stimuli in the color matching experiment with complex stimuli regarding the level of complexity. The same optimization method as before was used. Table 9.2 shows the resulting values.

Tab. 9.2 – Values of the constant α for the stimuli with different visual complexity levels in the color matching experiment with complex stimuli

Stimulus	Complexity Scale	$\alpha(1)$	$\alpha(2)$	$\frac{\alpha(2)}{\alpha(1)}$
Square with no texture	15	1.59	3.11	1.94
Cube with high frequency low depth texture	50	1.21	2.65	2.17
Spiky shaped with low frequency high depth texture	85	0.65	3.84	5.90

From Table 9.2, we see that as the complexity scale of the stimuli increased, the ratio of $\frac{\alpha(2)}{\alpha(1)}$ increased as well. This means that as the stimulus became more complex, less light contribution of the background and more light contribution of the foreground was perceived. The predictions of the tristimulus values were then used as input to CAM16 to predict the appearance in AR. The surrounding was set to 'dim' and the background white was used as the white point. The results of Jab predictions are presented in Figures 9.7, 9.7, and 9.9.

Figures 9.7, 9.8, and 9.9 show the predicted appearance by the second approach in CAM16 UCS a'-b' space. In these plots, the black diamond shows the color of the background, blue diamonds show the average matched color by the observers, green circles depict the predictions by the second approach and the magenta diamonds depict measurements of the mix light transferred to Jab using CAM16. From the figures, it is clear that the second approach improves appearance predictions by CAM16 (also see Table 9.3). This improvement is specifically notable for results of the color matching experiment with complex stimuli. Similar results were obtained in terms of J as well.

9.3.3 Other Approaches

Other approaches were also tested. One other approach was to add impacts of simultaneous contrast (local adaptation) to the second approach. In this approach (Approach3/ XYZ+White), after the tristimulus values were predicted using the second approach, the white point was also modified regarding the background color (see Equation 5.1); the tristimulus values of the predicted mix and the modified white point were then used as input to CAM16 to achieve appearance parameters.

Another approach was to combine the first and the second approach together (Approach4 /XYZ+CAM). In this case, after predicting the tristimulus values of the mix using the second approach, the tristimulus values were used as input to CAM16. Then the output Jab was modified using the first approach. Since these approaches did not improve the predictions (and in many cases worsened them, the results of these approaches are not depicted in figures and are only compared to the other approaches in Table 9.3.

Performance Comparison

Table 9.3 shows the performances of all the taken approaches.

As we see from Table 9.3, all the approaches improve CAM16 predictions from just using the measured mix as an input to CAM16 with no modifications. XYZ approach has very good results for all the datasets. When comparing XYZ approach and XYZ+CAM approach, it is notable that XYZ+CAM approach (combining approach

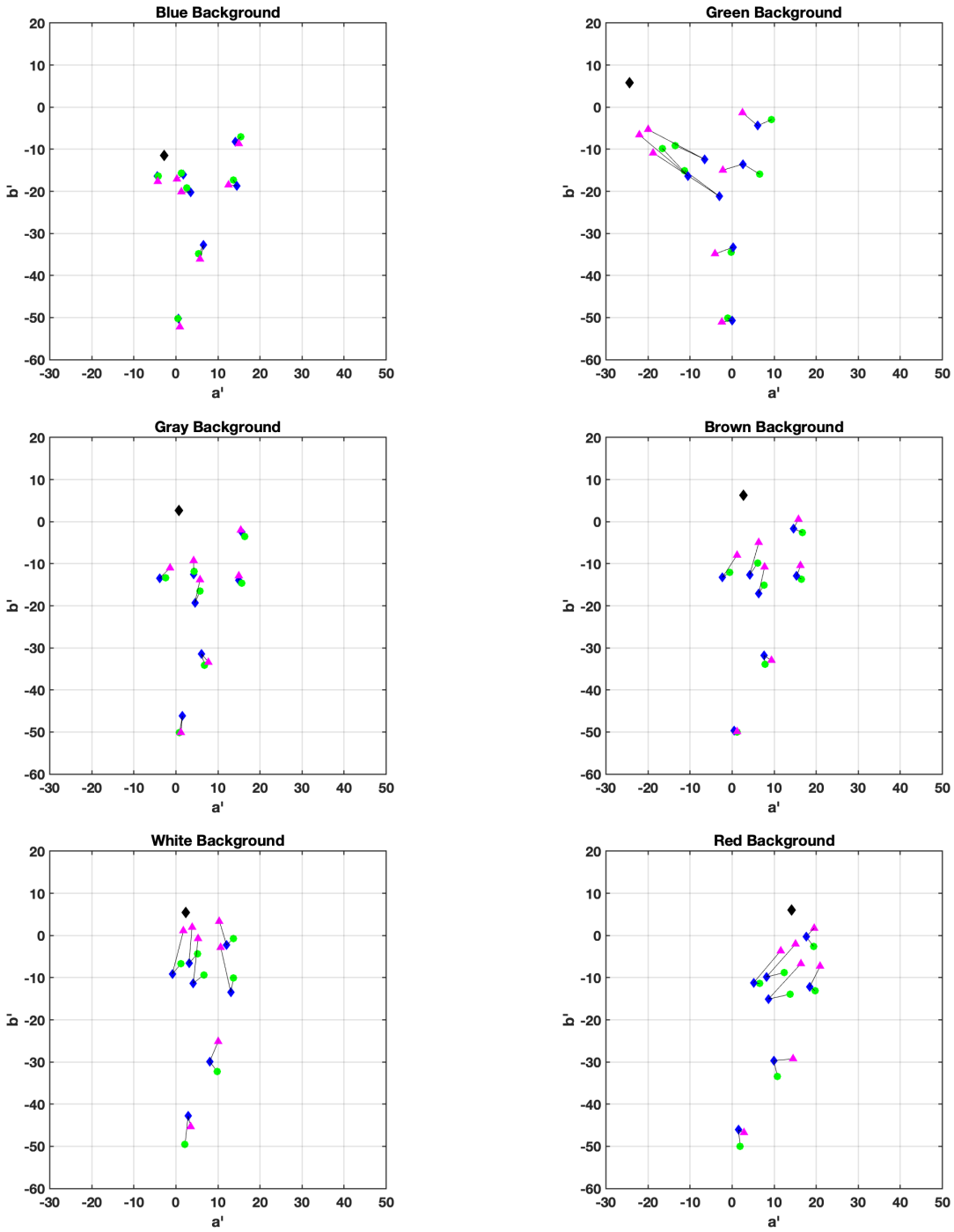

Fig. 9.7 – Results of using XYZ approach to predict perception of the mixed content in AR in CAM16 UCS space for color matching experiment with simple stimuli (warm light session). The black, magenta, blue and green diamonds represent background color, measured mix color average color match by observers and predicted color by tristimulus modification approach respectively.

one and two) has slightly better results than XYZ approach for the results of color matching experiment with

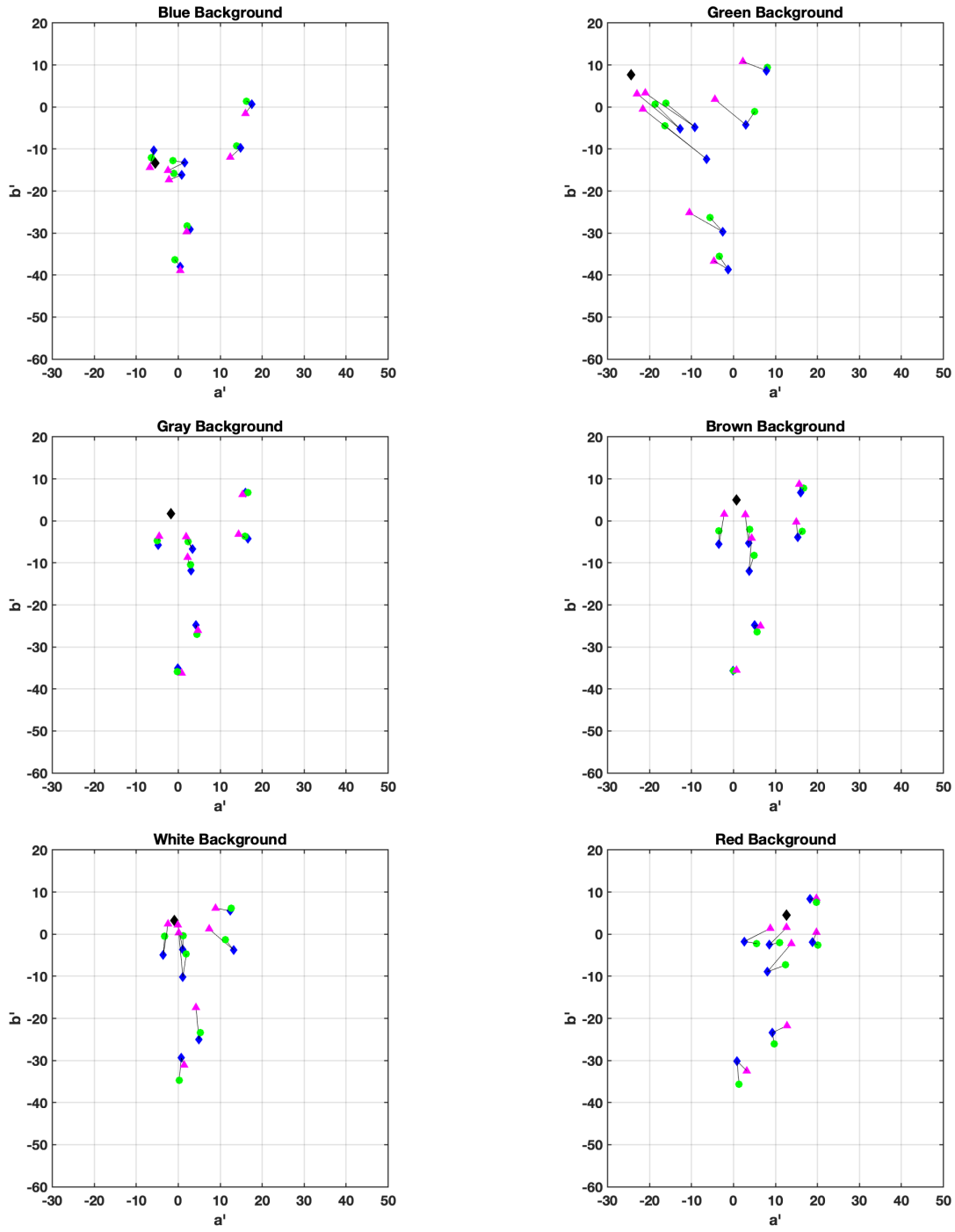

Fig. 9.8 – Results of using XYZ approach to predict perception of the mixed content in AR in CAM16 UCS space for color matching experiment with simple stimuli (cool light session). The black, magenta, blue and green diamonds represent background color, measured mix color average color match by observers and predicted color by tristimulus modification approach respectively.

simple stimuli (Cool light). However, XYZ+CAM approach is very less accurate in predicting the appearance

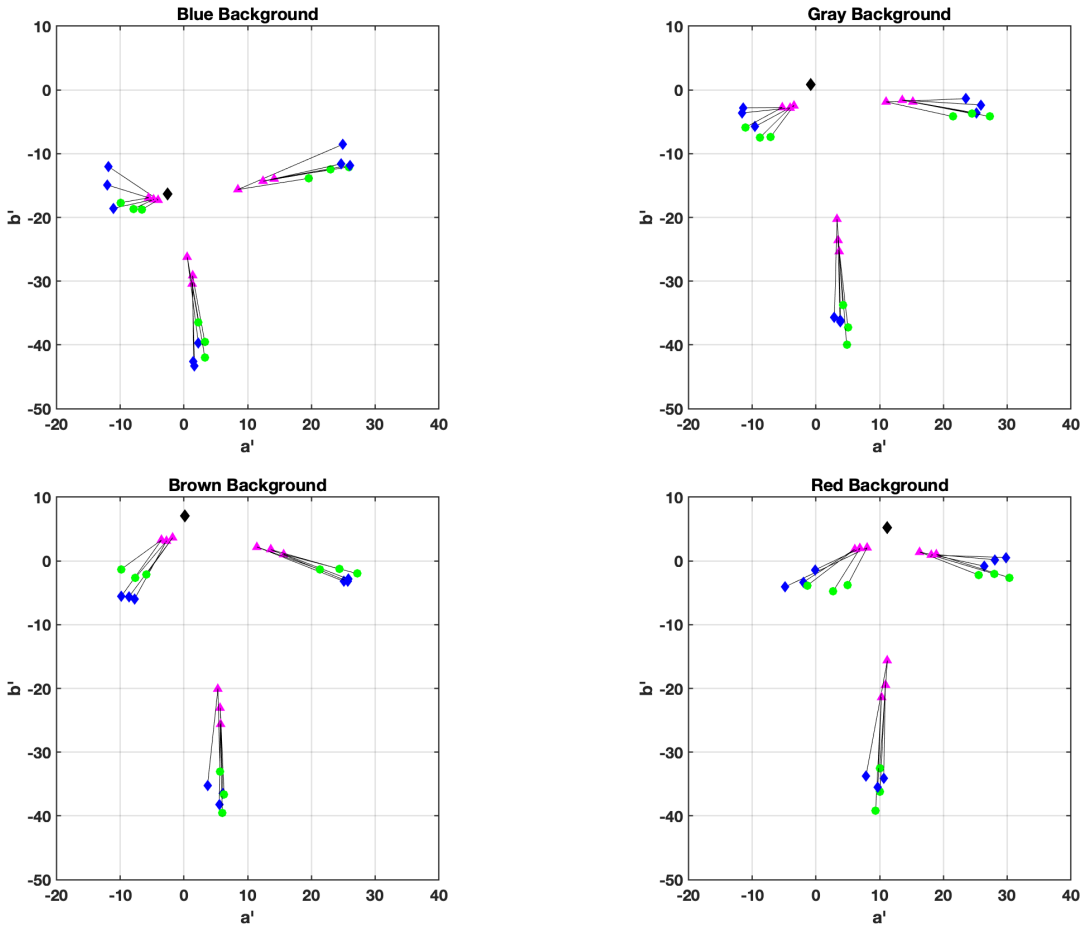

Fig. 9.9 – Results of using XYZ approach to predict perception of the mixed content in AR in CAM16 UCS space for color matching experiment with complex stimuli. The black, magenta, blue and green diamonds represent background color, measured mix color average color match by observers and predicted color by tristimulus modification approach respectively.

Tab. 9.3 – Comparison of the performances of each approach to model color appearance in AR

Average Euclidean difference (J'a'b')	Measured mix	Approach 1	Approach 2	Approach 3	Approach 4
Experiment with simple stimuli (Warm light)	17.92	12.57	6.87	17.64	6.95
Experiment with simple stimuli (Cool light)	14.96	10.67	6.49	14.40	5.47
Experiment with complex stimuli	42.13	26.24	10.90	11.10	34.06

for the results of color matching experiment with complex stimuli compared to XYZ approach. Overall, XYZ approach gives the best results.

9.4 Summary

In this chapter, all the results of the performed experiments (discussed in previous chapters) were used to model color appearance for AR. Four approaches were tested. The first approach (CAM approach) was to modify CAM16 predictions (using measured mix tristimulus values as input). Second approach was based on researches done on transparency. In Approach 2 (XYZ approach), the tristimulus values of the mix color were predicted from the background and foreground tristimulus values. Approach 3 (XYZ+White) added local adaptation to Approach 2 and Approach 4 (XYZ+CAM) was a combination of Approach 1 and 2. The steps of the approaches were explained and the predictions by them were calculated for all the datasets of the 3D and 2D color matching experiments. Comparison of the performances showed that Approach 2 (XYZ approach) performs best among all the approaches. The α values were fitted to the used datasets in this approach and from the results it seems that α depends on the visual complexity of the stimuli. Using this approach for future datasets, the α values should be fitted for the new dataset.

10 Conclusions

The color appearance of real objects and images have been studied and modeled for decades. However, with the arrival of augmented reality technology, there is a new need to study and model color appearance in such environment. AR is a combination of real world and display images superimposed over it, having applications in many areas such as design, education, medicine, gaming etc. Since AR is a relatively new technology, most of the efforts have been focused on bringing this technology to life and therefore the focus has been more on the technology sides of it. However, if the future of AR is to be widely used as the new human-computer interaction platform, understanding color perception in this environment and being able to control it would be vital. In order to model color appearance in AR, different experiments were designed and performed to answer different questions. Instead of starting from zero, the available color appearance model CAM16 was used as a base to build upon the modifications needed for AR. This color appearance model was used as it is one of the most comprehensive color appearances and it is reversible.

At first, some measurements were done in AR environment to better understand the light mixture in AR. An AR simulator was built to have a controllable AR environment to perform the measurements and other experiment. The AR simulator included a light booth with controllable lighting, a display and a half-silvered mirror to optically superimpose the display content over the physical background, which was inside the light booth. Measurements were done from simple 2D solid color patches printed and put under two different lighting, a warm light and a cool light with similar brightness level, simple 2D solid color patches as overlays (depicted on the display and measured from the observer's point of view (reflected from the half-silvered mirror), and the mix appearance of the overlay (foreground) patches over the real physical patches under the two lighting. These measurements showed that when the overlay patches are superimposed on the physical background patches, the mix color convergence from the color of the overlay patch towards the color of the physical background patch. This trend was similar for both lighting sessions.

Next, color perception in the AR simulator was studied. For this purpose, a psychophysical color matching experiment was designed. Six physical background colors were chosen for the 2D solid color background patches and seven different colors were chosen for the foreground patches (smaller than the background patches). Only 2D solid patches were used in the design of the stimuli to keep the experiment simple and only include the impact of background and foreground color and the lighting and not shape or texture. The stimuli were presented in pairs with a patch overlaid on a randomly chosen color background and the other

patch overlaid on black adjacent to the color background. In order to have this presentation of stimuli, the physical background was designed to have a black column in the middle. Observers were asked to modify the patch overlaid on black in terms of hue, chroma and lightness to match it to the color of the patch overlaid on the color background. The results of the color matching were then compared to predictions by CAM16. The measurements of the mix colors (foreground patch overlaid on the background patch) and the tristimulus values of the white physical background (as the adapting white point) was used as input to CAM16. This comparison showed that CAM16 is not accurate in predicting the color appearance in AR environment. The predictions were closer to background color than what the observer had perceived.

A question that was interesting to answer was how different is color perception in AR from color perception from a single display? Because after all, AR is simply showing display content in front of your eyes and it's transparent. To answer this question, the previous color matching experiment was replicated on a single display. The colors of background and foreground were re-rendered on the display and to replicate the mix appearance, whenever a similar presentation to having an overlay patch on a physical patch was meant to be presented, the color of the mix appearance would be presented on the middle of the color background. Observers were asked to do the same task as in previous color matching experiment: to modify the patch on black background in terms of hue, chroma and lightness to match it to the small patch on the color background patch. The results of this experiment were then compared to results of the color matching experiment in the AR simulator and it was noted that the two datasets were statistically significantly different. This means that although the AR environment consists of display content overlaid on the physical world, the perception of color in AR environment is not simply similar to display color perception. This is might be due to differences in adaptation states for the two experiments or due to a difference in phenomenology (since in the experiment performed in the AR simulator the background was a real physical object while in the display experiment it was an image).

The next step to study color perception in AR was to study the color perception of more visually complex stimuli than simple 2D patches with solid colors. This was necessary as in real applications of AR, 3D and more complex objects are depicted as overlays and just modeling the color perception in AR for simple patches would not represent those cases. Therefore, a new experiment was needed to be designed. However, first it was needed to have a scale of visual complexity. This was necessary because in order to implement impacts of the visual complexity in AR color appearance model, a scale was needed. This resulted in designing a scaling experiment for visual complexity. This experiment was a psychophysical direct scaling having stimuli with two different base shapes (square and circle), these shapes were extended to different complexity levels. In case of the square, the shapes included a square, a cube and a spiky shaped stimulus and in case of the circle these were circle, sphere and a blob. Also, different levels of texture were applied. There were stimuli with no texture (visual complexity level 1), low depth texture with high frequency (visual complexity level 2) and high depth texture with low frequency (visual complexity level 3). A graphical user interface (GUI) was

designed including two anchor stimuli (15 and 85 %) and a slider to represent the visual complexity scale. The stimuli would be depicted randomly and the observers would use the slider to scale the visual complexity of the test stimulus. The results showed that as the dimension of the shape increased (from 2D to 3D), the visual complexity increased as well. Also, stimuli with high depth and low frequency textures were perceived as more complex. The choice of basic shape did not impact the visual complexity for example there was no difference between the square and circle in terms of visual complexity. The results of this experiment were also used to build a scale for visual complexity of the used stimuli which could be used later in the modeling.

The next experiment was designed to study color perception in AR for more visually complex stimuli. This was a color matching experiment similar to previous color matching experiments. However, instead of having only simple 2D stimuli with solid color, the stimuli included both 2D and 3D objects with different texture levels. Observers were asked to do the same task and the experiment was done using the AR simulator. The new stimuli were also measured using a Photo research PR655 spectrophotometer and these measurements were used as input to CAM16 color appearance model to predict the color appearance for these stimuli. For the stimuli with texture. These measurements would average the color over the devices aperture (1 degree). By comparing the predictions by CAM16 and the average matched color by the observers it was noted that the predictions are not accurate and become less accurate as the visual complexity increases.

The results of all the experiments were then used to build up approaches to model color appearance in AR environment. CAM16 was used as the base model and then some steps were added to include the perceptual phenomena in AR environment. As it was resulted from previous experiments, the predictions by CAM16 were always closer to the background color than the average matched color by the observers. This was implied in the first approach to make the predictions closer to the average of the observers' perceived color. Adding the impact of visual complexity however would not change the results significantly while it would add to the cost for the model. For this reason, this was excluded from the new model. In the second approach, tristimulus values of the mixed content was predicted using the background and foreground color tristimulus values. This approach was based on transparency perception modeling researches. The results of this approach showed more accurate predictions than approach 1. Two other approaches were tested as well. In approach 3, local adaptation was added to the first approach predictions and in Approach 4, the first two approaches were combined. The results showed that Approach 2 (predicting tristimulus values of the mixed content) had the best predictions among all approaches.

In this dissertation, color appearance in AR was studied. Datasets were built using measurements of the light in AR environment and performing psychophysical experiments. Color perception in AR and form a regular display was compared which showed that they are different (probably a difference in adaptation state). A psychophysical scaling experiment was performed to scale the visual complexity of stimuli in AR. This was important as stimuli with different visual complexity evoke different levels of transparency. The results of the

experiments were used to model color appearance in AR. Four approaches were taken. The best approach was based on modeling the tristimulus values of the mixed content based on the background and foreground color.

10.1 Future Work

There are still interesting questions to answer in order to fully understand color perception in AR environment and be able to control it. An important area is building more datasets and testing the model performance with independent datasets. Since there has not been much effort on studying color perception in AR, there is not a big dataset available. Therefore, more effort can be done to produce more psychophysical color datasets to better model the color perception in AR. Also, there is more research needed to analyze and model the α parameter in the approach 2.

One important subject is adaptation. In previous experiments, adapting white point was assumed to be the average of the white background present in the scene and the display white (color matching experiment in AR for 2D stimuli discussed in Chapter 5) or the white background present in the scene (for the color matching experiment with more visually complex stimuli discussed in Chapter 8 and the model discussed in Chapter 9). However, it would be interesting to conduct experiments to verify what is adapting white point in different scenarios in AR environment.

Another interesting topic is color perception and adaptation dynamically. As AR is intended to be used dynamically and while moving through different environments (indoor and outdoor), it is very important to understand the adaptation and color perception in such cases.

Depth level can also be further investigated by conducting experiments with the virtual content (overlay) presented in different depth levels. In all the performed experiments discussed in this dissertation, the virtual overlays were always registered at the same depth level as the real physical background. However, this would not be the case in real applications of AR and the virtual content might be presented at different levels. Therefore, it is necessary to study the impact of having the virtual overlay at different depth levels on perception of the mix appearance in AR.

10.2 Publications

10.2.1 Journal Publications

- N. Hassani, M.J. Murdoch, "Investigating Color Appearance in Optical See-Through Augmented Reality," Color Research & Application. 2019; 44(4) 492-507 https://doi.org/10.1002/col.22380

- N. Hassani, M.J. Murdoch , "New Approaches to Predict Color Appearance in Optical See-Through Augmented Reality ," Color Research & Application (**In Preparation**)

10.2.2 Conference Publications

- N. Hassani, Susan.P Farnand, "Color Discrimination Threshold for Medical Test Devices," Society for Imaging Science and Technology, pp.60-66 (2017)

- N. Hassani, M.J. Murdoch, "Color appearance modeling in augmented reality," ACM Symposium on Applied Perception, pp.132-132 (2018)(poster session)

- N. Hassani, M.J. Murdoch, " Scaling the Visual Complexity of simple graphical psychophysical experiments," (**In Preparation**)

11 Appendix A: Light Measurements in AR

Tables below show measurements performed inside the AR simulator from the illuminants (a cool and a warm light), background patches, virtual foreground content and the mix color. All the measurements were performed from the observer's point of view(through the half-silvered mirror).

Tab. 11.1 – Measured illuminants inside the AR simulator from a perfect reflecting diffuser put at the bottom of the booth

Light	X	Y	Z
Cool light	6.198	6.477	4.033
Warm light	7	6.425	1.796

Tab. 11.2 – Measured background patches inside the AR simulator under the warm light

Background color	X	Y	Z
Green	1.006	1.803	0.3772
Blue	2.052	2.114	1.247
Brown	1.857	1.616	0.3319
Gray	1.629	1.519	0.4328
Red	1.867	1.284	0.2387
White	7.464	6.856	1.928

Tab. 11.3 – Measured background patches inside the AR simulator under the cool light

Background color	X	Y	Z
Green	1.006	2.073	0.7478
Blue	2.018	2.293	2.785
Brown	1.595	1.6	0.7251
Gray	1.438	1.533	0.9718
Red	1.486	1.138	0.5074
White	6.605	6.908	4.309

Tab. 11.4 – Measured foreground patches inside the AR simulator under the warm light

Foreground color	X	Y	Z
Brown	0.4851	0.4332	0.6014
Green	0.5833	0.6893	0.783
Orange	3.762	2.795	1.303
Blue	1.532	1.134	5.574
Red	2.175	1.535	1.606
Purple	0.3458	0.2682	0.8473
White	15.47	15.64	27.73

Tab. 11.5 – Measured foreground patches inside the AR simulator under the cool light

Foreground color	X	Y	Z
Brown	0.4441	0.4042	0.5328
Green	0.5438	0.6456	0.6977
Orange	3.467	2.588	1.13
Blue	1.361	1.035	4.835
Red	1.982	1.407	1.398
Purple	0.3105	0.2468	0.7386
White	14.19	14.52	24.66

Tab. 11.6 – Measured mix patches inside the AR simulator under the warm light

Background color	Foreground color	X	Y	Z
Green	Brown	1.519	2.224	1.038
	Green	1.614	2.503	1.239
	Orange	5.203	4.867	1.801
	Blue	2.685	3	6.492
	Red	3.409	3.448	2.112
	Purple	1.355	2.038	1.292
	White	18.42	19.4	31.58
Blue	Brown	2.403	2.387	1.824
	Green	2.518	2.684	2.019
	Orange	6.252	5.142	2.602
	Blue	3.63	3.209	7.526
	Red	4.369	3.658	2.942
	Purple	2.241	2.208	2.085
	White	20.3	20.44	34.48
Brown	Brown	2.276	2.014	0.9167
	Green	2.372	2.273	1.11
	Orange	5.829	4.564	1.602
	Blue	3.349	2.747	5.951
	Red	4.093	3.1850	1.92
	Purple	2.113	1.84	1.151
	White	18.48	18.57	29.42
Gray	Brown	1.942	1.786	0.9904
	Green	2.059	2.058	1.171
	Orange	5.324	4.206	1.669
	Blue	2.987	2.494	5.897
	Red	3.67	2.905	1.981
	Purple	1.819	1.637	1.222
	White	17.58	17.64	29.22
Red	Brown	2.212	1.606	0.6759
	Green	2.292	1.825	0.8192
	Orange	5.161	3.718	1.221
	Blue	3.042	2.207	4.588
	Red	3.727	2.583	1.458
	Purple	2.065	1.463	0.8551
	White	15.48	15.22	23.27
White	Brown	7.498	6.867	2.296
	Green	7.569	7.081	2.431
	Orange	10.32	8.879	2.826
	Blue	8.31	7.435	6.109
	Red	8.919	7.788	3.051
	Purple	7.372	6.729	2.455
	White	20.31	19.89	24.51

Tab. 11.7 – Measured mix patches inside the AR simulator under the cool light

Background color	Foreground color	X	Y	Z
Green	Brown	1.512	2.466	1.363
	Green	1.619	2.755	1.539
	Orange	5.148	5.084	2.075
	Blue	2.641	3.23	6.654
	Red	3.377	3.665	2.39
	Purple	11.347	2.287	1.577
	White	18.34	19.57	31.79
Blue	Brown	2.321	2.492	3.193
	Green	2.437	2.792	3.369
	Orange	6.123	5.22	3.937
	Blue	3.527	3.299	8.767
	Red	4.266	3.757	4.272
	Purple	2.172	2.319	3.417
	White	20.07	20.35	35.55
Brown	Brown	2.001	1.973	1.27
	Green	2.107	2.243	1.457
	Orange	5.522	4.499	1.962
	Blue	3.063	2.707	6.181
	Red	3.79	3.132	2.259
	Purple	1.851	1.806	1.52
	White	18.01	18.34	29.45
Gray	Brown	1.752	1.774	1.436
	Green	1.831	2.012	1.6
	Orange	5.045	4.142	2.086
	Blue	2.757	2.466	6.201
	Red	3.424	2.856	2.385
	Purple	1.594	1.599	1.658
	White	17.11	17.35	29.18
Red	Brown	1.834	1.458	0.9242
	Green	1.919	1.683	1.089
	Orange	4.78	3.556	1.461
	Blue	2.654	2.046	4.789
	Red	3.315	2.421	1.691
	Purple	1.692	1.314	1.103
	White	15.05	15.01	23.29
White	Brown	6.782	7.017	4.587
	Green	6.847	7.222	4.716
	Orange	9.593	9.02	5.1
	Blue	7.598	7.583	8.443
	Red	8.203	7.923	5.347
	Purple	6.645	6.871	4.753
	White	19.62	20.06	26.99

12

Appendix B: Color matching in AR simulator with simple stimuli

Tables below show the average matched color by the observers in terms of XYZ. The tables show what XYZ was matched for each foreground background combination (presented in the table).

Tab. 12.1 – Average matched XYZ by the observers for the color matching for sessions with the warm light on

Background color	Foreground color	X	Y	Z
Green	Brown	1.00	1.19	0.89
	Green	1.46	1.84	1.70
	Orange	5.14	4.56	1.91
	Blue	2.42	2.32	6.44
	Red	3.15	2.98	1.91
	Purple	1.60	1.73	2.89
	White	18.56	18.95	32.77
Blue	Brown	1.14	1.11	1.08
	Green	1.48	1.61	1.37
	Orange	5.60	4.62	2.90
	Blue	2.59	2.08	6.46
	Red	3.66	2.87	2.75
	Purple	1.05	0.96	1.46
	White	17.63	17.83	31.46
Brown	Brown	1.16	1.06	0.85
	Green	1.44	1.47	1.17
	Orange	4.80	3.78	1.47
	Blue	2.26	1.80	5.28
	Red	3.20	2.46	1.81
	Purple	1.17	0.98	1.28
	White	17.34	17.59	28.68
Gray	Brown	0.91	0.82	0.70
	Green	0.90	0.98	0.81
	Orange	4.12	3.18	1.31
	Blue	1.90	1.51	4.88
	Red	2.56	1.93	1.59
	Purple	1.45	1.37	2.31
	White	14.90	15.10	24.83
Red	Brown	1.21	0.98	0.70
	Green	1.86	1.63	1.20
	Orange	5.08	3.81	1.40
	Blue	2.14	1.57	4.42
	Red	3.25	2.34	1.76
	Purple	0.90	0.69	0.90
	White	15.31	15.30	22.76
White	Brown	4.08	3.78	1.62
	Green	4.43	4.27	1.98
	Orange	6.11	5.12	1.97
	Blue	3.65	3.13	5.49
	Red	5.53	4.72	3.48
	Purple	4.27	3.91	2.06
	White	14.21	14.03	19.88

Tab. 12.2 – Average matched XYZ by the observers for the color matching for sessions with the cool light on

Background color	Foreground color	X	Y	Z
Green	Brown	1.29	1.68	1.41
	Green	1.39	1.90	1.69
	Orange	6.06	5.49	2.47
	Blue	3.036	3.01	8.95
	Red	2.95	2.91	2.42
	Purple	0.99	1.24	1.82
	White	20.10	20.75	36.11
Blue	Brown	1.91	1.89	2.56
	Green	1.47	1.69	1.96
	Orange	5.74	4.69	3.28
	Blue	2.74	2.40	7.91
	Red	3.40	2.80	3.26
	Purple	1.24	1.24	2.27
	White	17.88	18.15	32.36
Brown	Brown	1.28	1.23	1.19
	Green	1.52	1.67	1.49
	Orange	5.20	4.21	2.07
	Blue	2.29	2.00	5.41
	Red	3.41	2.77	2.46
	Purple	0.91	0.85	1.36
	White	17.09	17.47	29.17
Gray	Brown	1.02	0.99	1.07
	Green	1.01	1.14	1.07
	Orange	4.20	3.33	1.58
	Blue	1.82	1.55	4.84
	Red	2.90	2.25	2.09
	Purple	0.65	0.61	1.05
	White	15.79	16.13	26.93
Red	Brown	1.21	1.02	0.86
	Green	1.56	1.53	1.19
	Orange	4.52	3.45	1.49
	Blue	2.16	1.68	4.92
	Red	3.16	2.36	1.97
	Purple	0.85	0.69	1.02
	White	15.76	16.13	23.73
White	Brown	4.02	4.18	3.26
	Green	4.34	4.68	3.85
	Orange	6.25	5.52	3.14
	Blue	5.34	5.07	9.50
	Red	4.91	4.34	3.71
	Purple	5.74	5.87	6.45
	White	17.26	17.71	24.58

13 Appendix B: Color matching on a display

Tables below show the average matched color by the observers for the color matching experiment on a display in terms of XYZ. The tables show what XYZ was matched for each foreground background combination (presented in the table).

Tab. 13.1 – Average matched XYZ by the observers for the color matching on a display

Background color	Foreground color	X	Y	Z
Green	Brown	2.09	2.72	3.11
	Green	1.97	2.70	3.21
	Orange	5.76	5.27	4.04
	Blue	3.28	3.60	12.66
	Red	4.84	4.68	4.96
	Purple	1.51	2.09	3.30
	White	16.84	16.91	43.10
Blue	Brown	1.99	1.95	3.93
	Green	1.90	2.11	4.03
	Orange	6.47	5.04	4.71
	Blue	3.10	2.63	12.57
	Red	4.37	3.43	5.81
	Purple	1.83	1.76	4.93
	White	17.36	17.12	43.47
Brown	Brown	1.71	1.59	2.06
	Green	2.13	2.17	2.56
	Orange	5.60	4.40	3.41
	Blue	2.99	2.46	9.60
	Red	4.20	3.31	4.18
	Purple	1.71	1.57	2.71
	White	18.21	17.64	45.53
Gray	Brown	1.23	1.14	1.73
	Green	1.42	1.51	2.10
	Orange	4.76	3.62	2.84
	Blue	2.22	1.79	8.42
	Red	2.91	2.21	3.12
	Purple	1.30	1.17	2.71
	White	15.57	15.18	40.18
Red	Brown	1.80	1.44	1.92
	Green	2.26	2.03	2.36
	Orange	5.13	3.76	2.68
	Blue	2.88	2.16	8.53
	Red	3.85	2.78	3.66
	Purple	1.51	1.19	2.17
	White	16.86	16.10	40.69
White	Brown	8.97	8.79	9.08
	Green	8.73	8.81	9.40
	Orange	9.38	8.11	7.10
	Blue	8.63	8.00	17.82
	Red	7.41	6.55	7.41
	Purple	11.71	11.51	13.20
	White	18.55	18.17	41.09

14

Appendix B: Color matching in AR simulator with Complex stimuli

Tables below show the average matched color by the observers for the color matching experiment for visually complex stimuli terms of XYZ. The tables show what XYZ was matched for each foreground background combination (presented in the table).

Tab. 14.1 – Average matched XYZ by the observers for the color matching experiment with visually complex stimuli

Background color	Foreground color	Stimulus	X	Y	Z
Blue	Green	Square	3.56	3.97	5.90
		Cube	3.11	3.56	4.77
		Spiky	2.55	2.94	3.75
	Blue	Square	6.22	5.26	19.07
		Cube	6.94	5.87	20.86
		Spiky	5.09	4.13	16.39
	Red	Square	8.00	6.29	7.56
		Cube	8.02	6.19	7.49
		Spiky	5.78	4.27	4.99
Brown	Green	Square	2.15	2.36	2.42
		Cube	2.25	2.53	2.51
		Spiky	1.50	1.71	1.77
	Blue	Square	4.47	3.45	13.22
		Cube	4.74	3.71	14.34
		Spiky	4.03	3.29	12.09
	Red	Square	6.62	4.95	4.73
		Cube	6.35	4.67	4.33
		Spiky	5.31	3.87	3.71
Gray	Green	Square	1.90	2.22	2.06
		Cube	1.67	1.98	1.77
		Spiky	1.41	1.64	1.73
	Blue	Square	4.16	3.33	12.72
		Cube	3.69	2.87	12.02
		Spiky	3.69	2.94	11.95
	Red	Square	6.06	4.48	4.14
		Cube	5.59	4.09	4.09
		Spiky	4.27	3.06	2.73
Red	Green	Square	2.28	2.24	1.87
		Cube	1.76	1.79	1.73
		Spiky	1.39	1.51	1.45
	Blue	Square	4.22	3.07	11.42
		Cube	4.66	3.48	12.88
		Spiky	3.54	2.51	11.27
	Red	Square	6.70	4.69	3.82
		Cube	5.70	3.99	3.32
		Spiky	4.82	3.36	2.94

References

[Azuma, 1997]
Azuma, Ronald T (1997). “A survey of augmented reality”. In: *Presence: Teleoperators & Virtual Environments* 6.4, pp. 355–385 (Cited on page 13).

[Bajorski, 2011]
Bajorski, Peter (2011). *Statistics for imaging, optics, and photonics*. Vol. 808. John Wiley & Sons (Cited on page 65).

[Beato, Zhang, Colbert, Yamazawa, and Hughes, 2009]
Beato, Nicholas, Yunjun Zhang, Mark Colbert, Kazumasa Yamazawa, and Charles E. Hughes (2009). “Interactive chroma keying for mixed reality”. In: *Computer Animation and Virtual Worlds* 20.2-3, pp. 405–415 (Cited on pages 13, 14).

[Beck, 1978]
Beck, Jacob (1978). “Additive and subtractive color mixture in color transparency”. In: *Attention, Perception, & Psychophysics* 23.3, pp. 265–267 (Cited on page 23).

[Beck, Prazdny, and Ivry, 1984]
Beck, Jacob, K Prazdny, and Richard Ivry (1984). “The perception of transparency with achromatic colors”. In: *Perception & psychophysics* 35.5, pp. 407–422 (Cited on pages 23–26, 29, 32).

[Bimber and Raskar, 2005]
Bimber, O. and R. Raskar (2005). *Spatial augmented reality: merging real and virtual worlds*. CRC press (Cited on pages 10, 12, 14, 15).

[Chen and D’Zmura, 1998]
Chen, Vincent J and Michael D’Zmura (1998). “Test of a convergence model for color transparency perception”. In: *Perception* 27.5, pp. 595–608 (Cited on page 23).

[CIE, 1986]
CIE (1986). “CIE Publication No. 15.2”. In: *Commission Internationale de l’éclairage, Vienna*, pp. 19–20 (Cited on pages 17, 50).

[CIE, 1998]
CIE (1998). “The CIE 1997 interim colour appearance model (simple version), CIECAM97s”. In: *Commission Internationale de l’éclairage, Vienna* (Cited on page 18).

[D'Zmura, Colantoni, Knoblauch, and Laget, 1997]
D'Zmura, Michael, Philippe Colantoni, Kenneth Knoblauch, and Bernard Laget (1997). "Color transparency". In: *Perception* 26.4, pp. 471–492 (Cited on pages 21, 22, 28, 46, 92).

[D'Zmura, Rinner, and Gegenfurtner, 2000]
D'Zmura, Michael, Oliver Rinner, and Karl R Gegenfurtner (2000). "The colors seen behind transparent filters". In: *Perception* 29.8, pp. 911–926 (Cited on pages 23, 24).

[Ekroll and Faul, 2002]
Ekroll, Vebjørn and Franz Faul (2002). "Perceptual transparency in neon color spreading displays". In: *Perception & psychophysics* 64.6, pp. 945–955 (Cited on pages 28, 29).

[Ekroll and Faul, 2013]
Ekroll, Vebjørn and Franz Faul (2013). "Transparency perception: The key to understanding simultaneous color contrast". In: *JOSA A* 30.3, pp. 342–352 (Cited on page 31).

[Fairchild, 2013]
Fairchild, Mark D (2013). *Color appearance models*. John Wiley & Sons (Cited on pages 17, 18).

[Fairchild and Berns, 1993]
Fairchild, Mark D and Roy S Berns (1993). "Image color-appearance specification through extension of CIELAB". In: *Color Research & Application* 18.3, pp. 178–190 (Cited on page 17).

[Faul, 2017]
Faul, Franz (2017). "Toward a perceptually uniform parameter space for filter transparency". In: *ACM Transactions on Applied Perception (TAP)* 14.2, p. 13 (Cited on page 30).

[Faul and Ekroll, 2002]
Faul, Franz and Vebjørn Ekroll (2002). "Psychophysical model of chromatic perceptual transparency based on substractive color mixture". In: *JOSA A* 19.6, pp. 1084–1095 (Cited on page 29).

[Faul and Ekroll, 2011]
Faul, Franz and Vebjørn Ekroll (2011). "On the filter approach to perceptual transparency". In: *Journal of Vision* 11.7, pp. 7–7 (Cited on pages 29, 30).

[Faul and Ekroll, 2012]
Faul, Franz and Vebjørn Ekroll (2012). "Transparent layer constancy". In: *Journal of Vision* 12.12, pp. 7–7 (Cited on page 30).

[Feiner, 2002]
Feiner, Steven K (2002). "Augmented reality: A new way of seeing". In: *Scientific American* 286.4, pp. 48–55 (Cited on page 1).

[Fleming, Jäkel, and Maloney, 2011]
Fleming, Roland W, Frank Jäkel, and Laurence T Maloney (2011). "Visual perception of thick transparent materials". In: *Psychological science* 22.6, pp. 812–820 (Cited on page 30).

[Gabbard, Swan, Zedlitz, and Winchester, 2010]
Gabbard, J. L., J. E. Swan, J. Zedlitz, and W. W. Winchester (Mar. 2010). "More than meets the eye: An engineering study to empirically examine the blending of real and virtual color spaces". In: *2010 IEEE Virtual Reality Conference (VR)*. 2010 IEEE Virtual Reality Conference (VR), pp. 79–86 (Cited on pages 33, 39, 43, 46).

[Gabbard, Swan, and Zarger, 2013]
Gabbard, Joseph L, J Edward Swan, and Adam Zarger (2013). “Color blending in outdoor optical see-through ar: the effect of real-world backgrounds on user interface color”. In: *2013 IEEE Virtual Reality (VR)*. IEEE, pp. 157–158 (Cited on pages 33, 34).

[Helmholtz and Southall, 2005]
Helmholtz, Hermann von and James Powell Cocke Southall (2005). *Treatise on physiological optics*. Vol. 3. Courier Corporation (Cited on page 19).

[Hincapié-Ramos, Ivanchuk, Sridharan, and Irani, 2014]
Hincapié-Ramos, Juan David, Levko Ivanchuk, Srikanth Kirshnamachari Sridharan, and Pourang Irani (2014). “SmartColor: Real-time color correction and contrast for optical see-through head-mounted displays”. In: *2014 IEEE International Symposium on Mixed and Augmented Reality (ISMAR)*. IEEE, pp. 187–194 (Cited on page 36).

[Ho, Saeedi, Kim, Shen, and Parviz, 2008]
Ho, H., E. Saeedi, S. S. Kim, T. T. Shen, and B. A. Parviz (2008). “Contact lens with integrated inorganic semiconductor devices”. In: *IEEE 21st International Conference on Micro Electro Mechanical Systems*, pp. 403–406 (Cited on page 9).

[Hunt, 1991]
Hunt, RWG (1991). “Revised colour-appearance model for related and unrelated colours”. In: *Color Research & Application* 16.3, pp. 146–165 (Cited on pages 17, 18, 30, 31, 50, 51).

[Ishihara, 1917]
Ishihara, Shinobu (1917). “Tests for color-blindness”. In: *Color and Imaging Conference*. Handaya, Tokyo, Hongo Harukicho (Cited on pages 48, 62).

[Kirschmann, 1892]
Kirschmann, August (1892). “Some effects of contrast”. In: *The American Journal of Psychology* (Cited on page 31).

[Kiyokawa, Billinghurst, Campbell, and Woods, 2003]
Kiyokawa, K., M. Billinghurst, B. Campbell, and E. Woods (2003). “An occlusion capable optical see-through head mount display for supporting co-located collaboration”. In: pp. 133–141 (Cited on page 16).

[LaserMagic]
, LaserMagic. *Holograms 3D Holographic Projection - Laser Magic Productions*. URL: `http://www.laser-magic.com/transscreen.html` (visited on Feb. 27, 2019) (Cited on page 11).

[Li, Li, Wang, Xu, Luo, et al., 2017a]
Li, Changjun, Zhiqiang Li, Zhifeng Wang, Yang Xu, Ming Ronnier Luo, et al. (2017a). “Comprehensive color solutions: CAM16, CAT16, and CAM16-UCS”. In: *Color Research & Application* 42.6, pp. 703–718 (Cited on pages 3, 47).

[Li, Li, Wang, Xu, Luo, et al., 2017b]
Li, Changjun, Zhiqiang Li, Zhifeng Wang, Yang Xu, Ming Ronnier Luo, et al. (2017b). “Comprehensive color solutions: CAM16, CAT16, and CAM16-UCS”. In: *Color Research & Application* 42.6, pp. 703–718 (Cited on pages 18, 50).

[Livingston, Barrow, and Sibley, 2009]
Livingston, M. A., J. H. Barrow, and C. M. Sibley (Mar. 2009). “Quantification of Contrast Sensitivity and Color Perception using Head-worn Augmented Reality Displays”. In: *2009 IEEE Virtual Reality Conference*. 2009 IEEE Virtual Reality Conference, pp. 115–122 (Cited on pages 34, 35).

[Luo, Cui, and Li, 2006]
Luo, M Ronnier, Guihua Cui, and Changjun Li (2006). “Uniform colour spaces based on CIECAM02 colour appearance model”. In: *Color Research & Application: Endorsed by Inter-Society Color Council, The Colour Group (Great Britain), Canadian Society for Color, Color Science Association of Japan, Dutch Society for the Study of Color, The Swedish Colour Centre Foundation, Colour Society of Australia, Centre Français de la Couleur* 31.4, pp. 320–330 (Cited on page 18).

[MacLeod and Boynton, 1979]
MacLeod, Donald IA and Robert M Boynton (1979). “Chromaticity diagram showing cone excitation by stimuli of equal luminance”. In: *JOSA* 69.8, pp. 1183–1186 (Cited on page 22).

[Menk and Koch, 2013]
Menk, C. and R. Koch (Feb. 2013). “Truthful Color Reproduction in Spatial Augmented Reality Applications”. In: *IEEE Transactions on Visualization and Computer Graphics* 19.2, pp. 236–248 (Cited on pages 34, 35).

[Merenda, Smith, Gabbard, Burnett, and Large, 2016]
Merenda, Coleman, Missie Smith, Joseph Gabbard, Gary Burnett, and David Large (2016). “Effects of real-world backgrounds on user interface color naming and matching in automotive AR HUDs”. In: *2016 IEEE VR 2016 Workshop on Perceptual and Cognitive Issues in AR (PERCAR)*. IEEE, pp. 1–6 (Cited on page 36).

[Metelli, 1970]
Metelli, F (1970). “An algebraic development of the theory of perceptual transparency.” In: *Ergonomics* (Cited on page 19).

[Metelli, 1974]
Metelli, Fabio (1974). “The perception of transparency”. In: *Scientific American* 230.4, pp. 90–99 (Cited on pages 19, 20, 24, 26, 29, 32).

[Metelli, Da Pos, and Cavedon, 1985]
Metelli, Fabio, Osvaldo Da Pos, and Adele Cavedon (1985). “Balanced and unbalanced, complete and partial transparency”. In: *Perception & psychophysics* 38.4, pp. 354–366 (Cited on page 26).

[Microsoft]
, Microsoft. *Microsoft HoloLens*. Microsoft HoloLens. URL: `https://www.microsoft.com/en-us/hololens/hardware` (Cited on page 15).

[Milgram and Kishino, 1994]
Milgram, P. and F. Kishino (1994). “A Taxonomy of Mixed Reality Visual Displays”. In: *IEICE Trans Inf. Syst.* E77-D.12, pp. 1321–1329 (Cited on page 7).

[Mirjalili and Parviz, 2012]
Mirjalili, R. and B. A. Parviz (2012). “Microlight-emitting diode with integrated Fresnel zone plate for contact lens embedded display”. In: *MicroNanolithography MEMS MOEMS* 11.3, pp. 033010–033010 (Cited on pages 9, 10).

[Moroney, Fairchild, Hunt, Li, Luo, et al., 2002]
Moroney, Nathan, Mark D Fairchild, Robert WG Hunt, Changjun Li, M Ronnier Luo, et al. (2002). "The CIECAM02 color appearance model". In: *Color and Imaging Conference*. Vol. 2002. 1. Society for Imaging Science and Technology, pp. 23–27 (Cited on pages 3, 17).

[Nakauchi, Silfsten, Parkkinen, and Usui, 1999]
Nakauchi, Shigeki, Pertti Silfsten, Jussi Parkkinen, and Shiro Usui (1999). "Computational theory of color transparency: Recovery of spectral properties for overlapping surfaces". In: *JOSA A* 16.11, pp. 2612–2624 (Cited on page 29).

[Nakayama, Shimojo, and Ramachandran, 1990]
Nakayama, Ken, Shinsuke Shimojo, and Vilayanur S Ramachandran (1990). "Transparency: Relation to depth, subjective contours, luminance, and neon color spreading". In: *Perception* 19.4, pp. 497–513 (Cited on page 27).

[Nayatani, Takahama, Sobagaki, and Hashimoto, 1990]
Nayatani, Yoshinobu, Kotaro Takahama, Hiroaki Sobagaki, and Kenjiro Hashimoto (1990). "Color-appearance model and chromatic-adaptation transform". In: *Color Research & Application* 15.4, pp. 210–221 (Cited on page 17).

[North, Mathieu, Bourquin, and Lucio, 2016]
North, Thibault, Wagner Mathieu, Stéphane Bourquin, and Kilcher Lucio (Sept. 2016). "Compact and High-Brightness Helmet-Mounted Head-Up Display System by Retinal Laser Projection". In: *Journal of Display Technology* 12, pp. 1–1 (Cited on page 16).

[Pandey, Liao, Lingley, Mirjalili, Parviz, et al., 2010]
Pandey, Jagdish, Yu-Te Liao, Andrew Lingley, Ramin Mirjalili, Babak Parviz, et al. (2010). "A Fully Integrated RF-Powered Contact Lens With a Single Element Display". In: *IEEE TRANSACTIONS ON BIOMEDICAL CIRCUITS AND SYSTEMS* 4.6, pp. 454–461 (Cited on page 9).

[Raskar, Welch, Low, and Bandyopadhyay, 2001]
Raskar, R., G. Welch, K.-L. Low, and D. Bandyopadhyay (2001). "Shader lamps: Animating real objects with image-based illumination". In: *Rendering Techniques*, pp. 89–102 (Cited on page 15).

[Ratnasingam and Anderson, 2017]
Ratnasingam, Sivalogeswaran and Barton L Anderson (2017). "What predicts the strength of simultaneous color contrast?" In: *Journal of vision* 17.2, pp. 13–13 (Cited on page 31).

[Ripamonti, Westland, and Da Pos, 2004]
Ripamonti, Caterina, Stephen Westland, and Osvaldo Da Pos (2004). "Conditions for perceptual transparency". In: *Journal of Electronic Imaging* 13.1, pp. 29–36 (Cited on page 28).

[Ryu, Kim, Lee, and Kim, 2016]
Ryu, Je-Ho, Jae-Woo Kim, Kang-Kyu Lee, and Jong-Ok Kim (2016). "Colorimetric background estimation for color blending reduction of OST-HMD". In: *2016 Asia-Pacific Signal and Information Processing Association Annual Summit and Conference (APSIPA)*. IEEE, pp. 1–4 (Cited on page 37).

[Shum, Cowan, Lähdesmäki, A. Lingley, and Parviz, 2009]
Shum, A. J., M. Cowan, I. Lähdesmäki, B. Otis A. Lingley, and B. A. Parviz (2009). "Functional modular contact lens". In: *Proc.SPIE* 7397, pp. 7397–7397–8 (Cited on page 9).

[Singh and Anderson, 2002]
Singh, Manish and Barton L Anderson (2002). “Toward a perceptual theory of transparency.” In: *Psychological review* 109.3, p. 492 (Cited on page 27).

[Smet, Smet, Cuypers, Weng, and Joshi, 2013]
Smet, H., J. Smet, D. Cuypers, C.-P. Weng, and P. Joshi (2013). “A Contact Lens With Built-In Display: Science Fiction or Not?” In: *SID Symposium Digest of Technical Papers* 44, pp. 8–11 (Cited on page 10).

[Sridharan, Hincapié-Ramos, Flatla, and Irani, 2013]
Sridharan, Srikanth Kirshnamachari, Juan David Hincapié-Ramos, David R Flatla, and Pourang Irani (2013). “Color correction for optical see-through displays using display color profiles”. In: *Proceedings of the 19th ACM Symposium on Virtual Reality Software and Technology*. ACM, pp. 231–240 (Cited on page 36).

[Sutherland, 1968]
Sutherland, Ivan E. (1968). “A Head-mounted Three Dimensional Display”. In: *Fall Joint Computer Conference, Part I*, pp. 757–764 (Cited on pages 7, 8).

[Talbot, 1834]
Talbot, H.F. (1834). “Experiments on light”. In: *Philosophical Magazine and Journal of Science* 5.29, pp. 321–334. eprint: `https://doi.org/10.1080/14786443408648474` (Cited on page 19).

[The Pokémon Company]
, The Pokémon Company, Niantic. *The Pokémon Company, Niantic*. URL: `https://www.pokemongo.com/en-us/` (Cited on page 13).

[Van Krevelen and Poelman, 2007]
Van Krevelen, D and R Poelman (2007). “Augmented reality: Technologies, applications, and limitations”. In: *Vrije Univ. Amsterdam, Dep. Comput. Sci* (Cited on page 1).

[Weiland, Braun, and Heiden, 2009]
Weiland, Christian, Anne-Kathrin Braun, and Wolfgang Heiden (2009). “Colorimetric and photometric compensation for optical see-through displays”. In: *International Conference on Universal Access in Human-Computer Interaction*. Springer, pp. 603–612 (Cited on page 36).

[Westland and Ripamonti, 2000]
Westland, Stephen and Caterina Ripamonti (2000). “Invariant cone-excitation ratios may predict transparency”. In: *JOSA A* 17.2, pp. 255–264 (Cited on pages 28, 29).

[Zhang and Murdoch, 2018]
Zhang, Lili and Michael J. Murdoch (2018). “Color Matching Criteria in Augmented Reality”. In: *Journal of Perceptual Imaging*, pp. 10506–1–10506–8 (Cited on page 39).